Investigating the By-Stander Effect of Hypericin Induced Photodynamic Therapy on Human Skin Cells

By:

Ana Popovic

PPVANA001

Submitted to the University of Cape Town
In fulfilment of the requirements for the degree

MSc (Med) in Cell Biology

Date of Submission: 18 August 2014

Supervisor: Dr Lester M. Davids

Department of Human Biology

Faculty of Health Sciences

University of Cape Town

Plagiarism Declaration

I, ……, hereby declare that the work on which this dissertation/thesis is based is my original work (except where acknowledgements indicate otherwise) and that neither the whole work nor any part of it has been, is being, or is to be submitted for another degree in this or any other university.

I empower the university to reproduce for the purpose of research either the whole or any portion of the contents in any manner whatsoever.

Signature: ……

Date: ……

Contents

List of Abbreviations

ALA	5-Aminolevunilic acid
AKT/PKB	Protein Kinase B
AP-1	Activator protein 1
ARF	Human ADP-ribosylation factor protein
BCC	Basal cell carcinoma
BAK	Bcl2 homologous antagonist killer
Bcl-2	B-cell lymphoma 2
Bid	BH3 interacting-domain death agonist
bFGF	Basic fibroblast growth factor
BRAF	V-raf murine sarcoma viral oncogene homolog B1
COX2	Cyclooxygenase
Cyt C	Cytochrome C
CDKN2A	Cyclin dependent kinase 2A
DAMPS	Damage associated molecular patterns
DCF	Dichlorofluoroscein
DCF-DA	2' 7' –dichlorofluorescein diacetate
DMEM	Dulbecco's Modified Eagles Medium
DMSO	Dimethyl Sulfoxide
DOPA	Dihydroxyphenylalanine
ECM	Extracellular matrix
ER	Endoplasmic reticulum
ERK	Extracellular signal regulated kinase
FACS	Fluorescent activated cell sorting
FADD	Fas associated death domain protein
FASL	Fas ligand
Fb	Primary human fibroblasts
FCS	Fetal Calf Serum
FDA	Food and Drug Administration
FETI	Melanocyte specific medium
GREENS	Keratinocytes maintenance medium
HDL	High density lipoproteins

HpD	Hematoporphyrin derivative
HYP	Hypericin
HYP-PDT	Hypericin induced photodynamic therapy
J/cm^2	Joules per surface unit of area
JNK 1	c-Jun N-terminal kinase 1
Kc	Primary human keratinocytes
KSFM	Keratinocyte specific medium
LD_{50}	Lethal dose
LDL	Low density lipoproteins
MAL	Methyl-aminolevunilic acid
MAPK	Mitogen activated protein kinase
Mc	Primary human melanocytes
MEK	Mitogen-activated protein/extracellular signal-regulated kinase
mins	Minutes
MITF	Microphthalmia-associated transcription factor
MMP2	Matrix metalloproteinase 2
Nd: YAG	neodymium-doped yttrium aluminium garnet
NMSC	Non-melanoma skin cancer
$^1O_2$	Singlet oxygen
$P38^{MAPK}$	P38 Mitogen activated protein kinase
$P16^{INK2A}$	Cyclin-dependent kinase inhibitor 2A, multiple tumor suppressor 1
PARP	Poly (ADP-ribose) polymerase
PBS	Phosphate buffered saline
PDT	Photodynamic therapy
PFA	Paraformaldehyde
PI	Propidium iodide
PIP 3	Phosphatidylinositol -3-trisphosphate
PKC	Protein kinase C
PTCH1	Protein patched homolog 1
PTEN	Phosphatase and tensin homolog
PVP	Polyvinylpyrrolidone

RAS	Rat sarcoma tumor suppressor protein
RGP	Radial growth phase
ROS	Reactive oxygen species
s	Seconds
SCC	Squamous cell carcinoma
SERCA 2	Sacro/endoplasmic Ca^{2+} ATPase 2
SOD	Superoxide dismutase
TGF- β	Transforming growth factor β
TNF-α	Tumor necrosis factor α
TP53	Tumor protein p53
TRAIL	Tumor necrosis factor-related apoptosis inducing ligand
TRPM1	Transient receptor potential cation channel subfamily M member 1
mW	Milli Watts
UVR	Ultraviolet radiation
VGP	Vertical growth phase
W	Watts
W/cm^2	Watts per surface unit of area
XTT	Cell proliferation kit II

List of Figures and Tables

Chapter 1: Literature Review

Chapter 2: Material and Methods

Chapter 3: Results

Chapter 4: Discussion

Abstract

Skin cancer is the most common cancer worldwide, and its incidence rate in South Africa is increasing. Photodynamic therapy (PDT) has been shown to be an effective treatment modality, through topical administration, for treatment of non-melanoma skin cancers. Our group investigates hypericin-induced PDT (HYP-PDT) for the treatment of both non-melanoma and melanoma skin cancers. However, a prerequisite for effective cancer treatments is efficient and selective targeting of the tumoral cells with minimal collateral damage to the surrounding normal cells, as it is well know that cancer therapies have bystander effects on normal cells in the body, often causing undesirable side effects.

PDT can induce a bystander effect, defined as indirect damaged induced into adjacent cells either via intercellular gap junctions or via diffusible ROS released in the microenvironment. It is therefore important to know the effects of HYP-PDT on the normal cell population surrounding the non-melanoma skin cancer or melanoma tumor. The aim of this project was to investigate the cellular and molecular effects of HYP-PDT on normal primary human keratinocytes (Kc), melanocytes (Mc) and fibroblasts (Fb) in an *in vitro* tissue culture model thus representing both the epidermal and dermal cellular compartments of human skin.

Cell viability and morphology analysis revealed a differential cytotoxic response to a range of HYP-PDT doses in all the human skin cell types. Fb were the most susceptible followed by Mc and then Kc. Fb cell viability was significantly different post 1μM (56%) ($p<0.001$); 2μM (48%) ($p<0.001$); 3μM (33%) ($p<0.001$) and 4μM (43%) ($p<0.001$) HYP-PDT. Similarly, distinct changes in Fb morphology were observed after a non-lethal (1μM) and lethal (3μM) dose of HYP-PDT. However, Mc were less susceptible than Fb to HYP-PDT doses, displaying significant differences in cell viability occurring at 2μM (60%) ($p<0.05$); 3μM (61%) ($p<0.05$) and 4μM (38%) ($p<0.001$). Distinct

changes in Mc morphology were also observed at both a non-lethal (1μM) and lethal (3μM) HYP-PDT dose. In contrast, Kc were the least sensitive to HYP-PDT compared to Mc and Fb as an initial significant difference in cell viability (79%) ($p<0.05$) only occurred at a dose of 4μM hypericin without causing significant morphological changes in Kc cellular integrity. Fluorescent microscopy displayed peri-nuclear localization of HYP in all the cell types and HYP was excluded from the nucleus of all 3 cell types.

Intracellular ROS levels measured in Fb at 3μM HYP-PDT, displayed a significant 3.8 fold ($p<0.05$) increase in ROS, but no significant difference in ROS levels occurred in Mc or Kc. Furthermore, 64% ($p<0.005$) early apoptotic Fb and 20% ($p<0.05$) early apoptotic Mc were evident; using fluorescence activated cell sorting (FACS), 24 hours post 3μM HYP-PDT. These results depict a differential response to HYP-PDT by different human skin cells suggesting an awareness of the efficacy and indeed, the bystander effect, when HYP-PDT is administered. Future directions include investigating whether the tumor microenvironment affects skin cancer cell response to HYP-PDT which contributes to improved targeting of tumor cells and sparing peri-tumoral normal cells.

Chapter 1: Literature Review

1.1. The Skin

The human body's largest organ is the skin (Figure 1.1.1 A), which has several important physiological functions regulating body temperature; protecting the body from mechanical and chemical stress and defending the body from pathogens in the external environment (Tobin, 2006). Human skin consists of two main layers (Figure 1.1.1 A) that are separated by the basement membrane: the superficial epidermis and the deeper dermis; with the subcutaneous fat layer (hypodermis) situated beneath the dermis (Powell & Soon, 2002; Tobin, 2006). The epidermis is architecturally arranged in 4 tiers named: the outermost stratum corneum, the stratum granulosum, the stratum spinosum and the startum basale (Powell & Soon, 2002; Tobin, 2006). These 4 tiers are populated primarily by keratin-producing keratinocytes that become increasingly more differentiated towards the stratum corneum layer. Some examples of keratins include: cell proliferation associated keratins (K5 and K14) and keratins which are expressed by differentiated keratinocytes (K1, K2, K10, K11) (Tobin, 2006).

In the stratum basale, residing on the basement membrane are pigment producing melanocytes (Figure 1.1.1 B) which extend their dendrites to several keratinocytes (Tobin 2006; Ortonne 2002). The ratio of melanocytes to keratinocytes in the epidermis is: 1:36 but in the basal layer, the dendrites of 1 melanocytes associate with approximately 5 keratinocytes (Haass & Herlyn, 2005). Melanocytes produce the body's endogenous sunscreen called melanin which is synthesized and stored in specialized organelles called melanosomes (Hearing, 2005; Ortonne, 2002; Thompson, Scolyer, & Kefford, 2005). Melanin is synthesized through a process called melanogenesis that involves the hydroxylation of tyrosine to dihydroxyphenylalanine (DOPA) by the rate limiting enzyme tyrosinase (Ortonne, 2002). Thereafter, DOPA is further oxidized to dopaquinone, a melanin precursor that yields the two different types of melanin: eumelanin –

black to brown and pheomelanin -yellow to reddish brown (Hearing, 2005; Ortonne, 2002).

Melanin not only attributes skin colour but also acts as an ultraviolet radiation (UVR) filter (Ortonne, 2002). Melanin-filled melanosomes are then transferred to keratinocytes via melanocyte dendrites and the melanin accumulates as a perinuclear cap in keratinocytes, thereby acting as a shield that absorbs and reflects UVR; preventing DNA damage (Hearing, 2005; Ortonne, 2002). Melanosomal transfer from melanocytes to keratinocytes can occur via several different mechanisms such as individual release of melanosomes from melanocyte dendrites which are taken up via phagocytosis by keratinocytes, membrane fusion of the two cell types; via filapodia extended from both cell types or via the shedding vesicle system (Ando et al., 2012; Mottaz & Zelickson, 1967; Scott, Leopardi, Printup, & Madden, 2002; Seiberg, 2001). Melanin is responsible for UVR-induced skin tanning and is an excellent free radical scavenger/antioxidant (Ortonne, 2002).

Other cell types present in the epidermis are immune Langerhans cells and nerve Merkel cells (Tobin, 2006). The basement membrane, which separates the epidermal and dermal layers, is made up of molecules that promote cell adhesion such as integrins, laminins and collagens (IV and VII), that also regulate keratinocyte migration from the stratum basale during processes such as wound healing (Powell & Soon, 2002; Tobin, 2006).

The dermis consists of fibroblasts interspersed in a dense amorphous extra cellular matrix (ECM), containing mostly collagen molecules (Frantz, Stewart, & Weaver, 2010; Tobin, 2006). To a lesser extent, the following glycoproteins also contribute to the ECM: fibronectin, elastin, laminin, fibrilin and TGF-β binding proteins (Frantz et al., 2010; Tobin, 2006). ECM proteins not only provide the skin with structural integrity, but are also important mediators of

cellular migration, adhesion and intercellular signaling (Frantz et al., 2010; Tobin, 2006). Fibroblasts are migratory cells that synthesize and degrade collagen and most of the ECM components, thereby shaping the dense fibrous and elastic meshwork of the dermis (Frantz et al., 2010; Tobin, 2006). Blood vessels, nerves, nerve receptors lymphatics, hair follicles, sebaceous glands and sweat glands are also situated in the dermis (Tobin, 2006). Therefore, the human skin is designed to protect the internal body from mechanical and external stresses especially, UVR which is a DNA damaging agent (Ortonne, 2002; Tobin, 2006).

A)

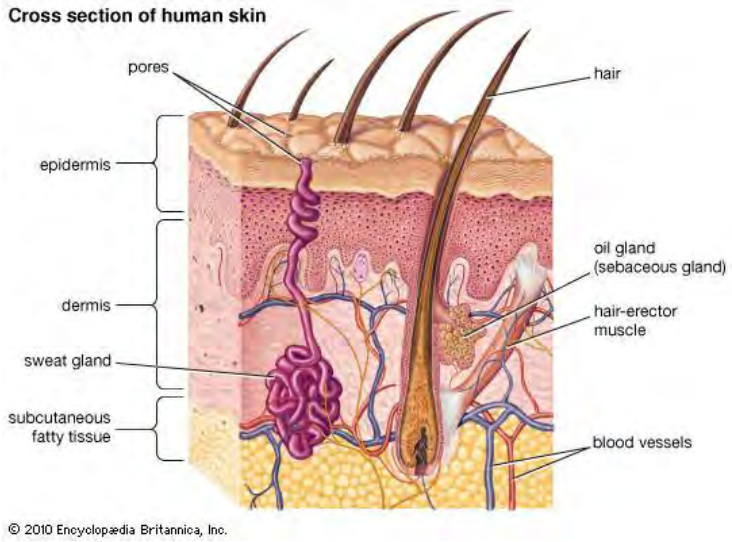

(http://kids.britannica.com/elementary/art-89672/Human-skin-has-three-layers-the-epidermis-the-dermis-and)

B)

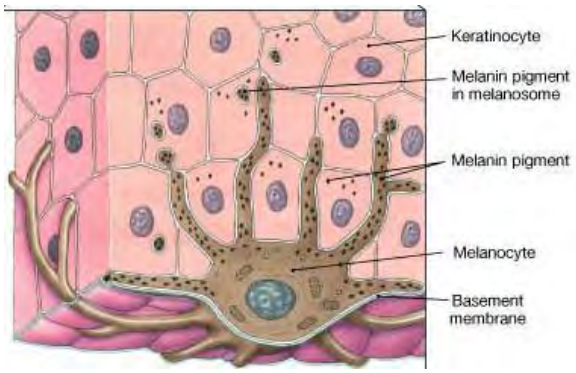

(http://droualb.faculty.mjc.edu/Lecture%20Notes/Unit%201/Integumentary%20with%20figures.html)

Figure 1.1.1: Cross section of human skin (A); Melanocyte and keratinocyte interaction at the basement membrane in the epidermis (B)

1.2. Skin Cancer

1.2.1. Skin Cancer Statistics

Skin cancer is the third most frequent malignancy in the world. It is subdivided into non-melanoma skin cancer (NMSC) and melanoma (Gray Schopfer et al., 2007). NMSC is the most common skin cancer type, accounting for 95% of all skin cancers with an estimated 2-3 million cases of NMSC occurring per year (Ahmed, Soyer, Saunders, Boukamp, & Roberts, 2008; Narayanan, Saladi, & Fox, 2010). Although rarely fatal, NMSC often results in aesthetic disfigurement, especially on the head, face and neck (Ahmed et al., 2008).

Melanoma, although only accounting for 5% of all skin cancers, has the greatest potential to metastasize and is responsible for approximately 85% of skin cancer related deaths (A. J. Miller & Mihm, 2006; Thompson et al., 2005). Shockingly, the prognosis for an estimated 14% of patients with metastatic melanoma is 5 years or less (A. J. Miller & Mihm, 2006). Furthermore, the WHO has estimated that melanoma has the fastest growing incidence rate compared to all cancers: doubling every 10-20 years (Lens & Dawes, 2004).

In a South African context, immuno-compromised patients are at a higher risk of getting NMSC (Lauth, Unden, & Toftgård, 2004). Subsequently, a recent study showed that HIV^+ subjects had a two times higher incidence rate of NMSC compared to HIV^- subjects (Silverberg et al., 2013). It is therefore concerning that the incidence rate of both NMSC and melanoma is increasing each year (Ahmed et al., 2008; Lens & Dawes, 2004; Thompson et al., 2005).

1.2.2. Causes of Skin Cancer

The predominant cause of skin cancer is ultraviolet radiation (UVR) which comprises UVA (315-400nm), UVB (280- 315nm) and UVC (100 – 280nm) wavelengths (de Gruijl, van Kranen, & Mullenders, 2001; Narayanan et al., 2010; Pfeifer & Besaratinia, 2012). UVC is filtered by the ozone layer and does not reach the earth's surface but UVA and UVB are able to penetrate the human skin and induce DNA damage and genetic mutations in human skin cells, thereby inducing skin cancer (Cadet, Mouret, Ravanat, & Douki, 2012; de Gruijl et al., 2001; Narayanan et al., 2010; Pfeifer & Besaratinia, 2012).

UVB penetrates the epidermis and is the main mutagenic culprit, as it can directly damage DNA by inducing cyclobutane pyrimidine dimers primarily by C-T transitions (Ahmed et al., 2008; Cadet et al., 2012; Narayanan et al., 2010). This results in CC to TT double base changes, known as the UVB signature; causing mutations in certain genes such as the tumor suppressor gene *TP53* in keratinocytes (Ahmed et al., 2008; Cadet et al., 2012).

UVA can penetrate both the epidermis and the dermis and can indirectly cause DNA damage via reactive oxygen species (ROS) (Ahmed et al., 2008; Cadet et al., 2012; Narayanan et al., 2010; Pfeifer & Besaratinia, 2012). Moreover, UVA more likely than UVB, causes DNA damage in basal keratinocytes in the stem-cell like layer at the basement membrane in the epidermis (Agar et al., 2004).

Furthermore, UVR-induced DNA damage can directly cause gene mutations, deregulation in DNA repair mechanisms, aberrant apoptosis, immuno-suppression, oxidative stress and stimulate the ECM to produce growth factors, thus promoting a cancer cell phenotype and a tumor microenvironment (Narayanan et al., 2010; Pfeifer & Besaratinia, 2012; Thompson et al., 2005). A skin cancer's microenvironment has a stiff

architecture as a result of ECM proteins and contains transformed fibroblasts, macrophages and T- lymphocytes (Celli, 2013; Frantz et al., 2010; Quail & Joyce, 2013; Vittar et al., 2013). Bidirectional communication exists between a cancer and its microenvironment which promotes angiogenesis, tumor proliferation, metastasis and tumor resistance (Frantz et al., 2010; Quail & Joyce, 2013; Vittar et al., 2013; Vittar et al., 2013)

1.2.3. Skin Cancer Types

NMSC presents either as basal cell carcinoma (BCC) or squamous cell carcinoma (SCC) and stems from mutations induced in keratinocytes however, due to genetic heterogeneity different genes can be mutated in keratinocytes (Lauth et al. 2004; Melnikova & Ananthaswamy 2005). Eighty percent of diagnosed skin cancers are BCC which is a slow growing and rarely metastatic keratinocyte derived cancer with mutations in the patched gene *PTCH1* and tumour suppressor *TP53* gene (de Gruijl et al., 2001; Lauth et al., 2004; Melnikova & Ananthaswamy, 2005). SCC is more aggressive and less frequent (1:4) than BCC that may occasionally metastasize (Lauth et al., 2004). SCC occurs as a result of mutations in *TP53; P16^{INK2A} genes, AP1* transcription factor complex and the pro-inflammatory cyclooxygenase (COX2) (Ahmed et al., 2008; Lauth et al., 2004).

Melanoma develops from genetic aberrations induced in melanocytes with the most common mutations in the *BRAF, N-RAS, CDKN2A and PTEN genes* (Gray Schopfer et al., 2007; A. J. Miller & Mihm, 2006; Thompson et al., 2005). Other less common mutations which result in a carcinogenic phenotype include MEK, ERK, ARF, P53, AKT and MITF proteins (Gray Schopfer et al., 2007; A. J. Miller & Mihm, 2006). Due to these genetic mutations and microenvironment changes, melanoma clonally expands in the epidermis; undertaking a radial form of clonal cellular expansion called

the radial growth phase (RGP) (A. J. Miller & Mihm, 2006). Unattended, these cells grow even more aggressively and adopt a vertical growth dimension which breaches the basement membrane and invades the dermis. This phase is called the vertical growth phase (VGP). However, it has been stipulated in a review by (Damsky, Theodosakis, & Bosenberg, 2014) that the progression from the RGP to the VGP is a very complex process. The aim of the VGP phase is expansion of the clone towards the blood vessels in the dermis which allows the final metastatic phase and consequential dissemination into the blood (A. J. Miller & Mihm, 2006).

During metastasis there is down regulation of certain adhesion molecules such as E-cadherin, Survivin and TRPM1 and upregulation of N-cadherin, $\alpha_V\beta3$ integrin and MMP2 (A. J. Miller & Mihm, 2006). Furthermore, there is some evidence that certain individuals have a genetic predisposition for melanoma susceptibility by inheriting a mutation in the *CDKN2A* gene which has been linked to a higher melanoma incidence rate, especially in people who live at lower altitudes and experience high UVR exposure (Thompson et al., 2005). Although individuals with a fairer skin type, often with European ancestry, are more susceptible to skin cancer than individuals with darker (pigmented) skin, darker skinned individuals can get skin cancer and their prognosis is often unsatisfactory due to late presentation and late diagnosis (Bradford, 2009).

1.2.4. Skin Cancer Treatment

Once a NMSC or a melanoma is diagnosed the current, golden standard of treatment is surgical resection (Freak, 2004; Ross, Cherpelis, Lien, & Fenske, 2013; Zhao & He, 2010). Thereafter, patients with aggressive skin cancers such as melanoma are usually treated with bouts of adjuvant therapy including chemotherapy or ionizing radiation (Thompson et al., 2005). However, melanoma is often resistant to these traditional therapies which is reflected by its high recurrence rate , poor patient prognosis and multi-drug

resistance (L M Davids & Kleemann, 2010; Fukunaga-Kalabis & Herlyn, 2012; Thompson et al., 2005). A need therefore exists for novel, adjuvant melanoma therapies (L M Davids & Kleemann, 2010).

Photodynamic therapy (PDT) is a promising, potential therapy for melanoma (Baldea, Filip, & Napoca, 2012; L M Davids & Kleemann, 2010). Furthermore, it is an effective treatment modality offered clinically in some parts of Europe and the USA for the treatment of NMSC, especially in NMSC that occurs on sensitive areas of the face, head and neck which are difficult to resect (Ross et al., 2013; Wan & Lin, 2014; Zhao & He, 2010). PDT is a minimally invasive therapy that results in good cosmetic outcome which can also be applied topically on cancerous skin lesions (Agostinis et al., 2011; Brown, Brown, & Walker, 2004; Ross et al., 2013; Wan & Lin, 2014; Zhao & He, 2010).

1.3. Photodynamic Therapy

1.3.1. The Principles of Photodynamic therapy (PDT)

PDT is a cancer treatment modality which is dependent on the interaction of light, a chemical compound know as a photosensitiser and oxygen in the tumor microenvironment (Agostinis et al., 2011; Dolmans, Fukumura, & Jain, 2003; Robertson, Evans, & Abrahamse, 2009). PDT was initially clinically used for the treatment of skin and bladder cancer in 1975 by Thomas Dougherty and in 1976 by J.F. Kelly, respectively. It was officially recognized as a cancer therapy in 1999, for the treatment of bladder cancer, upon FDA approval in Canada (Ackroyd, 2001; Dolmans et al., 2003).

Currently, PDT is clinically used for the treatment of several cancers including bladder, lung, esophageal, breast, brain, head and neck, pancreatic, ophthalmic, prostate, liver, bile duct, sarcoma, nasopharyngeal,

cutaneous T-cell lymphoma and BCC (Agostinis et al., 2011; Brown et al., 2004; Hopper, 2000). Furthermore, dermatologists not only use PDT routinely in clinics for the treatment of BCC but also for other dermatological conditions such as psoriasis and actinic keratosis (Ross et al., 2013; Zhao & He, 2010). However, the treatment of SCC and melanoma skin cancers is currently being investigated (Ross et al. 2013; Wan & Lin 2014; Morton et al. 2008). Moreover, in South Africa, PDT is an emerging cancer therapy and is being offered to patients in some private practices.

PDT involves the topical or systemic administration of a photosensitiser which upon light activation, becomes excited and gains energy (Figure 1.3.1) resulting in an unstable molecule which must transfer an electron and release energy in order to return to the lower energy level and more stable ground state (Agostinis et al., 2011; Plaetzer, Krammer, Berlanda, Berr, & Kiesslich, 2009; Stapleton & Rhodes, 2003). Therefore, the photosensitiser must release energy (Figure 1.3.1) by either donating an electron to a biomolecule (Type I) or to O_2 molecules (type II) in the microenvironment (Castano et al, 2004). These 2 photochemical reactions produce consequential intracellular reactive oxygen species (ROS) in the vicinity of photosensitiser activation and the type II reaction is most favored by photosensitizers due to thermodynamic laws and results in the formations of the highly reactive and short lived singlet oxygen ($^1O_2$) species (Calzavara-Pinton, Venturini, & Sala, 2007; Castano et al., 2004). $^1O_2$ is extremely unstable and can further transfer electrons and induce ROS-mediated lipid and protein peroxidation (Castano et al., 2004; Plaetzer et al., 2009).

An accumulation of ROS in target cancer cells can cause damage to organelles, leading to multifaceted triggering of cell death pathways such as apoptosis, necrosis and autophagy, resulting in cancer cell death and subsequent tumour destruction (Agostinis et al., 2011; Plaetzer et al., 2009; Robertson et al., 2009). Furthermore, PDT may potentially infer anti -tumor immunity by eliciting the innate and adaptive immune response as well as

inducing anti-vascular effects by causing vasoconstriction in the tumour microenvironment (Agostinis et al., 2011; Castano, 2006).

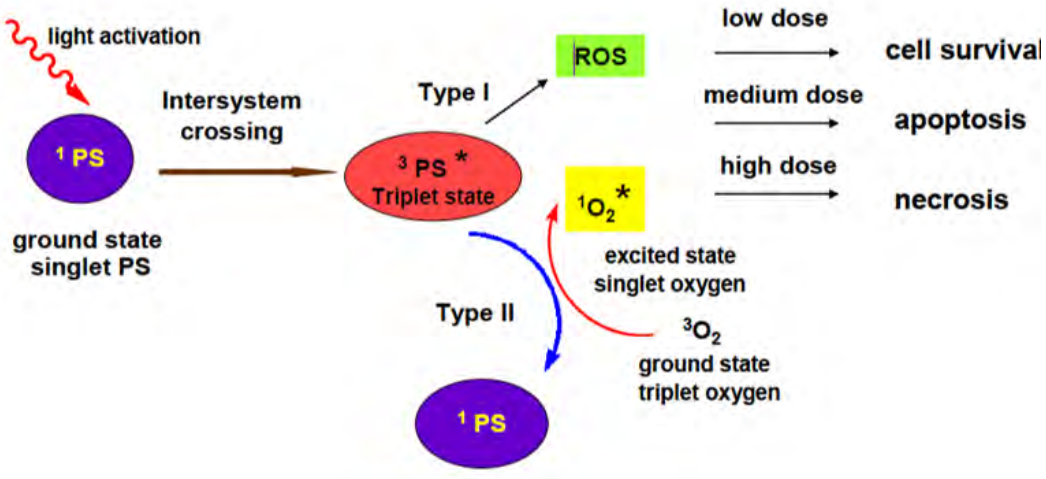

Figure 1.3.1: The basic principles of PDT (Karioti & Bilia, 2010)

As a cancer therapy, PDT offers several advantages compared to current cancer therapies (Agostinis et al., 2011). These include minimal invasiveness and high tumour specificity which can be attributed to 3 key factors: photosensitizers are specifically bioengineered to target cancer cells; cytotoxic effects of photosensitizers are limited to the vicinity of their localization within a cell and the light dose during PDT can be directed to irradiate only the tumor tissue with the aid of improved photo-technology (Agostinis et al., 2011; Dolmans et al., 2003). Furthermore, PDT does not interfere with the outcome of other cancer therapies and can be used adjunctively with other therapies such as surgery and chemotherapy (Agostinis et al., 2011; Zhao & He, 2010). Additionally, PDT can be used to treat internal cancers of the body with repeated PDT doses which can be administered to outpatients in clinics as they do not require hospitalization

(Castano et al., 2004; Morton et al., 2008; Ross et al., 2013; Wan & Lin, 2014). Moreover, PDT of NMSC and other dermatological conditions ensues a good cosmetic outcome and PDT of internal insitu tumors results in organ preservation (Brown et al., 2004; Ross et al., 2013).

Despite, the advantages of PDT, its main disadvantage is that PDT is not currently used to treat patients with systemic and metastatic cancers because PDT has great cancer lesion specificity (Agostinis et al., 2011; Hopper, 2000). However, with the advancement in technology of light delivery instruments; this disadvantage is becoming a possibility in the near future (Agostinis et al., 2011). Furthermore, some of the side effects associated with PDT of BCC are: pain, itching, edema, erythema and inflammation, epithelial abrasion, pustules and skin hyper pigmentation but there are currently investigations into the use of sunlight as a PDT light source to reduce pain and discomfort experienced by patients undergoing PDT of NMSC and Bowens disease (a form of SCC) (Wan & Lin 2014; Ross et al. 2013).

1.3.2. PDT Efficacy and Outcome: Photosensitisers

The synergistic actions of photosensitiser and light in the presence of O_2, are required for successful PDT outcome (Agostinis et al., 2011; Dolmans et al., 2003; Plaetzer et al., 2009). Investigating the ideal photosensitiser and its complimentary light source is therefore important as it may lead to improved PDT efficacy (Allison et al., 2004; Castano et al., 2004; Stapleton & Rhodes, 2003; Zhao & He, 2010).

Crucial characteristics of an ideal photosensitiser include high tumour selectivity, maximal and rapid accumulation, retention in cancer cells and an effective and fast clearance rate from the body (Allison et al., 2004; Detty, Gibson, & Wagner, 2004; Mojzisova, Bonneau, & Brault, 2007; Robertson et al., 2009). Ideally, the photosensitiser should be a single and chemically pure

compound which is inert and non-toxic in the dark that can be stored effectively (Agostinis et al., 2011; Castano et al., 2004; Mojzisova et al., 2007). It is also important for the photosensitiser to have a have a high quantum yield, enabling it to generate sufficient $^1O_2$ upon light absorption (Castano et al., 2004; Detty et al., 2004).

The first FDA approved (1993) photosensitizer was intravenous hematoporphyrin derivative (HpD), known commercially as Photofrin® (Table 1.3.2) that was initially a water soluble mixture of porphyrins and is now used in a more purified form as porfimer sodium (Agostinis et al., 2011; Calzavara-Pinton et al., 2007; Mojzisova et al., 2007) However, Photofrin® demonstrated several clinical shortfalls including poor selectivity and specificity for tumors compared to normal tissue with patients experiencing prolonged light-sensitivity of the skin, lasting between 4 and 10 weeks post-PDT (Allison et al., 2004; Castano et al., 2004; Detty et al., 2004). Despite these disadvantages, Photofrin® continues to be used in clinics worldwide to treat several cancers (Table 1.3.2) but it is not the most widely used photosensitiser for PDT of skin cancers specifically (Ross et al., 2013; Wan & Lin, 2014).

5-Aminolevunilic acid (ALA), commercially known as Levulan®, is used clinically worldwide (Table 1.3.2) as a topical photosensitiser for the treatment of superficial and nodular BCC, Bowen's disease (a form of SCC) and other dermatological conditions such as actinic keratosis (Ross et al., 2013). ALA is an endogenous photosensitizer because it is metabolized in the intracellular haem pathway to protoporphyrin IX which is the photoactive molecule that induces $^1O_2$ production upon light activation (Calzavara-Pinton et al., 2007). Despite its efficacy as a topical photoensitizer, ALA is a small lipophilic molecule and therefore has relatively weak penetration into skin tissue (Wan & Lin 2014).

ALA which is methylated with an ester to form methyl-aminolevunilic acid (MAL; Metvix®) is clinically used in several European countries, New Zealand and Australia for the treatment of BCC and *in situ* SCC (Table 1.3.2) (Wan & Lin 2014). MAL has improved tissue penetration compared to ALA as it is slightly more hydrophobic thereby penetrating more easily across plasma cell membranes and entering skin cancer cells more readily (Stapleton & Rhodes, 2003). The drawbacks of ALA and MAL such as poor selectivity when administered systemically, their shallow tissue penetration and reported pain during light exposure in clinics encouraged further investigation of improved photosensitisers for PDT (Agostinis et al., 2011; Allison et al., 2004; Calzavara-Pinton et al., 2007; Castano et al., 2004; Detty et al., 2004; Ross et al., 2013; Wan & Lin, 2014).

Currently, several novel photosensitizers are being tested in clinics around the world (Table 1.3.2). These include chlorins, bacteriochlorins, benzoporphyrin derivatives, pthalocyanines and porphycenes (Agostinis et al., 2011; Mojzisova et al., 2007). These photosensitizers have been named second generation photosensitizers due to less reported skin photosensitivity and their activation by longer wavelengths of light (>600nm) (Calzavara-Pinton et al., 2007; Mojzisova et al., 2007). Although both of these are desirable characteristics, shorter wavelengths of light comprise higher energy (Alexiades-Armenakas, 2006; Karrer, Szeimies, Hohenleutner, & Landthaler, 2001; Mang, 2004). Therefore, the combination of light penetration depth and light energy must produce sufficient $^1O_2$ to cause cytotoxicity (Castano et al., 2004). In order to improve photosensitizer uptake and intracellular localization, photosensitizers are often coupled to carrier molecules such as: antibodies, peptides, nanoparticles or are encapsulated in lipids or other bio materials. (Agostinis et al., 2011; Konan, Gurny, & Allémann, 2002; Vandongen, Visser, & Vrouenraets, 2004).

Table 1.3.2 Photosensitizers Currently Used During Clinical PDT (Agostinis et al., 2011)

PHOTOSENSITIZER	STRUCTURE	WAVELENGTH, nm	APPROVED	TRIALS	CANCER TYPES
Porfimer sodium (Photofrin) (HPD)	Porphyrin	630	Worldwide		Lung, esophagus, bile duct, bladder, brain, ovarian
ALA	Porphyrin precursor	635	Worldwide		Skin, bladder, brain, esophagus
ALA esters	Porphyrin precursor	635	Europe		Skin, bladder
Temoporfin (Foscan) (mTHPC)	Chlorine	652	Europe	United States	Head and neck, lung, brain, skin, bile duct
Verteporfin	Chlorine	690	Worldwide (AMD)	United Kingdom	Ophthalmic, pancreatic, skin
HPPH	Chlorin	665		United States	Head and neck, esophagus, lung
SnEt2 (Purlytin)	Chlorin	660		United States	Skin, breast
Talaporfin (LS11, MACE, NPe6)	Chlorin	660		United States	Liver, colon, brain
Ce6-PVP (Fotolon), Ce6 derivatives (Radachlorin, Photodithazine)	Chlorin	660		Belarus, Russia	Nasopharyngeal, sarcoma, brain
Silicon phthalocyanine (Pc4)	Phthalocyanine	675		United States	Cutaneous T-cell lymphoma
Padoporfin (TOOKAD)	Bacteriochlorin	762		United States	Prostate
Motexafin lutetium (Lutex)	Texaphyrin	732		United States	Breast

Abbreviations: ALA, 5-aminolevulinic acid; AMD, age-related macular degeneration; Ce6-PVP, chlorin e6-polyvinypyrrolidone; HPD, hematoporphyrin derivative; HPPH, 2- (1-hexyloxyethyl)-2-devinyl pyropheophorbide-a; MACE, mono-(L)-aspartylchlorin-e6; mTHPC, m-tetrahydroxyphenylchlorin; nm indicates nanometers; SnEt2, tin ethyl etiopurpurin.

1.3.3. PDT Efficacy and Outcome: Light Source Activation

Once the photosensitiser has been internalized by cancer cells, the tumor lesion is irradiated with an appropriate light source that should ideally correspond to the peak absorption peak of the photosensitiser (Robertson et al., 2009). Various light sources may be used for photosensitiser activation during PDT including laser light, UV lamps, white light, light emitting diodes (LEDs), short arc plasma discharge lamps, xenon lamps and more recently, sunlight (Alexiades-Armenakas, 2006; Calzavara- Pinton, 2007; Mang, 2004; Ross et al., 2013).

Lasers, the most common light source used during PDT (Ross et al., 2013; Wan & Lin, 2014) exist as several different types - diode lasers emitting continuous wave light (red, green or blue) or intense pulsed light, potassium titanyl phosphate lasers, pulse dye lasers, infrared lasers, CO_2 lasers, argon lasers and Nd:YAG lasers (Karrer et al., 2001; Mang, 2004; Ross et al., 2013; Wan & Lin, 2014). Diode lasers are the most popular because they are small, cost effective and have automated dosimetry and calibration rendering them practical and relatively easy to use by the clinician (Alexiades-Armenakas, 2006; Karrer et al., 2001; Mang, 2004). Moreover, lasers can be attached to one or several flexible fiber optic cables and endoscopes that allow for the irradiation of interstitial tissues, internal organs and tumors (Alexiades-Armenakas, 2006; Mang, 2004).

PDT efficacy is dependent on the light dose which is measured by two key parameters: fluence of the light beam and the fluence rate (Hamblin & Huang, 2013; Splinter & Hooper, 2007; Vo-Dinh, 2003). The first important parameter fluence (J/m^2), is the amount of light energy that reaches a unit of area, taking into account that some of the energy is lost due to light by diffusion and scattering when it penetrates tissue (Hamblin & Huang, 2013; Splinter & Hooper, 2007; Vo-Dinh, 2003). The second important parameter in light delivery is the fluence rate (W/cm^2), defined as the power (light energy per unit of time) that is delivered taking into account that energy is dissipated by diffusion and scattering upon tissue penetration (Hamblin & Huang, 2013; Splinter & Hooper, 2007; Vo-Dinh, 2003). The fluence and power of the light beam emitted by diode lasers can be adjusted manually or automatically which allows for improved light dosimetry during PDT and enables the user/laser to calculate accurate irradiating time (Splinter & Hooper, 2007).

Characteristics of an ideal light source include maximal absorption by a photosensitizer, good tissue penetration, a high fluence rate to generate $^1O_2$ in minimal irradiating time, precise targeting of tumour tissue and minimal skin photosensitivity and discomfort (Alexiades-Armenakas, 2006). Although

there is currently no ideal photosensitizer and its complementary light source for PDT of skin cancers; up and coming PDT research is aiming to address this, by investigating novel photosensitisers and their possible light sources for the treatment of skin cancers, especially melanoma skin cancer (Ross et al. 2013; Wan & Lin 2014).

1.4. The Photochemical and Photophysical Properties of Hypericin

Hypericin (HYP) is a deep red pigment primarily found in the leaves and flowers of the plant *Hypericum perforatum L.* commonly known St John's Wort (Figure 1.4.1 A) which can be extracted from this plant using high performance liquid chromatography (Krammer & Verwanger, 2012; A. L. Miller, 1998; Zobayed, Afreen, Goto, & Kozai, 2006). Although HYP is a natural photosensitiser, it can also be chemically synthesized using successive oxidations of its precursor emodin anthraquione to yield protohypericin, which upon light exposure, is converted to hypericin (Karioti & Bilia, 2010; Van de Putte, Roskams, Vandenheede, Agostinis, & de Witte, 2005; Zobayed et al., 2006). HYP is a lipophilic, polycyclic, aromatic naphthodianthrone (Figure 1.4.1 B) that is stable in solution and at room temperature and can be stored at -20°C in the dark (Karioti & Bilia, 2010; Van de Putte et al., 2005).

The photophysics of HYP include optimum light absorption at 560-595nm (green-orange visible light spectrum) (Figure 1.4.1 C) and red fluorescence emission at 600-640nm in organic solvents (Kiesslich, Krammer, & Plaetzer, 2006; Theodossiou, Hothersall, Witte, Pantos, & Agostinis, 2009). According to laser spectroscopy analyses, HYP is a potent natural promising photosensitiser because it has strong electron donating potential in polar solvents and therefore has a high quantum yield that results in generous $^1O_2$ production upon light activation (Theodossiou et al., 2009). Therefore,

hypericin induced PDT (HYP-PDT) can initiate potent cytotoxic consequences in cancer cells but this is primarily dependent on the localization of HYP upon light activation and to a lesser extent the dose of HYP, the uptake/incubation time of HYP and the light dose used to activate HYP (Agostinis, Vantieghem, Merlevede, & de Witte, 2002).

High tumour selectivity *in vivo* is also another important characteristic of HYP, for example in mice, HYP accumulation in subcutaneous tumor tissue was 16 fold higher in concentration than normal skin and muscle surrounding tissue after intravenous administration of HYP (5mg/kg) (Chen & de Witte, 2000).

A)

Adapted from (Karioti & Bilia, 2010)

B)

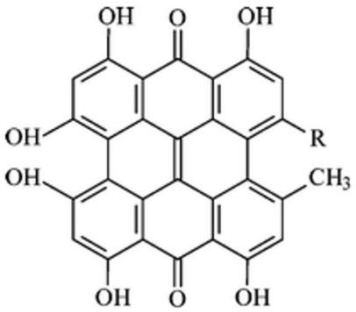

Adapted from (Nahrstedt & Butterweck, 2010)

C)

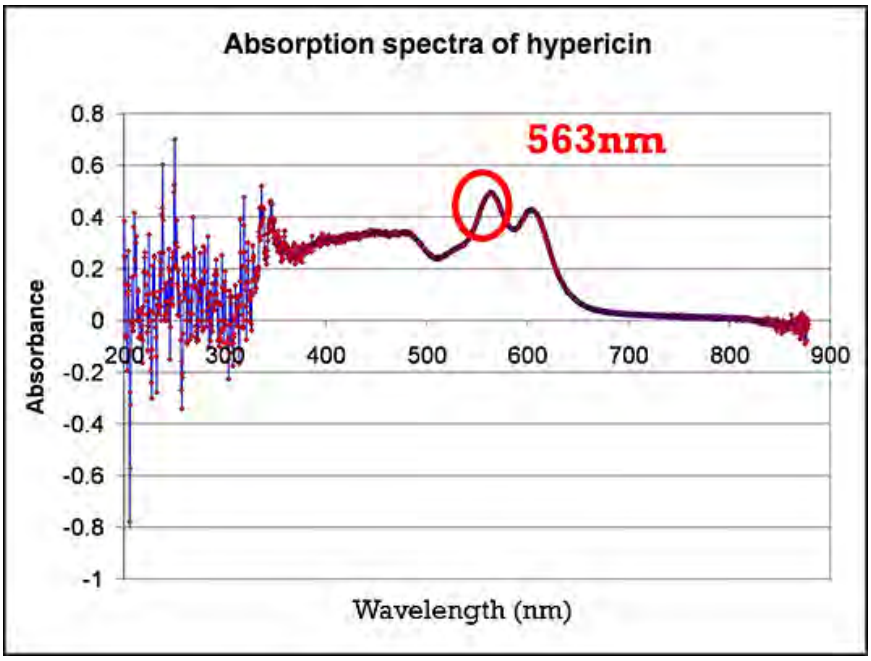

Figure 1.4.1: *Hypericum perforatum L.* (St John's Wort) (A); HYP chemical structure (B) and HYP absorption spectrum with the peak absorption peak at 563nm (C)

1.5. Hypericin Uptake and Localization

HYP is a monobasic salt in physiological solutions and due to its hydrophobicity it forms aggregates in physiological aqueous environments (Agostinis et al., 2002; Krammer & Verwanger, 2012). This allows HYP to bind readily to low density lipoproteins (LDL); high density lipoproteins (HDL) and serum albumin in the blood and can therefore be transported systemically around the body (Lavie, Mazur, Lavie, & Meruelo, 1995). HYP solubility can be improved by conjugating it to biomolecules such as polyvinylpyrrolidone (PVP) for improved transport and delivery to the tumor tissue (Kubin et al., 2008).

Once the HYP and LDL/HDL complexes reach the interstitial tissue, HYP can be taken up by LDL/HDL receptor mediated endocytosis or via passive diffusion after dissociation from the LDL/HDL molecules; because the hydrophobic moieties of HYP can interact with cholesterol molecules of the hydrophobic regions in plasma cell membranes allowing for easy breaching across the plasma membrane (Jori & Reddi, 1993; Karioti & Bilia, 2010; Siboni et al., 2002; Van de Putte et al., 2005). Furthermore, HYP can also interact with micromolecules in the tumor microenvironment such as collagen and can penetrate through the tumor microenvironment ECM, possibly because of the decrease in E-cadherin and loss of intracellular adhesion in tumor tissue (Krammer & Verwanger, 2012; Van de Putte et al., 2005).

In vivo, HYP is preferentially taken up by cancer cells because cancer cells have more LDL/HDL extracellular receptors compared to normal cells however, this is not the case *in vitro* as HYP is taken up readily by both normal and cancer cells via passive diffusion (Kamuhabwa, Agostinis, D'Hallewin, Kasran, & de Witte, 2000; Siboni et al., 2002). The rate of HYP uptake can vary depending on the dose and cell type; although the current

recommended uptake time for HYP *in vitro* is 2- 4 hours (Agostinis et al., 2002; Kiesslich et al., 2006; Theodossiou et al., 2009).

Once HYP is inside a cell, it preferentially localizes to organelle membranes and has been reported to localize in the membranes of the ER, mitochondria, Golgi apparatus, lysosomes and melanosomes but this localization which seems to be correlative with uptake, is cell type and dose-dependent (Agostinis et al., 2002; L M Davids & Kleemann, 2010; Kleemann, Loos, Lang, Scriba, & Davids, 2014; Krammer & Verwanger, 2012; Skalkos et al., 2006; Theodossiou et al., 2009). Furthermore, HYP localization in the nucleus although rare, has been reported after prolonged periods of time and at very high doses (>20μM) (Krammer & Verwanger, 2012).

1.6. Cytotoxic Effects of Hypericin-Induced Photodynamic Therapy

Activated HYP generates ROS in the vicinity of its localization because $^1O_2$ has a very short half-life (<0.04μs), and can diffuse a distance of approximately 20nm (Davies, 2003; Moan & Berg, 1991). This infers that hypericin-induced photodynamic therapy (HYP-PDT) ROS induced cell damage, occurs mostly in cell and organelle membranes in the form of protein and/or lipid peroxidation (Agostinis et al., 2002; Davies, 2003; Krammer & Verwanger, 2012; Moan & Berg, 1991). Subsequently, HYP-PDT can lead to different forms of cell death such as apoptosis or necrosis or may induce cell survival via autophagy, although autophagy has recently been deemed a cell death mechanism (Agostinis et al., 2002; Mikeš, Jendželovský, & Fedoročko, 2013; Ouyang et al., 2012; Shen, Kepp, & Kroemer, 2012; Theodossiou et al., 2009).

Briefly, apoptosis results in cell shrinkage, chromatin condensation, DNA fragmentation and membrane blebbing preceding the formation of apoptotic

bodies, (membrane enclosed vesicles containing cellular debris) which are efficiently phagocytozed by neighboring cells; thereby avoiding an immunogenic response (Fiers, Beyaert, Declercq, & Vandenabeele, 1999; Kerr, Wyllie, & Currie, 1972). In contrast, necrosis induces a powerful immune response because of cellular content spillage once the cell cytoplasm and organelles swell and the plasma membrane has burst (Fiers et al., 1999). Autophagy ensures recycling of damaged organelles by means of enzymatic degradation in membrane bound autophagasomes that become fused with lysosomes containing hydrolases (Levine & Klionsky, 2004). However, persistent autophagy can instigate cell death as essential organelles get degraded cell metabolism and integrity is compromised; which can lead to apoptosis (Marino, Niiso-Santo, Baechrecke, & Guido, 2014; Rubio et al., 2012; Shen et al., 2012).

1.7. HYP-PDT Induced Apoptosis

Apoptosis is regulated by complex intracellular pathways (Figure 1.7.1) (Marino et al., 2014; Ouyang et al., 2012; Vandenabeele, Galluzzi, Vanden Berghe, & Kroemer, 2010). Briefly, the key mediators of apoptosis are the cytoplasmic caspases (9; 8; 3; 5; 7) (Figure 1.7.1), which are proteolyticly cleaved in a cascade fashion that induces translocation of poly (ADP-ribose) polymerase PARP into the cell nucleus which is then able to cleave DNA into fragments (Hengartner, 2000). The caspase cascade can be activated by either the intrinsic or the extrinsic apoptotic pathway (Ouyang et al., 2012).

The extrinsic pathway (Figure 1.7.1) is initiated by the binding of death ligand to their death receptors such as: tumor necrosis factor α (TNF α); tumor necrosis factor-related apoptosis inducing ligand (TRAIL) and Fas ligand (FASL) at the cell membrane which leads to receptors clustering and associating with adaptor proteins such as Fas associated death domain protein (FADD); leading to caspase activation (Ashkenazi & Dixit, 1999). The intrinsic apoptosis pathway (Figure 1.7.1) involves mitochondrial membrane

compromise after an insult and subsequently releasing cytochrome C (Cyt C) into the cytosol through a “leaky” mitochondrial membrane (Green & Walczak, 2013; Hengartner, 2000). Cyt C release is induced by key apoptotic proteins: B cell lymphoma 2 (Bcl 2); BAK and Bid and it allows Cyt C to form complexes with other apoptotic proteins to activate the caspase cascade (Fadeel, Zhivotosky, & Orrenius, 1999; Green & Walczak, 2013).

If HYP localizes in the mitochondrial membrane, HYP-PDT down regulates matrix metalloprotease 1; inhibits protein kinases such as PKC and impairs mitochondrial function thereby inducing apoptosis (Agostinis et al., 2002). HYP- PDT has been shown to activate the intrinsic apoptotic pathway by up regulating Bcl2; inhibiting mitochondrial membrane hexokinase, inducing Cyt C release, activating the caspase cascade; and causing DNA fragmentation (Agostinis et al., 2002; Karioti & Bilia, 2010; Kiesslich et al., 2006; Theodossiou et al., 2009). The extrinsic apoptotic pathway involving cathepsin D release and the lysosomal pathways has also been reported due to HYP-PDT (Agostinis et al., 2002; Kiesslich et al., 2006; Theodossiou et al., 2009).

Furthermore, should activated HYP reside in the ER, $^{1}O_{2}$ can damage the sarco/endoplasmic Ca^{2+} ATPase 2 (SERCA 2) pump which causes release of Ca^{2+} from ER Ca^{2+} stores into the cytosol (Buytaert et al., 2006). Ca^{2+} can act as a 2^{nd} messenger molecule in the cytosol and activate PKC and the pro-apoptotic protein BAK, which stimulates the extrinsic apoptotic cascade via mitochondrial membrane permealization and Cyt C release (Agostinis et al., 2002; Buytaert et al., 2006). Furthermore, HYP-PDT treated cells may also send “eat me” signals via damage associated molecular patterns (DAMPs) such as heat shock protein 70 (HSP 70) and calreticulin which are externalized and can induce an immunogenic response to ensure opsonization of dead cells and possibly infer anti-tumor immunity (Garg & Agostinis, 2014; Garg et al., 2013).

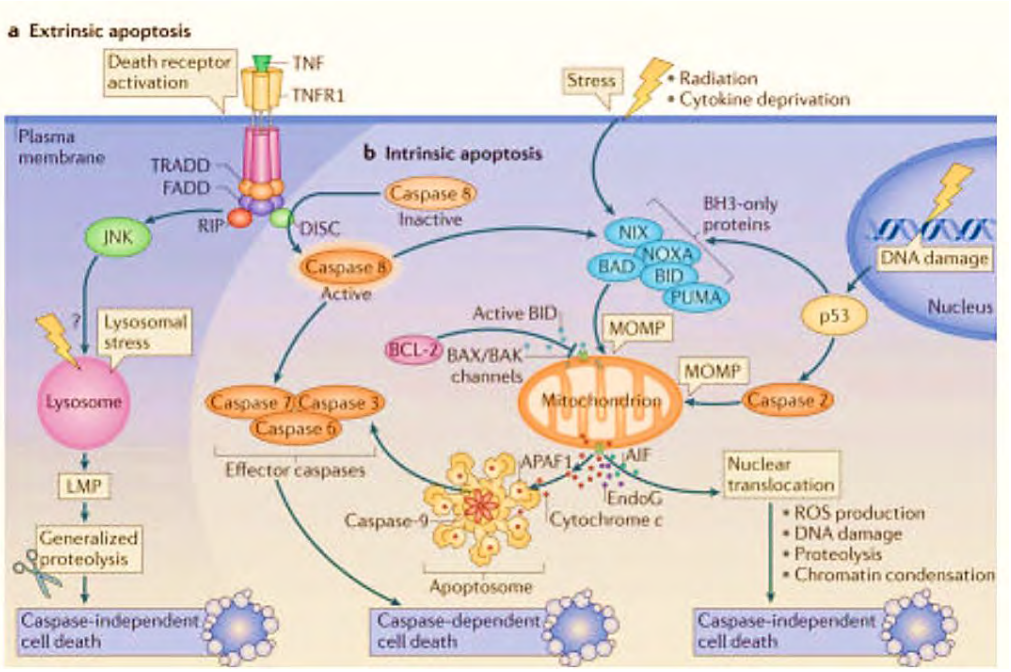

Figure 1.7.1: The mechanism of apoptosis (Adapted from Marino et al. 2014)

1.8. HYP-PDT and Prosurvival Effects

Some of the pro-survival mechanisms which have been associated with HYP-PDT include up regulation of: JNK 1, MAPKs; PIP 3; ERK 2; ceramides, cyclin dependent kinases and some second messenger molecules (Assefa et al., 1999; Oleinick & Evans, 2010). Furthermore, an increase in the activity of antioxidants such as superoxide dismutase (SOD) and glutathione have also been observed immediately post HYP-PDT which may contribute to cancer cell resistance to HYP-PDT (Agostinis et al., 2002; Karioti & Bilia, 2010; Kiesslich et al., 2006; Kubin, Wierrani, Burner, Ualth, & Grünberger, 2005; Theodossiou et al., 2009). It is important to note that the cellular response to HYP-PDT is dependent on a number of factors: the cell type; the dose of HYP; the dose of light and most importantly where inside

the cell the HYP is residing when it gets activated by light and produces ROS (Agostinis et al., 2002; L M Davids & Kleemann, 2010; Theodossiou et al., 2009).

1.9. HYP-PDT and *In Vitro* Skin Cancer Studies

We, and others have investigated the cytotoxic effects induced by HYP-PDT in human skin cancer cells (Davids et al. 2008; Davids et al. 2009; Sanovic et al. 2009; Blank et al. 2003; Sharma & Davids 2012; Gyenge et al. 2013; Hadjur et al. 1996; Sharma et al. 2011).

A study by Sanovic et al. 2009, conducted gene profiling using gene microarray analysis of apoptotic genes in A431 SCC cells at 1.5; 3; 5 and 6 hours post HYP – PDT. Upregulation of pro-survival proteins $p38^{MAPK}$ JNK, ERK and RAS were observed when cells were treated with HYP, only (in the dark) or low concentrations (< 3μM) of HYP-PDT (Sanovic et al., 2009). However, they also reported on possible indications of apoptosis genes being upregulated such as ERK and RAS and perinuclear localization of HYP; when cells were treated with a higher dose (200ng/ml) of HYP-PDT; incorporating a longer HYP uptake time (16hrs) (Sanovic et al., 2009). Another study that used a different SCC cell line (SQ2) showed that these cells experienced a G2-M cell cycle arrest as a result of heat shock protein 90 and 70 ubiquitination, after treatment with HYP in the dark (Blank et al., 2003).

Our group reported on a novel “double hit/day strategy” approach by treating human SCC cells with multiple, consecutive HYP-PDT doses, which resulted in rapid necrotic cell death (Sharma & Davids, 2012). In corroboration, Gyenge et al. 2012, recently reported a 30% increase in apoptosis and increased ROS levels in UMB-SCC745 and UMB-SCC969 (head and neck SCC cells) were observed 3 hours post HYP-PDT (Gyenge et al., 2012). Furthermore, in a different study by the same group, 96% cell death was

observed at a dose of 2.5µg/ml HYP (5hr incubation) which was activated with white light (Gyenge, Emina et al., 2013). Interestingly, they also showed that the cytotoxicity of HYP alone was higher than when cells were treated with a 1:1 mixture of HYP and the photosensitiser mTHPC (Gyenge, Emina et al., 2013).

With regards to melanoma cells, our group has investigated the effect of HYP-PDT and established an effective "killing does" of 3µM HYP which was activated with UVA (Lester M Davids et al., 2008). Interestingly, HYP-PDT induced different cytotoxic responses in pigmented UCT Mel-1 and unpigmented UCT Mel-3 cells: UCT Mel-3 cells underwent apoptosis and UCT Mel-1 cells underwent necrosis with the pigmented UCT Mel-1 cells being less susceptible to HYP-PDT than the unpigmented UCT Mel-3 cells (Lester M Davids et al., 2008). This supported the hypothesis stipulated by Hadjur et al. 1996, that melanin present in pigmented (melanotic) melanoma cells may play a role in melanoma cell response to HYP-PDT (Hadjur et al., 1996).

Furthermore, our laboratory did two follow up studies which involved depigmenting pigmented UCT mel1 cells with tyrosinase inhibitors (block melanogenesis pathway) kojic acid and phenylthiourea; preceding HYP-PDT treatment that rendered the pigmented UCT Mel-1 cells more sensitive to HYP-PDT, similarly to unpigmented A375 melanoma cells (Sharma et al., 2011; Sharma, Davids, & Krishna V. Sharma and Lester M.Davids, 2012). Lastly, using electron microscopy, our group also established that an initial autophagic response is induced in both unpigmented and pigmented human melanoma cells, 4 hours post treatment with 3µM HYP-PDT (Davids et al. 2009).

Another interesting approach used pulsed laser therapy as the light modality of HYP-PDT by testing different light wavelengths (514nm – 593nm) and using different exposure times (5-120s) to activate a range of HYP (0.1-2mM) concentrations in order to suggest a LD_{50} dose of light and HYP for SNU-1 SCC cells (Bublik et al., 2006). Several different laser settings were

effective in activating HYP to achieve LD_{50} of SNU-1 cells (Bublik et al., 2006).

Further *in vitro* studies are needed to elucidate the cellular mechanisms induced by HYP-PDT in human skin cancer cells, in order to fully understand the mechanism of action of HYP-PDT in this system.

1.10. HYP-PDT and *In Vivo* Skin Cancer Studies

To date, few *in vivo* studies have been published on HYP- PDT (A Boiy, Roelandts, & de Witte, 2011; A Boiy, Roelandts, van den Oord, & de Witte, 2008; Annelies Boiy, Roelandts, & de Witte, 2007; Head, Luu, Sercarz, & Saxton, 2006). One group tested a range of HYP does (0.1- 10µg/ml) and different wavelengths of light on SNU 1 (SCC) cells before intralesionally injecting these cells into nude mice and allowing the tumors to grow over a period of 6-8 weeks (Head et al., 2006). HYP-PDT resulted in regression of tumors which were originally smaller than $0.4cm^2$ but PDT was ineffective in the treatment of larger tumors (Head et al., 2006). Another group investigated topical application of 0.1% HYP on mice skin and suggested that 24 hours is needed for homogenous HYP distribution in UVR induced skin tumors in mice and that HYP tissue penetration can be improved using lipid carriers and esterification of HYP (A Boiy et al., 2008; Annelies Boiy et al., 2007).

Two clinical studies have been carried out investigating HYP-PDT and non-melanoma skin cancer (Alecu et al., 1998; Kacerovská, Pizinger, Majer, & Smíd, 2008). Alecu et al, 1998, stipulated that HYP-PDT targeted tumors selectively as no necrosis or tissue damage was observed in surrounding tissue but the effectiveness of HYP-PDT was dose dependent with higher doses almost completely eradicating tumors with a favorable cosmetic outcome (Alecu et al., 1998). This study included 8 SCC and 11 BCC patients and HYP was administered intralesionaly to SCC patients (40-100mg) 3-5 times during 2-4 weeks and to BCC patients (40-200mg) 3-5

times during 2-6 weeks therefore, not only the dose of HYP but also the frequency and duration of HYP-PDT affected the outcome (Alecu et al., 1998). However, another treatment protocol was used by Kacerovska et al. 2008, to treat 8 actinic keratosis patients, 21 BCC patients and 5 Bowmen's disease (SCC) patients: HYP (2mg/ml) was administered topically (10mm thick onto lesion) for 2 hours and activated with red light (75 J/cm^2); which was carried out once each week, for 6 weeks (Kacerovská et al., 2008). Promising results suggested that 50% of actinic keratosis patients; 28 % of BCC patients and 40% of Bowman's disease patients had successful outcome post HYP-PDT with the histological analysis showing complete eradication of 11% of the BCC and 40% of the bowmen's disease lesions (Kacerovská et al., 2008).

The discrepancies between treatment protocols in these two studies are evident as there is currently no standardized regime for clinical HYP-PDT for the treatment of skin cancers. Furthermore, *in vivo* PDT is influenced by several factors such as the method of HYP administration, the irradiation protocol, the type of tumor and the oxygenation levels in the tumor (Agostinis et al., 2011, 2002). However, both studies showed some promising results that support HYP-PDT as a potential treatment option for NMSC despite more clinical trials with increased patient sample sizes, being required. To our knowledge, no clinical trials have been conducted to investigate HYP-PDT for the treatment of melanoma.

1.11. The Bystander Effect of HYP-PDT on Normal Cells

A bystander effect, defined as indirect damaged induced into adjacent cells either via intercellular gap junctions or via diffusible ROS released in the microenvironment, has been shown to occur during PDT (Dahle, Kaalhus, Moan, & Steen, 1997; Dahle, 2000). It is well know that cancer therapies have bystander effects on normal cells in the body which often cause undesirable side effects (De Angelis, 2008; Ehmann, Heinemann, & Wollenberg, 2011; Langer et al., 1989). As PDT has been shown to be

effective through topical administration to treat skin cancers, it is important to know what its effect, if any, is on the normal cells population surrounding the NMSC or Melanoma.

Till now, very few studies have investigated the effect of HYP-PDT on normal skin cells. To our knowledge, us and a few other *in vitro* studies have been the only groups that have investigated the effect of HYP-PDT on normal human skin cells (Bernd et al., 1999; Lester M Davids et al., 2008; Hadjur, Richard, Parat, Favier, & Jardon, 1995; Kashef, Borghei, & Djavid, 2013; Rezusta et al., 2012; Traynor et al., 2005). However, most of these studies used immortalized cell lines such as the HaCaT immortalized keratinocyte cell line (Bernd et al., 1999; Lester M Davids et al., 2008; Rezusta et al., 2012); MRC5 immortalized fibroblast cell line (Hadjur et al., 1995) and Hermes 4 immortalized melanocyte cell line (Lester M Davids et al., 2008). Furthermore, 2 of these studies investigated the effects of HYP-PDT on primary human fibroblasts (Kashef et al., 2013; Rezusta et al., 2012) but these concentrated on the effect of HYP-PDT as an antimicrobial agent.

The novelty of this study is therefore the *in vitro* investigation into the effects of HYP-PDT on normal human skin cells representing both the epidermal (melanocytes and keratinocytes) and dermal (fibroblasts) components of the skin. These in turn, provide insight into the reaction of these potential cells in the tumor microenvironment.

1.12. Aims

1) To optimize tissue culture of primary human keratinocyte (Kc), melanocytes (Mc), and fibroblasts (Fb) from neonatal foreskins.
2) To determine the effects of HYP-PDT on the cell viability of primary human skin cells.

3) To evaluate intracellular ROS production post HYP-PDT in primary human skin cells.
4) To assess the effects of HYP-PDT on cell morphology of primary human skin cells.
5) To analyze apoptosis in primary human skin cells post HYP-PDT.

Chapter 2: Materials and Methods

2.1. In Vitro Human Skin Cell Culture Model

2.1.1. Isolation of Primary Human Skin Cells

Primary human skin cells were isolated from human neonatal, adult foreskins and human tissue obtained from plastic and reconstructive surgeries via full consent and approval by our institutional board (REC REF 493/2009). Briefly, skin tissue was collected in Dulbecco's Modified Eagles Medium (DMEM) (Highveld Biological, South Africa; Appendix A) supplemented with antibiotics (100 U/ml penicillin / 100µg/ml streptomycin; Appendix A) (Sigma- Aldrich: P3032/S91370) and stored at 4ºC. Skin tissue was cut into smaller pieces (5mm X 2.5mm) and sub-merged in 5mg/ml of dispase solution (Sigma-Aldrich: D4693) overnight at 4ºC. The epidermis was then separated from the dermis according to standard protocols (Appendix A).

Primary human melanocytes (Mc) and keratinocytes (Kc) were further isolated from the epidermis by incubating the smaller epidermal samples in trypsin supplemented with 0.1% glucose (Appendix A) in a 37ºC water bath for 15 minutes. This suspension was triturated every 5 minutes to disaggregate the tissue into a cellular suspension. The suspension was then filtered through a 70µm Whatman filter (BD BioSciences, USA). To exclude tissue debris, the cell suspension was pelleted at 3000 rpm for 5 minutes at room temperature. The pellet was then resuspended in complete cell-specific (Mc or Kc) media (section 2.1.2); depending on whether Mc or Kc were the desired cell type. The settled cells were denoted passage 0 and fresh specific complete medium was added to the cells once they had adhered overnight.

Primary human fibroblasts (Fb) were isolated from dermal samples by placing the whole tissue piece underneath a glass coverslip (Marienfeld Laboratory Glassware, Germany) in a 35mm tissue culture dish (Greiner Bio-

one, Germany); containing complete cell-specific medium (section 2.1.2). Thereafter, Fb spontaneously migrated away from the fixed tissue onto the tissue culture dish. After 10 days, the glass coverslip was removed and the settled Fb were denoted as passage 0. Mc, Kc and Fb were cultured for 2-3 weeks to obtain pure cell populations.

2.1.2. Tissue Culture Conditions

Fb, Mc and Kc were cultured in different cell specific complete media in a tissue culture incubator (MCO-175M, Sanyo, United Scientific, South Africa) at 37 ºC in a humidified atmosphere with 5% CO_2. Fb were cultured in DMEM (Highveld Biological, South Africa) (Appendix A) supplemented with 10% (v/v) heat inactivated fetal bovine serum (FCS) (Highveld Biological; Appendix A) and antibiotics (100 U/ml penicillin / 100µg/ml streptomycin; Appendix A) (Sigma- Aldrich: P3032/S91370). Mc were cultured in Mc specific medium (FETI) (Appendix A). Kc were cultured in Kc specific medium (KSFM) (Gibco®, Life technologies, United Kingdom) supplemented with: 25mg bovine pituitary extract (BPE); 2.5µg epidermal growth factor (EGF) and antibiotics (Appendix A) (Gibco®, Life Technologies: 17005034; 130 28-014; 10450 013, United Kingdom). However, when Kc were cultured for periods exceeding passage 3 and during experiments, they were maintained in a different Kc-specific medium called GREENS (Appendix A).

Trypsin/EDTA (Appendix A) was used to lift adherent Fb and Mc whereas commercial TrypLE™ Express (Gibco®, Life Technologies, United Kingdom) or commercial trypsin/EDTA (Gibco®, Life Technologies, United Kingdom) were used to lift adherent Kc from tissue culture dishes. Additionally, FCS (included in complete medium) was used as a trypsin inhibitor, when lifting cells from tissue culture dishes. Cultured primary human skin cells used in all experiments did not exceed passage 12 and cells were viewed frequently under a bright field microscope (Olympus Microscope Model CK2, Olympus

Microscopes). Routine weekly mycoplasma tests were employed with Hoechst nuclear dye (Appendix A) to maintain sterility in all cultures. Cells were often pooled from different dishes and patients in order to obtain enough cells for an experiment (one biological repeat).

2.1.3. Growth Curves

Growth curves were conducted over a period of 7 days using: Fb, Mc and Kc to establish the seeding efficiency of these cells and to investigate their growth dynamics. Fifty thousand ($5x10^4$) Fb and Mc and $1.5x10^5$ Kc were seeded in triplicate in 35mm cell culture dishes (Greiner-Bio One, Germany) in cell-specific complete medium. The day on which cells were seeded was designated as day 0 and Mc were counted manually on days: 1, 3, 5 and 7 and Kc were counted on days: 2; 3; 5 and 7 using a haemocytometer (Neubauer improved, Marienfeld Laboratory Glassware, Germany). This experiment included 3 technical repeats, within each biological repeat and included 3 biological repeats (n=3).

2.2. Photodynamic Therapy (PDT)

2.2.1. Hypericin Preparation

Hypericin (HYP) extract from the species *Hypericum perforatum L.* (Sigma-Aldrich: 56690, 99% purity) was prepared in 1ml of 100% dimethyl sulfoxide (DMSO) (Merck: 8.02912.1000) to obtain a 2mM stock solution (Appendix A), which was further stored in 20µl aliquots at –80ºC. A 20µM working stock was freshly prepared in phosphate-buffered saline (1xPBS) which was further diluted in complete media to attain the required concentrations during all PDT experiments. All experiments involving HYP were carried out under subdued light conditions due to the light-sensitivity of HYP.

2.2.2. *Laser Light Activation*

HYP was activated with a yellow/green light emitted from a diode pumped, solid state, continuous wave, tunable laser that emits a light beam of exactly 561nm; which is delivered via a fibre optic cable. This laser was obtained via a grant from the National Laser Centre at the Centre for Scientific and Industrial Research (NLC-LREHGOO-CON-001). The power and fluence of the light dose were kept constant at 20mW and 5J/cm^2 respectively, for all experiments involving laser light to activate hypericin. The irradiation time was calculated using the following equation:

Equation 2.1: Laser Irradiation Time

Time (s) = Fluence (J/cm^2) / Power density= (W/cm^2)
*power density = fluence rate (W/cm^2)

The irradiation time used in our experimental set up was dependent on the area of the bottom of the well or dish which was being irradiated (Table: 2.21). The size of the laser-light beam was adjusted, using the aperture connected to the light-emitting fibre optic cable, to the exact area of the bottom of the well or dish used in different experiments. Therefore, light refraction from the sides of the well or dish did not need to be accounted for when calculating the light dose. Dark (unirradiated) controls were covered with foil at all times and were not exposed to the laser light.

Table 2.2.1: Laser parameters Used to Calculate Irradiating Time of Tissue Culture Dishes during HYP-PDT Treatment Protocol

Dish/ well size	**Diameter (cm)**	**Area (cm^2)**	**Fluence (J/cm^2)**	**Power (W)**	**Fluence rate/power density (W/cm^2)**	**Calculation using equation 1**	**Irradiation time**
1well /96 well plate	0.5	0.196	5	0.02	0.02/ 0.196	5/ (0.02/0.196)	49s
35mm dish	3.5	9.621	5	0.02	0.02/9.621	5/ (0.02/9.621)	2405s = 40mins
1 well /24 well plate	1.5	1.767	5	0.02	0.02/1.767	5/ (0.021/1.767)	421s =7mins

2.2.3. Hypericin Induced Photodynamic Therapy (HYP-PDT)

HYP-PDT involved treating primary human skin cells with hypericin (HYP) and laser light. Briefly, cells were incubated for 4 hours at 37ºC in a 5% CO_2 humidified tissue culture incubator (MCO-175M, Sanyo. United Scientific, South Africa) with various doses of HYP (0.5μM - 4 μM), in cell-specific complete media (Appendix A). Following the incubation period, cells were

rinsed twice with 1xPBS (Appendix A) and irradiated in 1xPBS. Irradiation time was dependent on the size of the well or dish (Table 2.2.1).

The following controls were included in all experiments:

- Untreated control: cells were not treated with HYP or light (C)
- Vehicle dark control: cells treated with 0.15% DMSO only (VC)
- Dark HYP controls: cells treated with HYP only (H)
- Light only control: cells treated with light only (L)
- Vehicle light control: cells treated with 0.15% DMSO and light (VL)
- HYP-PDT: cells treated with HYP and activated with light (H+L)

Post-irradiation, the wells were replenished with fresh medium. As HYP is sensitive to auto-oxidation, all experiments involving HYP-PDT were: carried out in subdued light conditions, all dark and untreated controls were plated in a separate unirradiated plate or dish and plates/dishes were covered with foil at all times.

2.3. Cell Viability Assay

Cell viability of Fb, Mc and Kc was assessed 24 hours post-HYP-PDT treatment; using the XTT metabolic-based viability assay (Cell proliferation kit II (XTT); Roche: 11465015001). Briefly, the cells were seeded in triplicate in 2 separate 96 well plates (TRP®, Switzerland: 92096) in 200µl of cell specific complete media. In order to obtain 80% confluency, $2x10^4$ Fb and $7x10^4$ Mc and Kc were seeded per well and allowed to adhere overnight. The following day, cells were treated with a range of HYP doses (0.5µM; 1µM; 2µM; 3µM; 4µM) as described in (section 2.2). Twenty four hours (24hrs) post HYP-PDT treatment, cell viability was assessed. The basis of the cell viability assay is the cleavage of the XTT tetrazolium salt by mitochondrial dehyrogenases to yield an orange formazan product. Thus, only metabolically active cells will induce a colorimetric change that is detected at an absorbance of 450nm. Following the kit's protocol, the final reading was done using an ELSIA plate

reader (VERSAmax^{TM} tunable microplate reader, Molecular Devices). In order to account for technical or pipetting error within an experiment, 3 technical repeats were included in each biological repeat. This experiment comprised 3 biological repeats (n=3).

2.4. Reactive Oxygen Species (ROS) Assay

A fluorescent-based ROS assay was used to detect intracellular ROS immediately after HYP-PDT treatment. This assay involved exposing the cells to the cell permeable non-fluorescent probe 2', 7'– dichlorofluorescein diacetate (DCF-DA), which upon oxidation by intracellular esterases in the presence of intracellular ROS, is cleaved to yield the fluorescent product dichlorofluorescein (DCF). Intracellular ROS is therefore indirectly measured by intracellular DCF fluorescence. Twenty thousand Fb ($2x10^4$) and $7x10^4$ Mc and Kc were seeded per well, in triplicate, in 200µl of cell specific complete medium, in 2 separate 96 well white plates (Greiner Bio- One: 655083, Germany). Once the cells had adhered overnight, Fb and Mc were both treated with 1µM and 3µM HYP- PDT and Kc were treated with 3µM and 4µM HYP- PDT according to the protocol described in section 2.2.

Immediately after HYP-PDT, 5µM of DCF-DA (Sigma-Aldrich: 35845) (Appendix A), prepared in cell specific complete medium, was added to each well (100µl). Following a 20 minute incubation at 37ºC, the DCF- DA containing medium was removed and the cells were washed twice with 100µl of 1xPBS (Appendix A) and fresh 1xPBS (100µl) was added to each well. The fluorescence was then measured using a fluorimeter (Cary Eclipse e104043731) at an excitation wavelength of 488nm and an emission wavelength of 535nm. The blank reading (1xPBS only) was deducted from each recorded value preceding data analysis. This experiment was conducted under subdued light conditions (section 2.2) and every biological repeat included 3 technical repeats. However, there were 3 biological

repeats for the Fb (n=3) and Kc (n=3) but 4 biological repeats were conducted using the Mc (n=4).

2.5. Cell Morphology Analysis

Cellular morphology of Fb, Mc and Kc was assessed 24 hours post HYP-PDT with phase and fluorescent microscopy. One hundred thousand ($1x10^5$) Fb and Mc and $1.5x10^5$ Kc were seeded directly onto glass coverslips (Marienfeld Laboratory Glassware, Germany) in 35mm tissue culture dishes (Greiner Bio- One, Germany) in 400µl of complete cell specific medium. Cells adhered to the glass coverslip in a drop of medium through surface tension overnight. Complete cell specific medium (1.6ml) was added to each 35mmm dish on the following day. Cells were then cultured from 2-7 days according to tissue culture conditions described in section 2.1.1, in order to achieve 80% confluency on the glass coverslips (Marienfeld, Germany). Cells were then subjected to HYP- PDT treatment using a dose of 1µM and 3µM HYP according to the protocol described in (section 2.2).

Twenty four hours post HYP-PDT treatment, 1µg/ml of Hoechst Live 33342 (Invitrogen, Molecular Probes: H1399) nuclear dye was added directly to the recovery medium for 20 minutes. After washing twice with 1xPBS (Appendix A) the cells were fixed with 4% paraformaldehyde (PFA) (Appendix A) for 20 minutes and mounted on glass slides (Marienfeld, Germany) with 50µl of mowiol (Appendix A) containing an anti-fade compound (N-propyl gallate) (Sigma- Aldrich, 204-498-2). Phase contrast images and their complementary multi-acquisition fluorescent images were acquired using the Zeis Axiovert 200M inverted fluorescent microscope (20X and 40X objectives).

The DAPI channel was used to view Hoechst Live, blue nuclear stain and the Cy3 channel to view HYP; as HYP has an inherent red fluorescence. The

camera exposure time was set according to the HYP- PDT treated cells viewed in the Cy3 channel because HYP yields an even brighter fluorescence upon light illumination, thereby minimizing HYP background fluorescence. Two biological repeats (n=2) were performed for this experiment using each cell type.

2.6. Apoptosis Analysis

Fluorescent activated cell sorting (FACS) was employed to determine early stage apoptosis and plasma cell membrane integrity 24 hours post HYP-PDT treatment. The two fluorophores that were used were Annexin V-FITC and propidium iodide (PI). Annexin V-FITC (green fluorophore) binds to phosphatidylserines, residing intracellularly on the plasma cell membrane, which become externalized at the onset of apoptosis. Annexin V-FITC bound to externalized phosphatidylserines fluoresces green and can be detected using FACS. PI is an intercalating agent and a red dye (red fluorophore) that is excluded from viable cells due to their intact plasma cell membranes. Cells therefore with compromised plasma cell membranes internalize the dye, making it a direct measure of plasma cell membrane integrity which can be correlated to cell viability or cell death.

One hundred thousand ($1x10^5$) Fb and Mc and $1.5x10^5$ Kc were seeded per well in a 24 well plate (Greiner Bio-one) in duplicate, in cell specific medium. Cells were cultured for 2-7 days as stipulated in (2.1.2) to achieve 80% confluency. Cells were then treated with 3μM HYP-PDT according to the protocol described in (2.2). Twenty four hours (24hrs) post HYP-PDT treatment, cells were processed for FACS analysis. This involved harvesting all cells, i.e. from the recovery medium and those adherent to the dish, with (trypsin/EDTA) (Appendix A) and centrifuging at 1000 rpm for 10 minutes to obtain cell pellets. The cells from duplicate wells were pooled in order to obtain sufficient cells (10 000 cells/events) per sample. The cell pellets were

re-suspended in 1ml of ice cold 1xPBS (Appendix A) and further centrifuged at 3000 rpm for 5 minutes. The pellets were then re-suspended in 300µl of Annexin V-FITC binding buffer (Appendix A) and placed in FACS tubes (BD Falcon, Biosciences, USA).

Four microliters (4µl) of Annexin V-FITC working solution (BD Biosciences USA: 556420) and 10µl of PI (50µg/ml) (Roche, Germany) (Appendix A) were added directly to the cells in Annexin V binding buffer. FACS sample processing was carried out in subdued light conditions. The samples were allowed to stand at room temperature for 15 minutes before FACS was carried out using the FACSAria 1 cell sorting machine (BD Biosciences, USA). All controls discussed in section 2.2, were included in this experiment and fluorophores were tested by adding Annexin V-FITC and PI separately to HYP-PDT treated cells. FACS data was analyzed using FlowJo Software Version 10.0.7.0. Three technical repeats were included in each biological repeat. Using each cell type, 3 biological repeats were conducted during this experiment (n=3).

Furthermore, prior to carrying out the above FACS cell death analysis experiment, we tested whether we could use PI in combination with HYP during FACS experiment because both HYP and PI are fluorophores which emit a red fluorescence. However, several studies had used PI when analyzing cell death induced by HYP-PDT *in vitro* (Du, Li, Olivo, Yip, & Bay, 2006; Huntosova et al., 2012; Kleban et al., 2006; Seitz et al., 2008). Therefore, Fb, Mc and Kc were treated with either HYP-PDT (no PI added) or stressed with 70% ethanol before adding PI. Interestingly, the FACSAria 1 cell sorting machine used could detect several red fluorophores in 4 different channels: PerCp-Cy5; Texas Red; APC and PE-A. HYP and PI showed a strong fluorescent signal in the form of a histogram peak in the: PerCp-Cy5; Texas Red and APC channels.

PI showed a strong positive fluorescence signal in the PE-A channel but HYP exhibited a minimal signal in the PE-A channel (Figure 2.6.1) as the number of positive events in the PE-A channel for HYP-PDT treated Fb, Mc and Kc was: 15.1%; 6.09% and 34% respective (Figure 2.6.1). However, the percentage of HYP negative events in the PE-A channel was significantly higher in: Fb (84.9%); Mc (93.9%) and Kc (66%). This suggested that HYP does not exude significant fluorescence in the PE-A channel which is also justified by the fluorescence emission peak of HYP (600-640nm) not corresponding to the emission peak of the PE–A channel (667nm). Furthermore, the mean fluorescent intensity of PI in the PE-A channel was measured (Table 2.6.1) as: 12.9; 3.1 and 16.1 fold higher than HYP mean fluorescent intensities in the PEA channel in Fb, Mc and Kc respectively (Table 2.6.1).

Therefore, we established that PI fluorescence intensity can be recorded using the PE-A channel due to the minimal overlap of HYP and PI red fluorescence in this channel and that we can indeed use PI to sort HYP-PDT treated cells that have compromised cell membranes.

A)

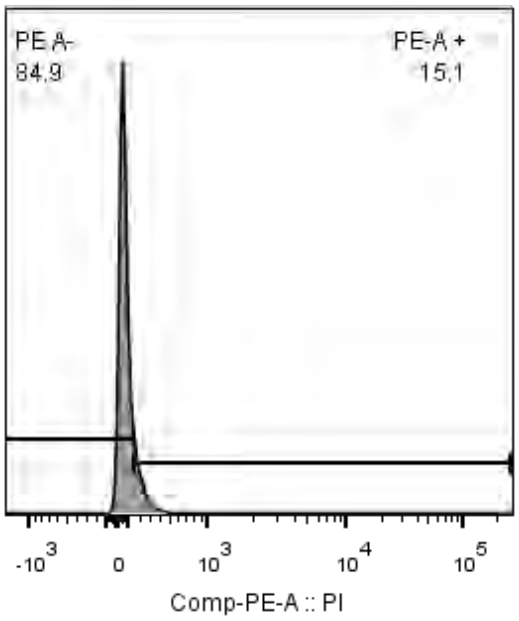
PE A-
84.9
PE-A +
15.1
-10^3
0
10^3
10^4
10^5
Comp-PE-A :: PI

B)

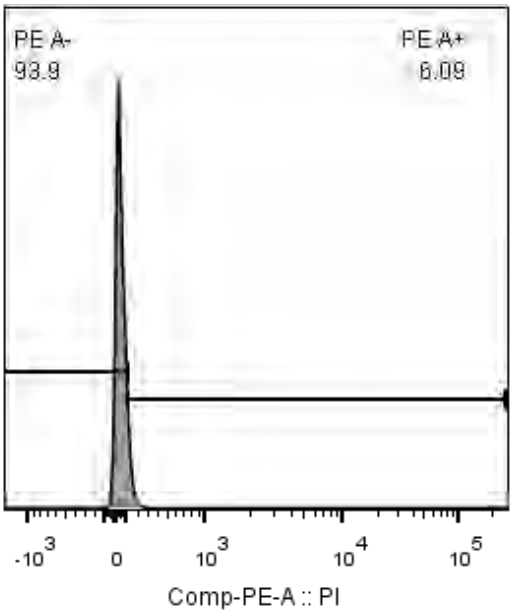
PE A-
93.9
PE A+
6.09
-10^3
0
10^3
10^4
10^5
Comp-PE-A :: PI

C)

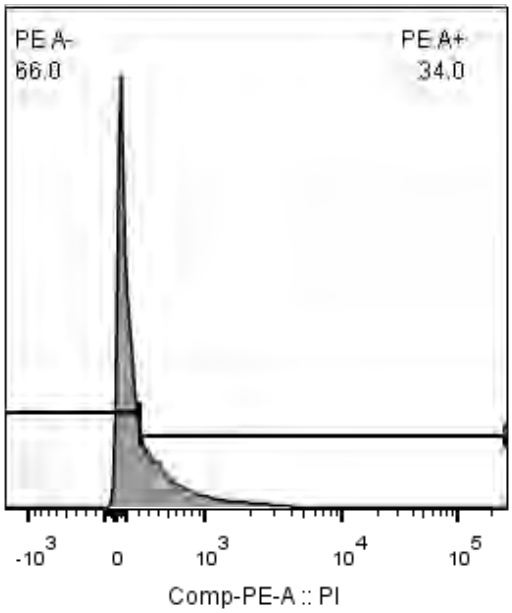
PE A-
66.0
PE A+
34.0
-10^3
0
10^3
10^4
10^5
Comp-PE-A :: PI

Figure 2.6.1: Percentage of positive and negative events in the PE-A (red) channel of HYP-PDT treated Fb (A); Mc (B) and Kc (C) represented as a histogram

Table 2.6.1: Mean Fluorescent Intensities of the PE-A (red) Channel

	Fb	Mc	Kc
PI Treated	597	71.9	1798
HYP Treated	46.2	23.1	112
Ratio: PI/ HYP	12.9	3.1	16.1
PI - HYP	550.8	48.8	1686

2.7. Data Analysis

Graphpad Prism (Version 5, Graphpad Software Inc.) was employed for data analysis of raw data. Raw data was normalized taking into account the mean and standard error mean (mean± SEM) and statistical differences were elicited using a one way ANOVA and Dunnet multiple comparison post-test. A One way ANOVA with Bonferroni post-tests was used to compare groups of data sets when comparing different cell types to each other. P-values less than: 0.05; 0.01 and 0.001 indicated significantly different values.

2.8. Methods Summary

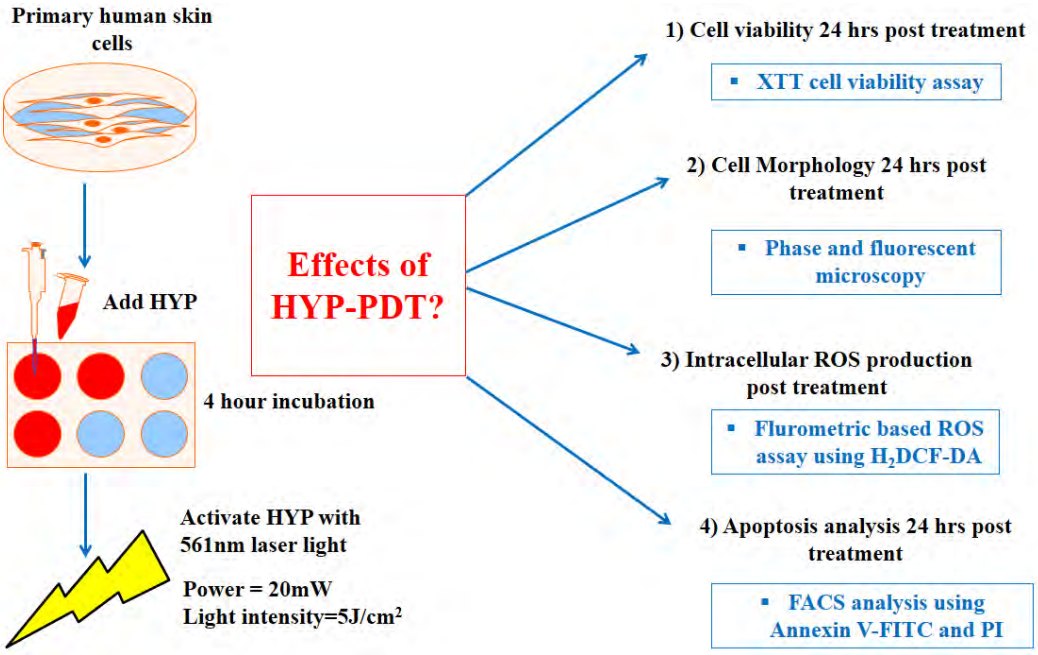

Chapter 3: Results

3.1 Growth Dynamics of Primary Human Skin Cells

In order to establish the growth dynamics of pure primary human keratinocyte (Kc), fibroblast (Fb) and melanocyte (Mc) monocultures, growth curves were performed over a period of 7 days. Once pure cultures had been obtained (See Section 2.1.1), $5x10^4$ Fb and Mc were seeded on Day 0 and counted on days: 1; 3; 5 and 7. Kc ($1.5x10^5$) were seeded on Day 0 and counted on days: 2; 3; 5 and 7.

Kc exhibited a poor seeding efficiency of 58% as $1.5x10^5$ cells were seeded on day 0 which reduced to $8.7x10^4$ cells on day 2 (Figure 3.1.1). However, the Kc grew at an improved rate (Figure 3.1.1) and grew exponentially from day 3 ($2.57x10^5$ cells) through today 7 ($7.27x10^5$ cells). In contrast, both Fb and Mc seeded well yielding a seeding efficiency of 100% ($5x10^4$) and 72% ($3.6x10^4$), respectively. Both cell types adopted a similar growth profile over 7 days (Figure 3.1.1) exhibiting cell numbers of $8.4x10^4$; $2.22x10^5$; $2.38x10^5$ Fb and $5.3x10^4$; $1.33x10^5$; $1.86x10^5$ Mc on days 3; 5 and 7, respectively (Figure 3.1.1). Therefore both Mc and Fb demonstrated a short lag phase followed by an exponential phase that proceeded to plateau from day 5 onwards (Figure 3.1.1). This occurred as a result of contact inhibition as Fb and Mc were vey confluent (>80%) when 35mm dishes were viewed with light microscopy.

The doubling time (Table 3.1.1), which is the time taken for cells to double in number during the exponential growth phase, was estimated visually from the graph for each skin cell type. The doubling time for Kc, Mc and Fb was ±2; ±3 and ±1.5 days, respectively (Table 3.1.1). Seeing that the doubling is indicative of cell proliferation, as cells with a smaller doubling time a higher growth rate; Fb had the fastest growth rate compared to Mc and Kc (Table 3.1.1). However, Kc had a slower growth rate than Fb but a faster growth rate

than Mc (Figure 3.1.1). Mc had the slowest growth rate compared to both Fb and Kc (Table 3.1.1).

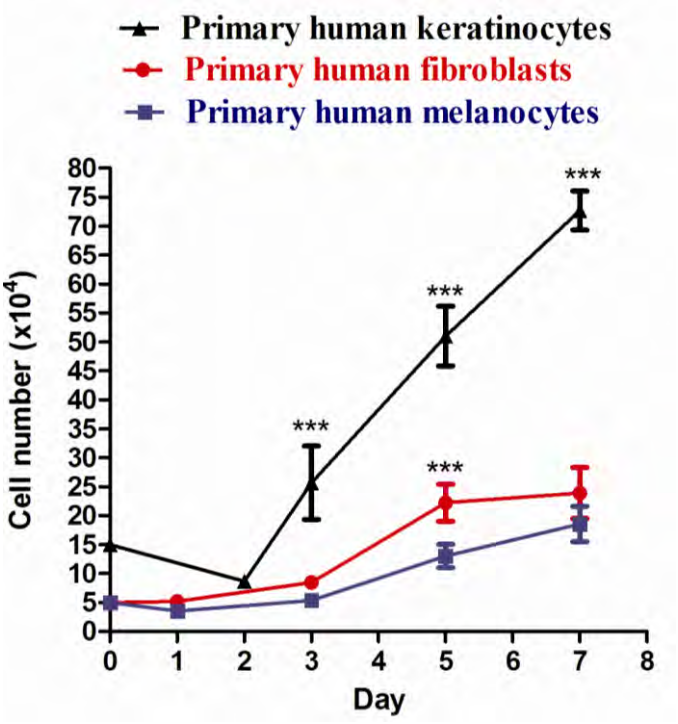

Figure 3.1.1: Growth curves of primary human skin cells over a period of 7 days. Doubling time of Kc, Fb and Mc: ± 2 days; ± 1.5 days and ± 3 days, respectively. (* = $p < 0.001$) (Mean; SEM) (n=3)**

Table.3.1. 1 Characteristics of Different Primary Human Skin Cells

Cell Type	Phase Contrast Image	Morphology	Doubling Time (Days)
Kc	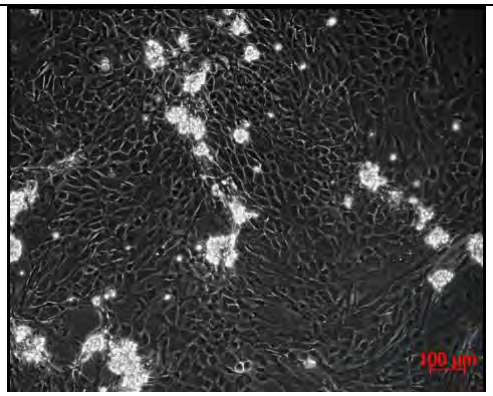	Large, tightly packed, cobblestone shaped	± 2
Mc	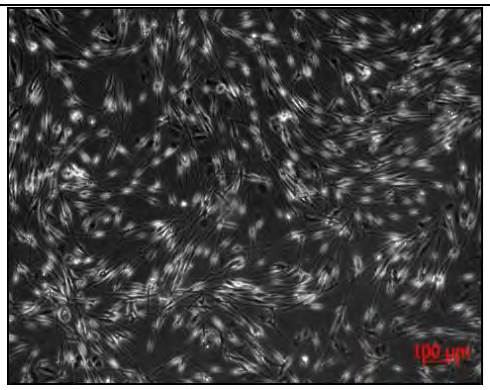	Small, round, bipolar dendrites	± 3
Fb	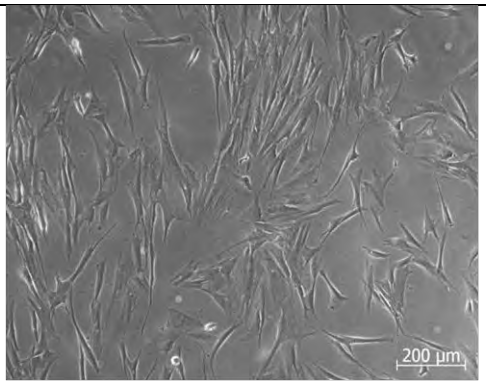	Spindle shaped	± 1.5

3.2 Cell Viability 24 Hours Post HYP-PDT

Having established the seeding efficiencies and growth dynamics of primary human skin cells, we investigated the effects of hypericin induced PDT (HYP-PDT) on cell viability. The XTT cell viability assay (Roche) was carried out 24 hours post-treatment.

Fb, Mc and Kc were treated with a range of HYP concentrations (0.25μM; 0.5μM 1μM; 2μM; 3μM; 4μM) in the dark which displayed no significant effect on cell viability in any of the 3 cell types compared to the vehicle control (Figure 3.2.1 A1; B1; C1; D); thus showing that HYP does not have a cytotoxic effect in the dark in these skin cells. However, activated HYP-PDT induced a dose-dependent response in Fb (Figure 3.2.1 A2; D) and a significant difference ($p<0.001$) in cell viability compared to the vehicle control, following different doses of HYP-PDT: 1μM (56%); 2μM (48%); 3μM (33%) and 4μM (34%). The LD_{50} is indicative of sensitivity to a drug/treatment with a smaller LD_{50} indicating a greater susceptibility to a treatment/drug. The LD_{50} for HYP-PDT treated Fb occurred at 1.75μM HYP-PDT (Figure 3.2.1 A2; D).

In Mc, (Figure 3.2.1 B2; D), HYP-PDT induced a significant difference in cell viability compared to the vehicle control following doses: 2μM (60%) ($p< 0.05$); 3μM (61%) ($p< 0.05$); 4μM (38%) ($p< 0.001$) HYP-PDT (Figure 3.2.1 B2; D). Interestingly, the LD_{50} for Mc occurred at 3.5μM HYP-PDT; which is a higher dose than the dose required to reach the LD_{50} for Fb. HYP-PDT induced an initial significant difference ($p< 0.05$) in cell viability (79%) in Kc at a dose of 4μM HYP-PDT (Figure 3.2.1 C1; D). Since 4μM HYP-PDT was the highest dose with which human skin cells were treated, the LD_{50} for Kc occurs at a greater dose than 4μM HYP-PDT; making Kc the least susceptible skin cells to HYP-PDT.

Furthermore, these different cytotoxic profiles were confirmed statistically (Figure 3.2.1 D) as the cell viability of Fb and Kc was significantly different at: 1μM ($p< 0.05$); 2μM ($p<0.05$); 3μM ($p< 0.001$) and 4μM ($p< 0.01$) HYP-PDT. Furthermore, a significant difference between Mc and Kc occurred at a dose of 4μM ($p<0.05$) HYP-PDT (Figure 3.2.1 D). Therefore, HYP-PDT induces different cell viability effects in different human skin cells: Fb being the most susceptible, Kc being the least susceptible and the Mc being more susceptible than Kc but less sesceptiable than Fb 24 hours post HYP-PDT.

A1)

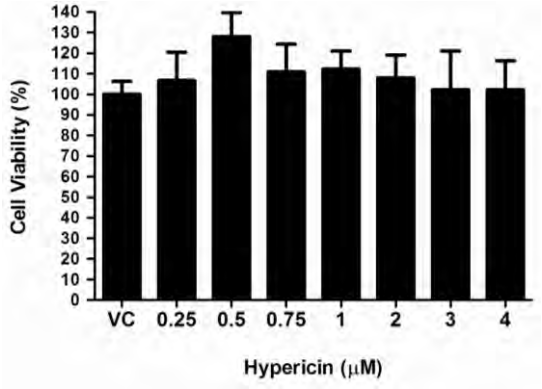

A2)

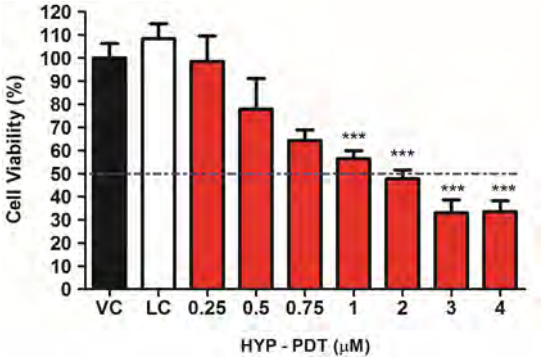

B1)

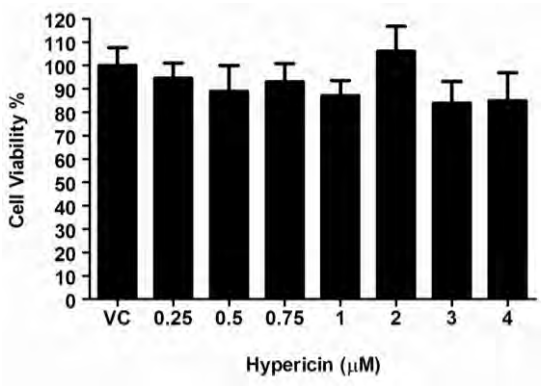

B2)

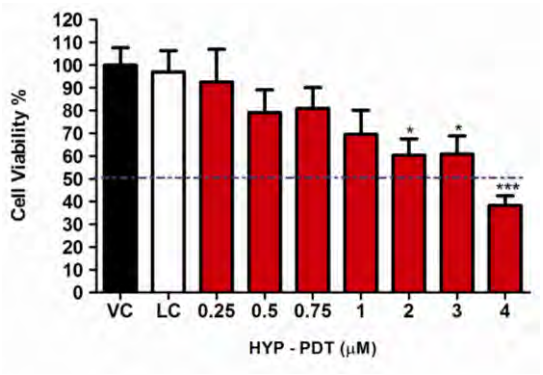

C1)

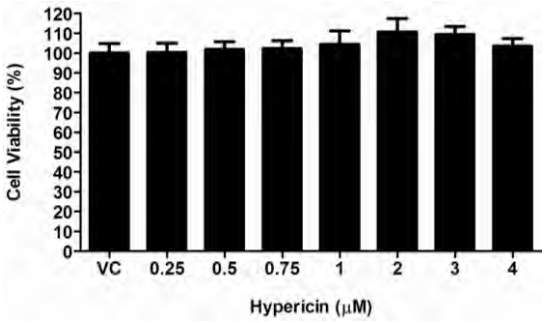

C2)

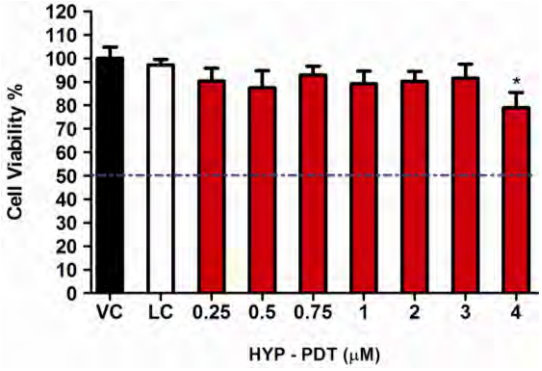

D)

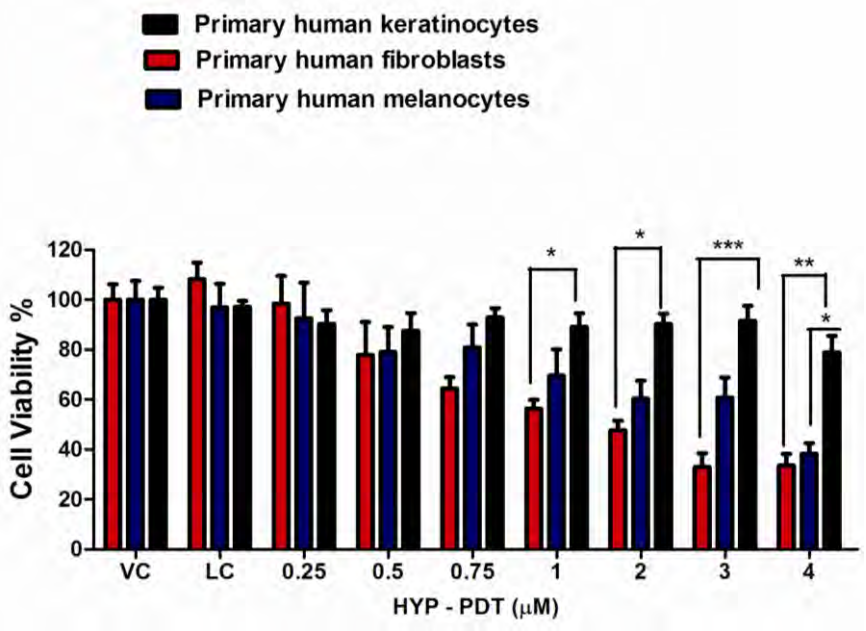

Figure 3.2.1: Cell viability assessed using the XTT cell viability assay at 24 hours in: Fb treated with HYP and no light (A1); Fb treated with HYP-PDT (A2); Mc treated with HYP and no light (B1); Mc treated with HYP-PDT (B2); Kc treated with HYP and no light (C1); Kc treated with HYP-PDT (C2) and skin cells (all types) treated with HYP-PDT (D). VC= vehicle control. LC= light control.
LD_{50} = dotted blue line. (*=p < 0.05; **= p < 0.01; ***= p < 0.001) (Mean; SEM) (n=3).

3.3 Cell Morphology 24 Hours Post HYP- PDT

Once the cytotoxic profiles of primary human skin cells in response to HYP-PDT had been established, we were interested in the effects of a non-lethal and lethal dose of HYP-PDT on cell morphology. Based on the cytotoxic profiles, Fb and Mc were treated with a non-lethal (1μM) and a lethal dose (3μM) of HYP-PDT. However, Kc were treated with the highest HYP-PDT doses (3μM and 4μM) as the lethal dose for Kc did not occur in our HYP-PDT concentration range. Thereafter, cells were stained with Hoechst nuclear dye and viewed using phase and fluorescent microscopy 24 hours post HYP-PDT.

Phase contrast images of Fb (left hand panel, Figure 3.3.1. A1; B1; C1; E1) revealed no morphological changes in Fb which were treated with light or HYP (1μM and 3μM) compared to the untreated control. However, a change in morphology was evident in treated Fb (1μM and 3μM HYP-PDT) (left hand panel Figure 3.3.1 D1; F1). Morphological alterations included: cell shrinkage or swelling and pronounced vacuolation in the cytoplasm (left hand panel Figure 3.3.1 D1; F1, see white arrows), but no evidence of apoptotic nuclei was observed.

Furthermore, the corresponding fluorescent images (right hand panel Figure 3.3.1 D2; F2, see white arrows) show perinuclear localization of HYP being displayed as red punctae. Although Hoechst stained nuclei (right hand panel Figure 3.3. D2; F2) appeared smaller 24 hours post HYP-PDT, HYP was excluded from the nucleus in Fb.

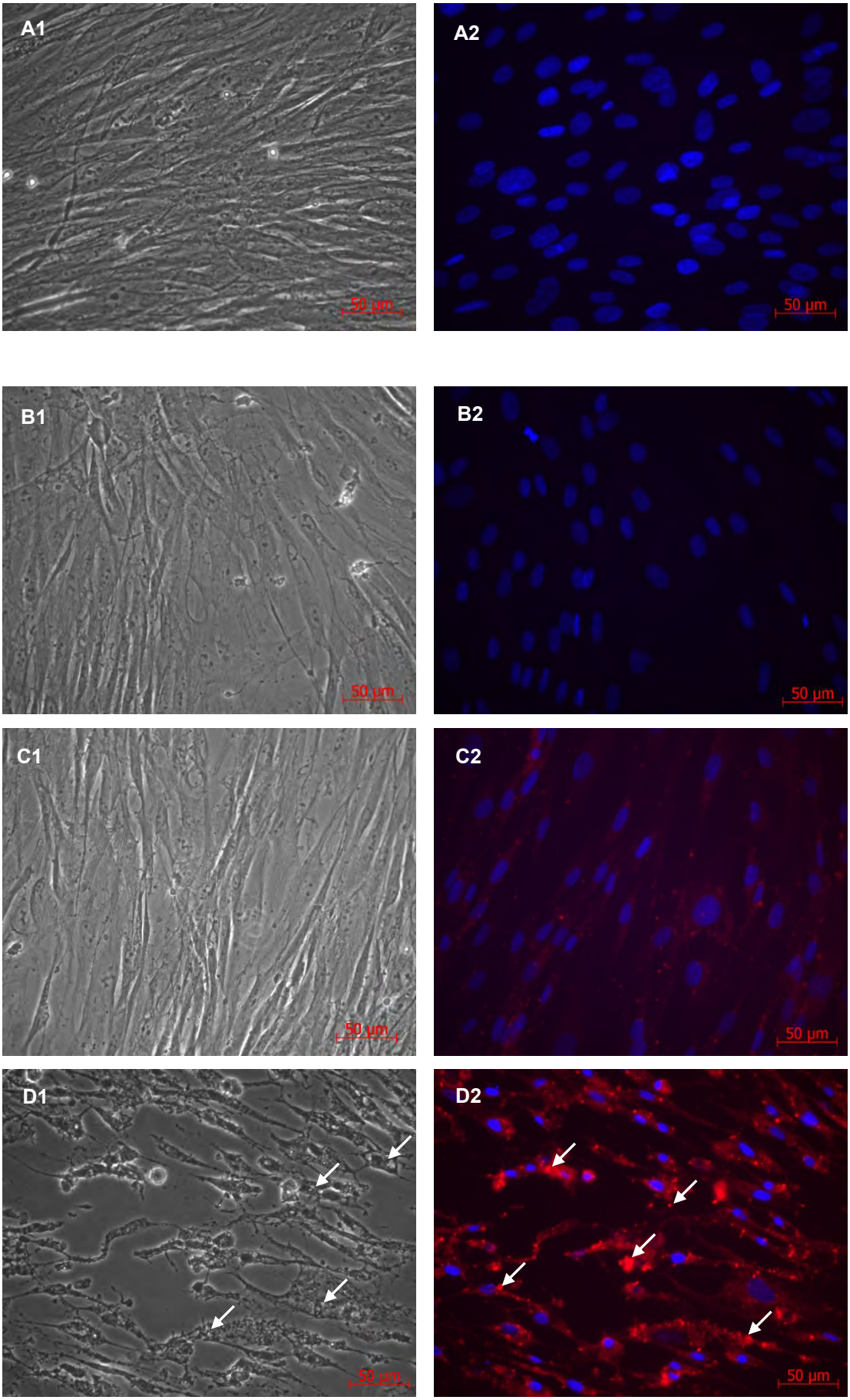
A1
50 µm
A2
50 µm
B1
50 µm
B2
50 µm
C1
50 µm
C2
50 µm
D1
50 µm
D2
50 µm

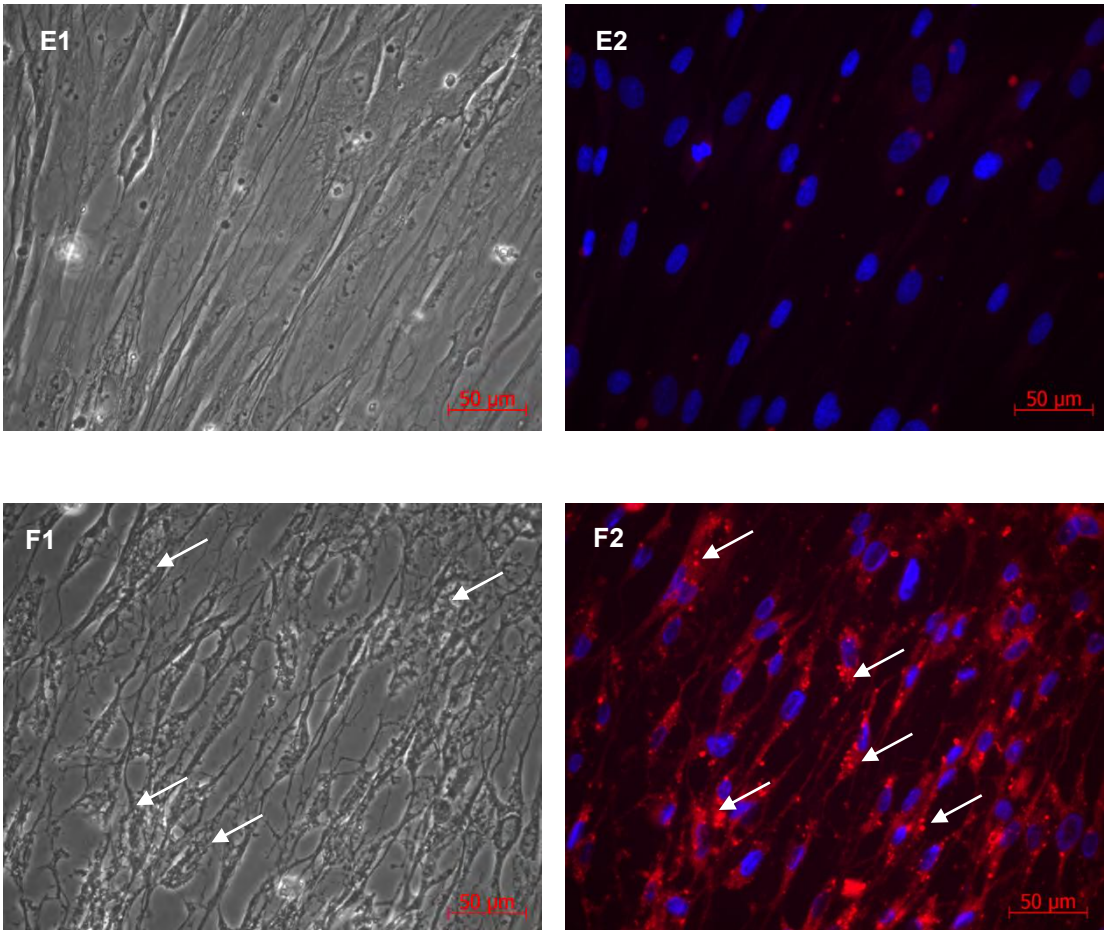

Figure 3.3.1: Fb stained with Hoechst nuclear dye (blue) and HYP (red) 24 hours post HYP-PDT. Phase contrast images on the left hand panel: white arrows pointing to vacuoles with corresponding fluorescent images on the right hand panel: white arrows pointing to HYP punctae. Untreated Control (A1 + A2); light control (B1 + B2); 1µM HYP (C1+ C2); 1µM HYP-PDT (D1 + D2); 3µM HYP (E1 + E2); 3 µM HYP-PDT (F1 + F2). Magnification = 400X. (n=2)

In Mc, phase contrast microscopy (left hand panel Figure 3.3.2 B1; C1; E1) did not exhibit morphological changes 24 hours post-treatment with HYP (1µM and 3µM) and light; as Mc looked similar to the bipolar, elegant cells with long slender dendrites observed in the untreated control (left hand panel Figure 3.3.2 B1). However, Mc which were treated with 1µM HYP-PDT (left hand panel Figure 3.3.2 D1) had retracted dendrites and had shrunk significantly with clear visual evidence of damaged cell membrane and cytoplasmic vacuoles (left hand panel Figure 3.3.2 D1, see white arrows).

Interestingly, Mc which were treated with 3μM HYP-PDT exhibited slight dendrite shrinkage and cytoplasmic vacuolation but maintained cell integrity (left hand panel Figure 3.3.2 F1), see white arrows.

The corresponding fluorescent images of Mc (right hand panel Figure 3.3.2 D2; F2, see white arrows) stained with Hoechst nuclear dye showed HYP localization in the cytoplasm with HYP aggregates, resembling bright red punctae. Similarly to the Fb, there was no evidence of HYP accumulation in melanocyte nuclei (right hand panel Figure 3.3.2 D2; F2) and there was no evidence of apoptotic nuclei with phase microscopy (left hand panel Figure 3.3.2 D1; F1).

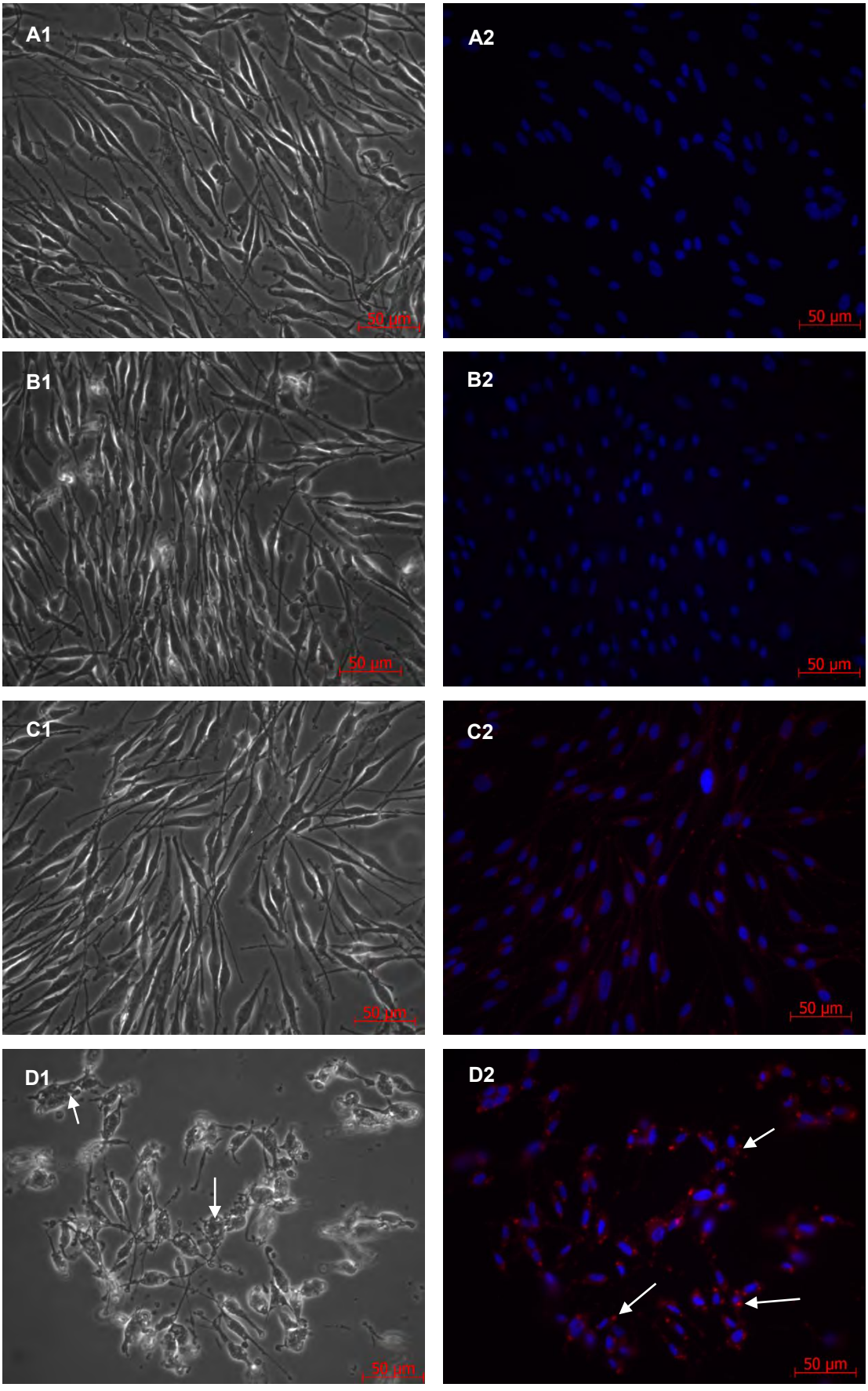
A1
50 µm
A2
50 µm
B1
50 µm
B2
50 µm
C1
50 µm
C2
50 µm
D1
50 µm
D2
50 µm

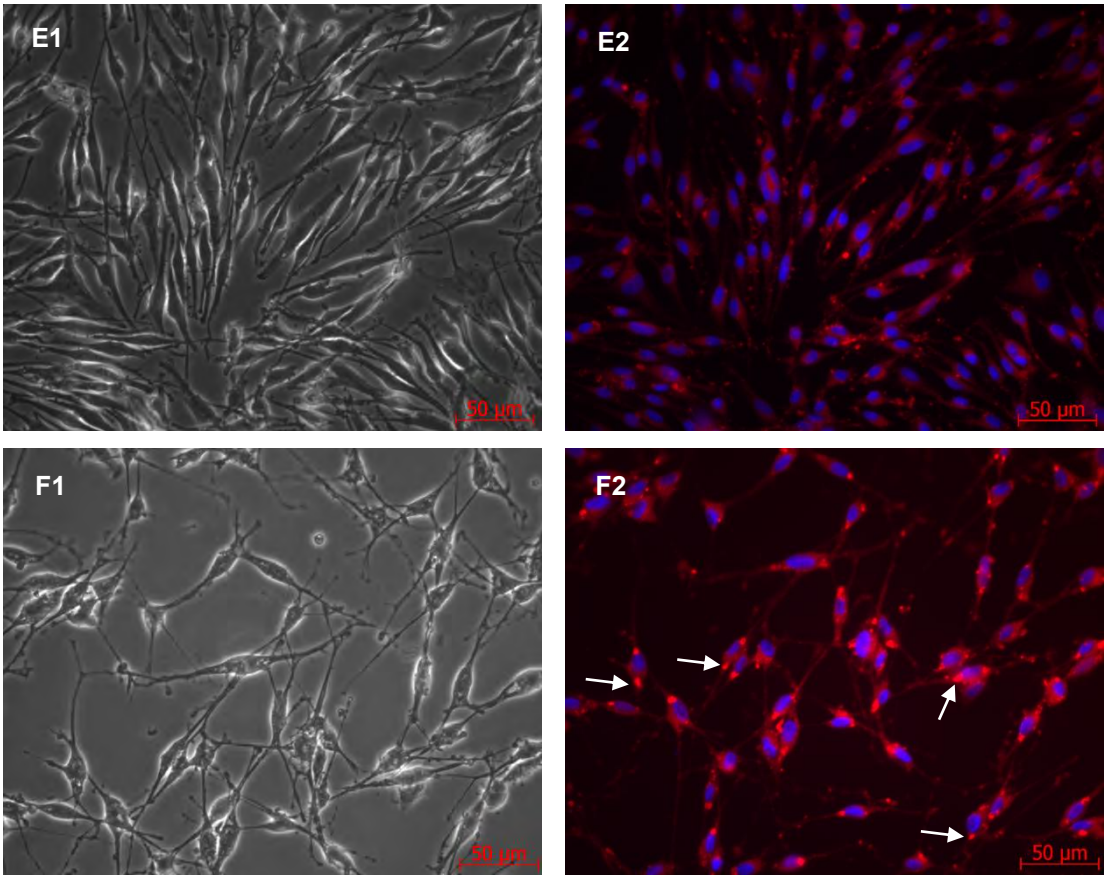

Figure 3.3.2: Mc stained with Hoechst nuclear dye (blue) and HYP (red) 24 hours post HYP-PDT. Phase contrast images on the left hand pane: white arrows pointing to vacuoles with corresponding fluorescent images on the right hand panel: white arrows pointing to HYP punctae. Untreated Control (A1 + A2); light control (B1 + B2); 1µM HYP (C1+ C2); 1µM HYP-PDT (D1 + D2); 3µM HYP (E1 + E2); 3 µM HYP-PDT (F1 + F2). Magnification = 400X. (n=2)

Despite having been treated with the highest HYP-PDT doses (3µM and 4µM), primary human Kc looked unaffected and remained 80-90% confluent (left hand panel, Figure 3.3.3 D1; F1). Furthermore, Kc maintained cell shape and integrity, looking very similar to the untreated control (left hand panel Figure 3.3.3 A1). At 4µM HYP-PDT exposure they did however display minimal evidence of cytoplasmic vacuolation (left hand panel Figure 3.3.3. F1, see white arrows).

The corresponding fluorescent images (right hand panel, Figure 3.3.3) of Kc had some blue background fluorescence possible due to antifade absorbing the Hoechst dye but blue healthy nuclei were evident. HYP localization in Kc was also perinuclear and red HYP aggregates distinguishable by red cytoplasmic punctae were also visible (right hand panel Figure 3.3.3 D2; F2, see white arrows).

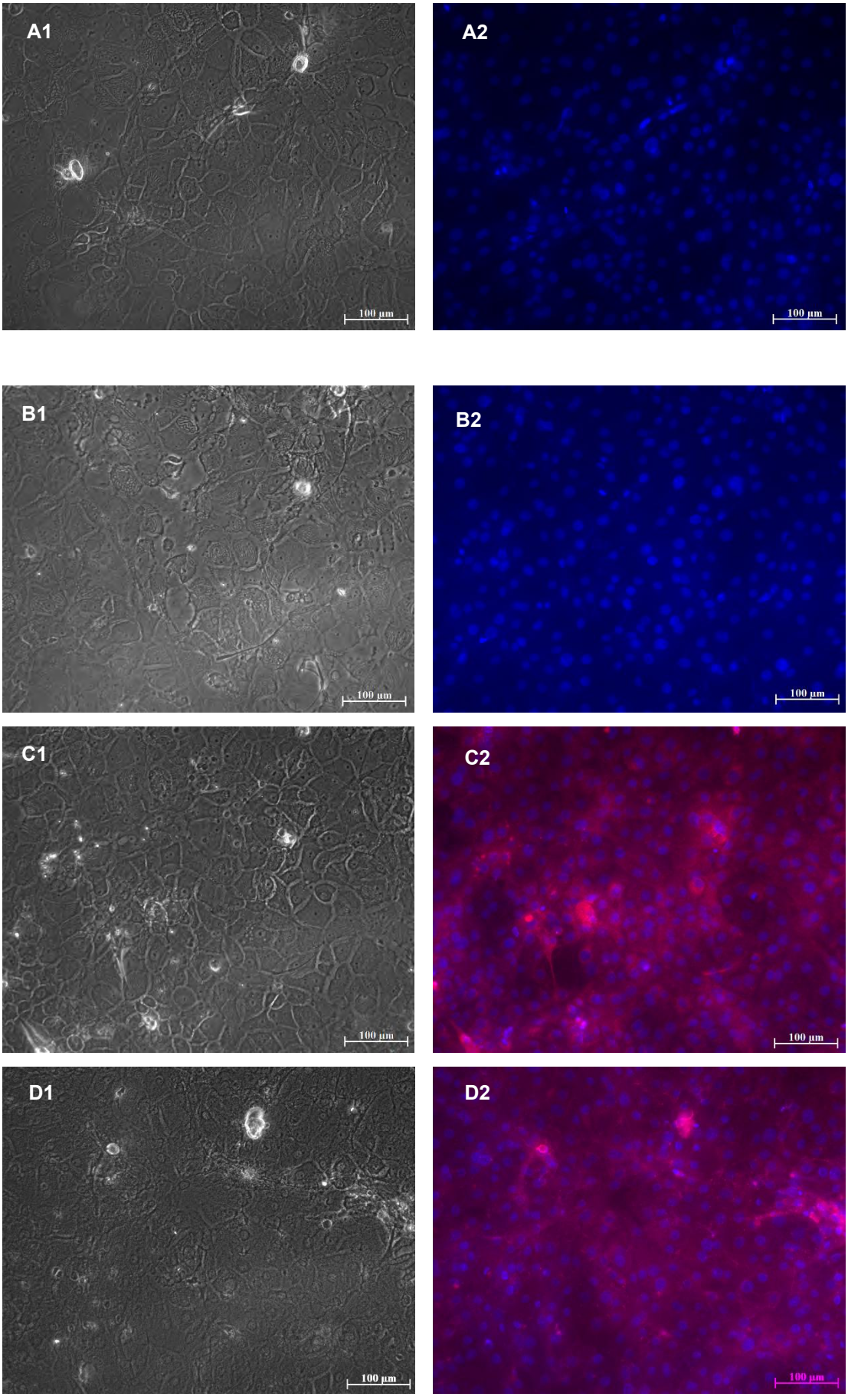
A1
A2
B1
B2
C1
C2
D1
D2
100 µm

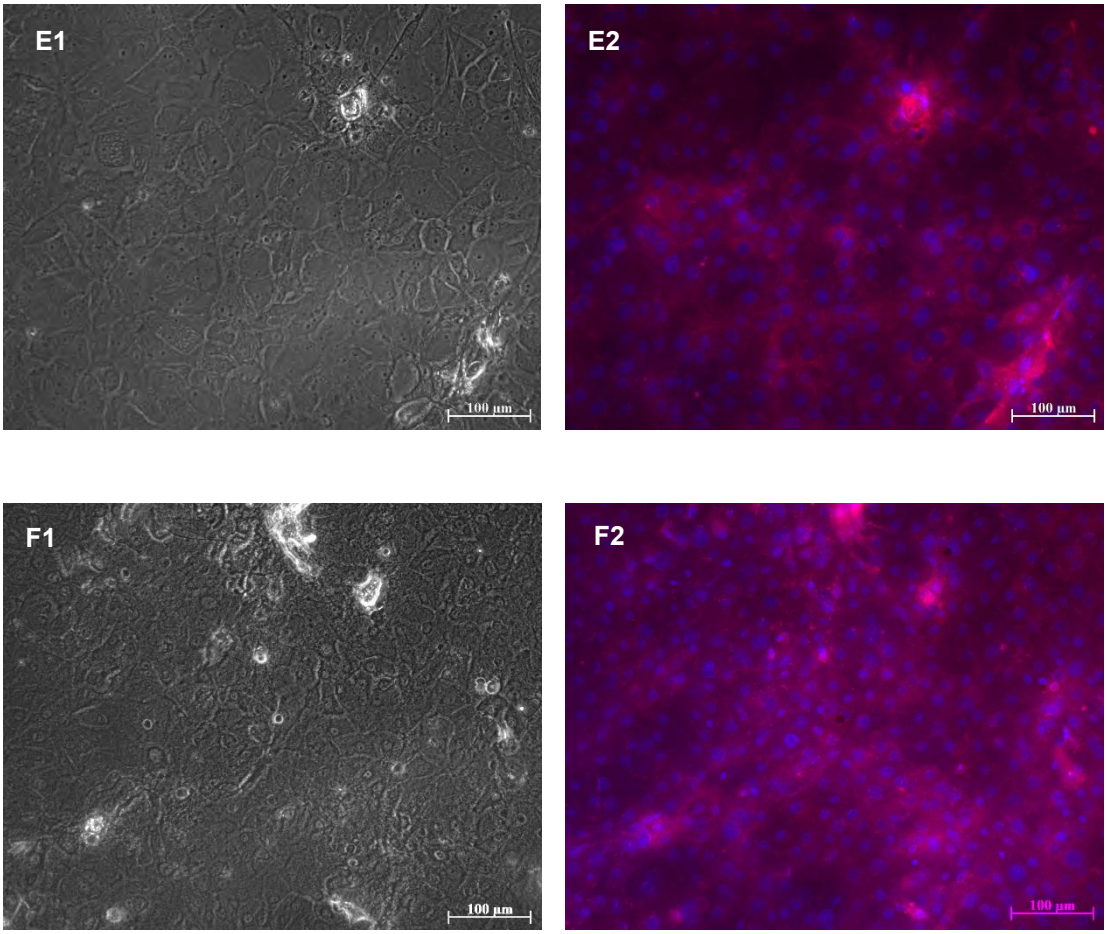

Figure 3.3.3: Kc stained with Hoechst nuclear dye (blue) and HYP (red) 24 hours post HYP-PDT. Phase contrast images on the left hand panel: white arrows pointing to vacuoles with corresponding fluorescent images on the right hand panel: white arrows pointing to HYP punctae. Untreated Control (A1 + A2); light control (B1 + B2); 3µM HYP (C1+ C2); 3µM HYP-PDT (D1 + D2); 4µM HYP (E1 + E2); 4µM HYP-PDT (F1 + F2). Magnification = 200X (n=3)

Therefore, both non-lethal and lethal doses of HYP-PDT induced distinct morphological changes, 24 hours post treatment, in Fb and Mc. However, the highest HYP-PDT doses did not induce distinct morphological changes in Kc. Interestingly, in all 3 cell types, HYP was excluded from the nucleus at the 24 hour time point.

3.4 Intracellular ROS levels 30 Minutes Post HYP-PDT

HYP induces its primary effect through production of intracellular ROS. Cellular damage is often dependent on the amount of ROS generated. It is therefore, necessary to quantify the HYP-PDT induced ROS. Intracellular ROS production was evaluated, 30 minutes post HYP-PDT, because HYP-PDT causes a cytotoxic response via consequential ROS once HYP is activated with light.

A fluorescence based ROS assay was used to measure intracellular ROS levels, 30 minutes post HYP-PDT, which employed the non-fluorescent probe DCF-DA that is cleaved to a fluorescent product by ROS. In order to prevent DCF-DA intracellular saturation, 5μM; 10μM and 20μM DCF-DA was tested using HYP-PDT (1μM and 3μM) treated Fb (Figure 3.4.1 A; B; C) and 5μM DCF-DA was identified as the optimum concentration for this assay.

Once we had optimized this assay, intracellular ROS levels were measured 30 minutes post HYP-PDT in all the primary cell types. A significant 3.8 fold increase (Figure 3.4.1 D) ($p < 0.05$) in ROS levels (Figure 3.4.1 D) occurred in Fb 30 minutes at a dose of 3μM HYP-PDT (Figure 3.4.1 D). However, a significant difference in intracellular ROS levels did not occur in Kc and Mc (Figure 3.4.1 D) post HYP-PDT.

Furthermore, intracellular ROS levels in Fb were significantly different ($p<0.001$) to intracellular ROS levels in Mc and Kc at a dose of 3μM HYP-PDT (Figure 3.4.1 D, see box). This correlated with the Fb being the most sensitive to HYP-PDT which was confirmed by cell viability and cell morphology analysis. Interestingly, intracellular ROS levels in Mc and Kc were not significantly different to each other post HYP-PD

A) B)

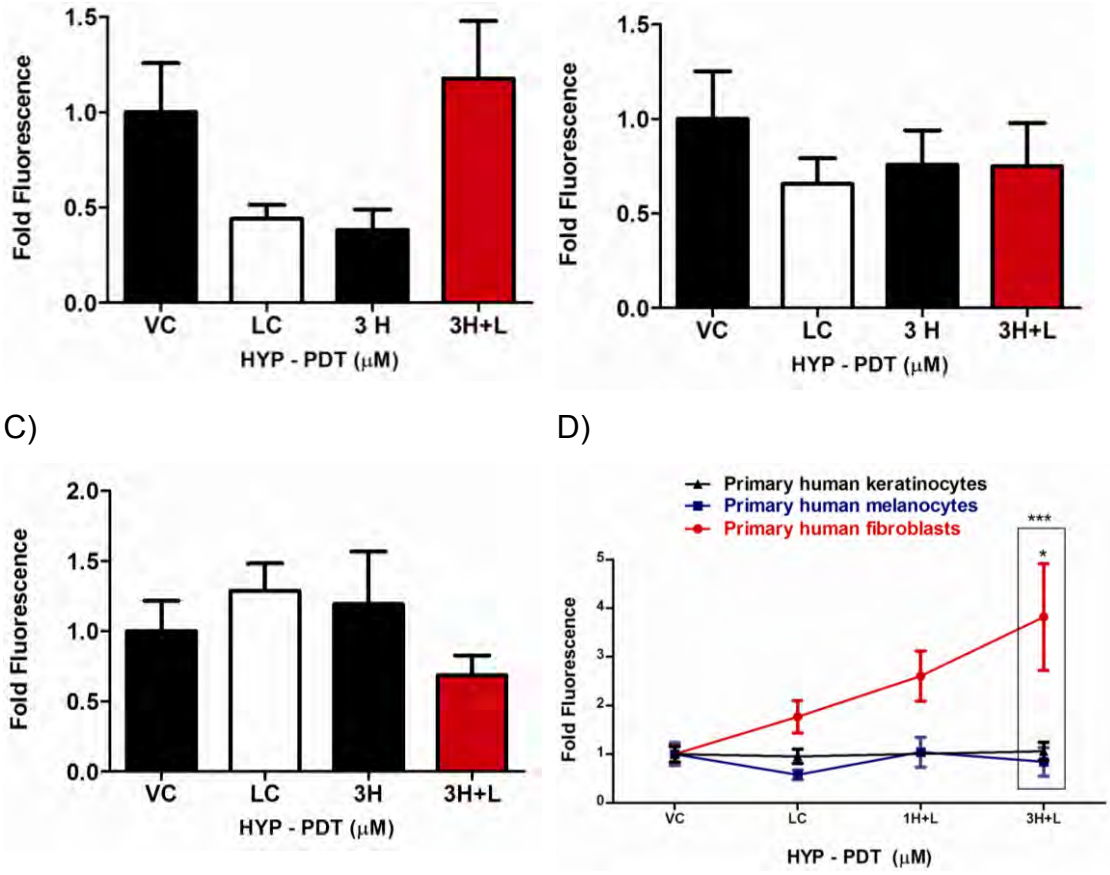

Figure 3.4.1: Intracellular ROS levels 30 minutes post HYP- PDT in Fb treated with 5μM H_2DCF-DA (A); Fb treated with 10μM H_2DCF-DA (B); Fb treated with 20μM H_2DCF-DA (C); all skin cell types treated with 5μM H_2DCF-DA (D). VC= vehicle control; LC= light control; 3H = 3μM HYP; 3H+L = 3μM HYP-PDT. (p=* < 0.05; p= * <0.001) (Mean; SEM) (n>3)**

3.5 Cell Death Analysis 24 Hours Post HYP-PDT

Even though apoptotic visualization was attempted with phase and fluorescent microscopy, Fluorescent activated cell sorting (FACS) is the

preferred method due sensitivity and accuracy. FACS was carried out 24 hours post HYP-PDT using Annexin V-FITC, an early apoptosis marker, and PI which is indicative of cell membrane integrity. Apoptosis analysis via FACS is sensitive and accurate because Annexin V-FITC measures phosphatidylserine externalization and PI is excluded by live cells with intact cell membranes. Therefore, different cell populations can be represented according to the 4 quartiles shown by the dot plot example in (Figure 3.5.1 A): cells in quartile 1 (Q1) are dead but not via apoptosis or necrosis; cells in quartile 2 (Q2) are necrotic; cells in quartile 3 (Q3) are undergoing early apoptosis and cells in quartile 4 (Q4) are viable.

Once different populations of Fb had been separated 24 hours post HYP-PDT, using FACS (Figure 3.5.1B); a significant ($P<0.001$) early apoptotic population (64%) was evident after treatment with 3μM HYP-PDT. However, a smaller, significant ($p< 0.05$) early apoptotic Mc population (20%) was prominent as a result of 3μM HYP-PDT (Figure 3.5.1 C) treatment. Interestingly, 3μM HYP treatment in the dark resulted in a significant ($p< 0.05$) early apoptotic (15%) Kc population (Figure 3.5.1 D) but 3μM HYP-PDT did not result in a significant early apoptotic Kc population. Furthermore, there were no significant necrotic cell populations in any of the skin cell types in the controls nor post HYP-PDT. Therefore, HYP-PDT induces a cytotoxic effect which results primarily in apoptotic cell death in Fb and Mc but not in Kc.

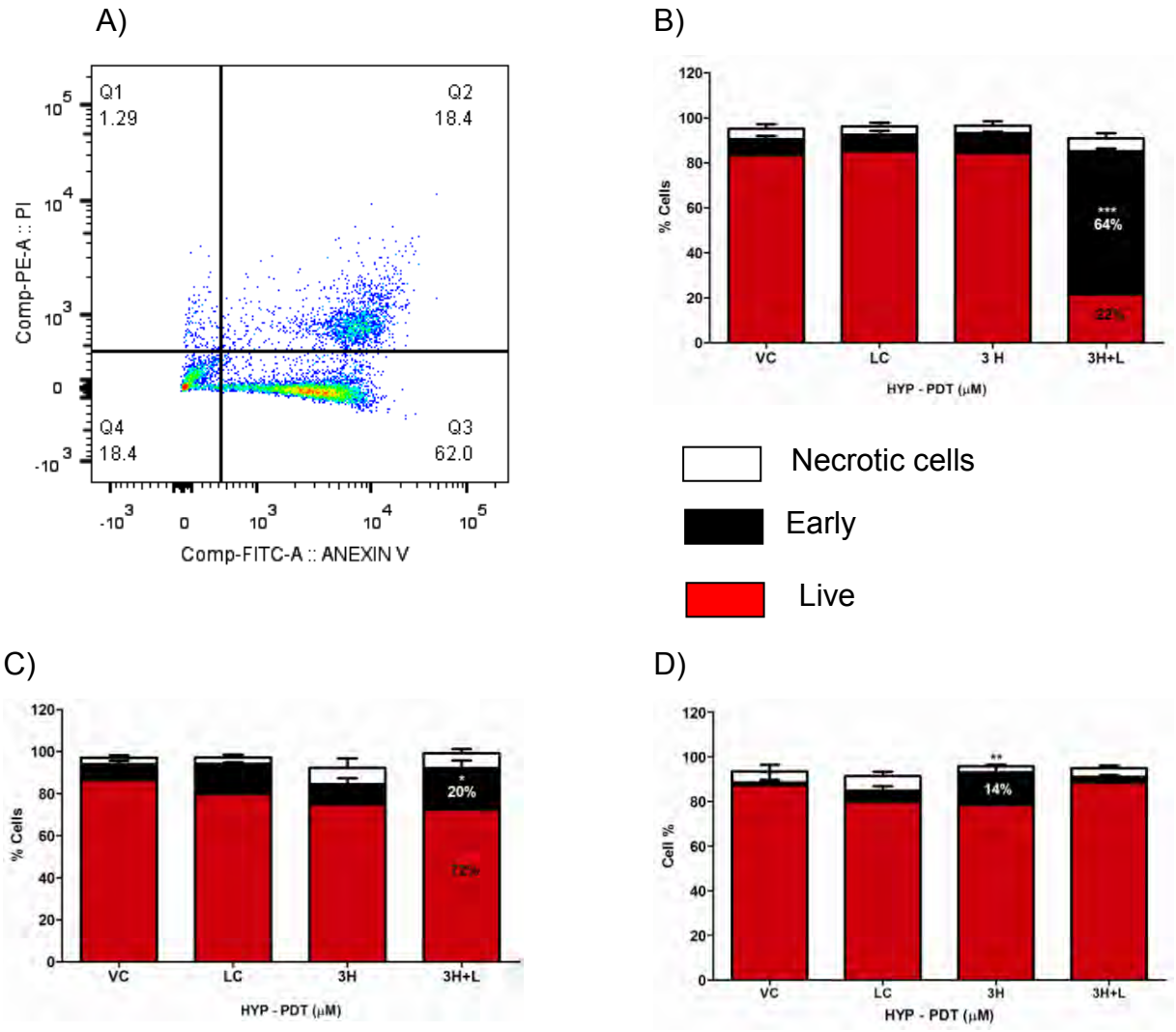

Figure 3.5.1: Cell death analysis 24 hours post HYP- PDT evaluated with FACS analysis using Annexin V–FITC and PI represented by the dot plot of cell populations and the 4 quartiles (A); Fb (B); Mc (C) and Kc (D). Red = viable cells. Black = early apoptotic cells. White = necrotic cells.
(*= p<0.05; ** = p < 0.01) (Mean; SEM) (n>3)

Chapter 4: Discussion:

Photodynamic therapy (PDT) is a promising cancer treatment modality which has been successful in the treatment of non-melanoma skin cancer (NMSC), especially basal cell carcinoma (BCC) but it's effectiveness in the treatment of squamous cell carcinoma (SCC) and melanoma skin cancer is currently being investigated, by our group and others (Agostinis et al. 2011; Braathen et al. 2007; Zhao & He 2010; Davids & Kleemann 2011) Our group is using a plant-based photosensitiser hypericin (HYP) due to its powerful cytotoxic effects in several cancer cells including cervical cancer cells; human myeloid leukemia cells; hepatocellular liver carcinoma cells and breast cancer cells (Barathan et al., 2013; Ferenc, Solár, Kleban, Mikes, & Fedorocko, 2010; Sacková, Fedorocko, Szilárdiová, Mikes, & Kleban, 2006; A Vantieghem, 1998).

An advantage of PDT as a skin cancer therapy includes topical administration to patients (Morton et al., 2008; Ross et al., 2013; Wan & Lin, 2014; Zhao & He, 2010). Following photosensitiser uptake, light is effectively directed onto the specific area of the skin that contains the cancerous lesion (Morton et al., 2008; Ross et al., 2013; Wan & Lin, 2014; Zhao & He, 2010). *In vivo,* a BCC, SCC and a superficial melanoma would be located in the epidermis but a SCC occurs predominantly in the basal layer of the epidermis (Ahmed et al., 2008; Lauth et al., 2004). In contrast, a melanoma may be superficial (radial and vertical growth phases, RGP and VGP) but also possesses the capability of breaching the basement membrane and growing vertically to metastasize into the blood vessels (A. J. Miller & Mihm, 2006).

As PDT is a promising topical skin cancer therapy, the surrounding normal tissue would be inescapable to photosensitiser exposure and irradiation during treatment (Braathen et al., 2007; Svanberg et al., 1994; Wang, Wang, Guo, & Xu, 2008; Zeitouni, Oseroff, & Shieh, 2003). It is therefore important to know how these cells are affected by treatment as they, being in the same

intimate environment, could have bearing on the success or efficacy of the treatment being applied. This is known as the “bystander effect”. With this in mind, this project investigated the effects of HYP-PDT on normal primary human skin cells as representative cell types of the peri-lesional cells to measure the bystander effect. Primary human melanocytes (Mc) and keratinocytes (Kc) were used as the epidermal cells and primary human fibroblasts (Fb) as the dermal representative. More specifically, the aims of this project investigated the *in vitro* effects of HYP-PDT on normal skin cell viability and morphology; intracellular ROS production and the induction of apoptosis post treatment.

4.1 Primary Human Skin Cells Have Different Growth Dynamics in Culture

Kc, Mc and Fb were isolated from human skin biopsies and neonatal foreskins after informed patient consent (see Ethics statement in methodology (see section 2.1.1). Thereafter, culture conditions were optimized and growth curves performed over a period of 7 days indicated that Fb had an excellent seeding efficiency (100%); Mc a good seeding (72%) efficiency but Kc exhibited a poor seeding efficiency (58%) by *in vitro* standards. Furthermore, the doubling time during the exponential growth phase was: ±2; ±3 and ±1.5 days for Kc, Mc and Fb, respectively. This indicated that Fb had the fastest growth rate compared to Mc and Kc; Mc the slowest growth rate and Kc grew slower than Fb but faster than Mc during the exponential phase.

The slower growth rate of Mc and Kc compared to Fb may have occurred because Mc and Kc grow in the same microenvironment, *in vivo* in the epidermis and rely on intercellular cytokines and growth factors for proliferation (Hirobe, 2005; Joshi et al., 2007; Nakazawa, Nakazawa, Collombel, & Damour, 1995; Valyi-Nagy, Murphy, Mancianti, Whitaker, &

Herlyn, 1990). However, Mc and Kc were cultured as monocultures in our *in vitro* system and did not experience intercellular interactions. Although Kc had the poorest seeding efficiency out of the 3 skin cells types, they proceeded to grow at an improved rate compared to Mc during the exponential phase, suggesting that Kc are less dependent on Kc-Mc interactions for proliferation compared to Mc. It is known that Mc are dependent on Kc derived factors for proliferation and even though Mc specific medium (FETI) (Appendix A) has several necessary growth factors such as endothelin and basic fibroblast growth factor (bFGF) it does not contain every Kc derived growth factor which Mc would be exposed to *in vivo that* may contribute to the suboptimum growth of Mc *in vitro* (Gordon, Mansur, & Gilchrest, 1989; R. Halaban, 1988; Ruth Halaban, 2000; Hirobe, 2005; Imokawa, Yada, & Miyagishi, 1992).

On the other hand, Fb were cultured efficiently and easily until 90% confluent. However they underwent contact inhibition at ±90% confluency and stopped proliferating, which was depicted in the plateau of Fb growth rate after day 5 (Abercrombie, 1970; Dietrich, Wallenfang, Oesch, & Wieser, 1997; Otten, Johnson, & Pastan, 1971). It is possible that Kc and Mc may have initiated contact inhibition at a lower confluency, thereby inhibiting proliferation and decreasing the growth rate. It was important to establish the growth dynamics of primary human skin cells to understand when they were in their exponential phase so that adequate conduction of experiments could take place with cells growing at their optimum.

4.2 HYP-PDT Induces Differential Cytotoxicity in Primary Human Skin Cells

The cytotoxic profile for primary human skin cells 24 hours post-HYP-PDT, demonstrated that HYP did not have any cytotoxic effects in the dark in primary human skin cells as there was no significant difference in cell viability

when cells were treated with various doses of HYP in the dark (0.25μM; 0.5μM; 0.75μM; 1μM; 2μM; 3μM; 4μM, (Figure 3.2.1). This result was not surprising as HYP has a cytostatic effect on cells and not a cytotoxic effect in the dark (Krammer & Verwanger, 2012; Kubin et al., 2005). However, activated HYP-PDT resulted in a LD_{50} that varied between HYP-PDT treated Fb, Mc and Kc at doses: 1.75μM; 3.5 μM and >4 μM HYP-PDT, respectively. As a lower LD_{50} is indicative of a higher susceptibility to a drug or treatment, Fb were the most susceptible cell type to HYP-PDT with Kc being the least susceptible and Mc being less susceptible than the Fb but more susceptible than the Kc.

As these are indeed all skin cells, the difference in LD_{50}'s between the cells, is interesting. Although the pigmentation levels in Mc were not quantified in this study, presence of melanin pigment could be a major contributor to the protection of melanocytes from ROS-induced PDT. This was corroborated by earlier work in melanoma where a decrease in the pigment, led to increased susceptibility to HYP-PDT. A further explanation could be that Mc and Kc have increased endogenous antioxidant levels (or sophisticated antioxidant responses) which may have inferred protection against ROS-based HYP-PDT induced cytotoxicity. This point ties in with the ultimate function of the Kc being the majority cell type of the epidermis, part of the barrier between the body and the external environment, and thus the most highly resistant skin cell to the HYP-PDT treatment at the 24 hour time point. Moreover, reports that the antioxidant levels in the epidermis are greater than the dermis, lend further support as to why the Fb were likely to be the most susceptible to HYP-PDT (Kohen, 1999; Shindo, Witt, Han, Epstein, & Packer, 1994). Additionally, our group established a killing does of 3μM HYP-PDT for human melanoma cells (Lester M Davids et al., 2008). We demonstrated in this study that 3μM HYP-PDT is indeed cytotoxic to Fb and Mc but not to Kc; it was therefore important to further analyze the effects for HYP-PDT using this particular dose.

4.3 HYP-PDT Induces Distinct Morphological Changes in Primary Human Skin Cells 24 hours post Treatment

HYP-PDT induced distinct morphological changes in both the Mc and the Fb whilst sparing the Kc at the lower concentrations Kc only suffered some effect when treated with the highest HYP-PDT doses (3μM and 4μM). Distinct changes in Fb morphology were apparent at 1μM (non-lethal dose) and 3μM (lethal dose) HYP-PDT, with phase contrast microscopy at both these doses exhibiting cell shrinkage and cytoplasmic vacuolation. It was surprising that Fb morphology was also compromised at both these doses. However, we could not compare the morphology of Fb to other studies which investigated HYP-PDT effects, as they did not carry out morphological analysis (Kashef et al., 2013; Rezusta et al., 2012).

A non-lethal dose (1μM) resulted in morphological changes in Mc; including cell shrinkage with associated dendrite retraction. Interestingly, at the lethal dose (3μM), Mc looked healthier with few cytoplasmic vacuoles and longer dendrites compared to treatment with the non-lethal dose (1μM). One explanation for this could be the inherent reaction to upregulate their intracellular antioxidant system (catalase, superoxide dismutase and glutathione) and increased production of melanin in response to the higher oxidative stress doses (Meyskens Jr., Farmer, & Fruehauf, 2001; Swalwell, Latimer, Haywood, & Birch-Machin, 2012).This is a well-known response in Mc and especially in their cancerous counterparts, melanoma (Hadjur et al., 1996; Picardo et al., 1996). Perhaps a tolerance to the HYP-PDT doses exist somewhere between 1μM and 3μM. Although this response was not quantified in this project, it would be intriguing to quantitatively measure it in the future.

Although 3μM HYP-PDT did not induce any morphological changes in Kc; few cytoplasmic vacuoles were evident with phase microscopy at a dose of 4μM HYP-PDT but cell integrity and shape was maintained. This was not surprising as 4μM HYP-PDT induced an initial significant difference in cell viability (79%) ($p < 0.05$) in these cells compared to the vehicle control.

4.4 HYP Localizes Perinuclearly in Primary Human Skin Cells

The enigma of why hypericin does not enter the nucleus and effect damage is ongoing and it seems in agreement with published literature that HYP localization in the nucleus occurs at doses exceeding 20μM hypericin or after incubation time exceeding 8 hours (Agostinis et al., 2002; Krammer & Verwanger, 2012; Theodossiou et al., 2009). In our system, fluorescent microscopy revealed perinuclear localization of HYP in distinct aggregates in all three cell types at a 24 hour time point. Furthermore, Kc staining with Hoechst nuclear dye could be improved by viewing cells immediately after staining without adding antifade to the mowiol because the antifade absorbed the Hoechst nuclear dye and caused a hazy deposition which was observed on the fluorescent images. Further co-localization experiments using confocal microscopy will need to be performed in order to determine exactly in which organelles HYP is localizing.

4.5 HYP-PDT Increased Intracellular ROS Levels in Fb but not in Kc or Mc

Since HYP-PDT induces cytotoxic damage via ROS production in the vicinity of activated HYP localization, intracellular ROS production was evaluated in Fb, Mc and Kc, 30 minutes post HYP-PDT. In Fb, a significant 3.8-fold increase in intracellular ROS correlated with the distinct morphological

changes and cell viability (33%) observed 24 hours post 3μM HYP-PDT. However, there was no significant intracellular ROS production in Mc and Kc at a 3μM HYP-PDT dose. Interestingly, although Mc were more susceptible to 3μM HYP-PDT than Kc, there was no significant difference in intracellular ROS levels between these two cell types, which may be attributed to the intracellular presence of melanin. Melanin is known to act as a ROS scavenger and "mop" up intracellular ROS when pigmented cells are oxidatively stressed (Chedekel & Zeise, 1999; Sander, Chang, Hamm, Elsner, & Thiele, 2004; Swalwell et al., 2012).

The insignificant intracellular ROS observed in Kc post treatment correlated with their resistance to 3μM HYP-PDT which was depicted by cell viability and cell morphology analysis. Since Mc transfer melanin to Kc, melanin may have protected Kc from ROS as melanin granules are situated around the nucleus in the cytoplasm, although the melanin content in Kc is much lower than in Mc (Van Den Bossche, Naeyaert, & Lambert, 2006; Wood et al., 1999). Furthermore, Kc may require longer than 4 hours for HYP uptake because HYP-PDT may not have induced a cytotoxic effect in Kc if insufficient HYP accumulated intracellularly upon light activation, which would have generated minimal $^1O_2$ and therefore the oxidative stress would have also been minimal. We chose a 4 hour incubation period for this study, as this was the optimized HYP uptake time determined by our group for human melanoma cells. However, we did not investigate HYP uptake time for Kc and this may be interesting to explore further when determining the LD_{50} for Kc.

Early Stage Apoptosis Occurred in Primary Fibroblasts and Melanocytes 24 hours post HYP-PDT Treatment. Seeing that an increase in intracellular ROS can lead to apoptosis, we in investigated whether HYP-PDT induced ROS can cause apoptosis in Fb, Mc and Kc (Martin & Barrett, 2002; Simon, Haj-Yehia, & Levi-Schaffer, 2000; Tan, Wood, & Maher, 2002). Despite there being no evidence of apoptotic nuclei in any of the 3 skin cell types during morphological analysis of HYP-PDT treated skin cells, more sensitive methods were needed to assess apoptosis. The cells viewed 24 hours post

HYP-PDT were adherent cells either at the early stage of cell death or resistant to the treatment as necrotic and late apoptotic cells would have lifted and been lost during the staining process. However, apoptotic (fragmented) nuclei is a characteristic of late stage apoptosis which would result in cells rounding up, lifting and inevitably being washed off the glass slides during the staining protocol (Gerschenson & Rotello, 1992; Saraste, 2000).

We therefore assessed apoptosis using fluorescent activated cell sorting (FACS) with the fluorophores Annexin V-FITC and PI - direct measures of early apoptosis and plasma cell membrane integrity, respectively. FACS analysis confirmed a significant early apoptotic Fb (64%) ($p<0.001$) and Mc (20%) ($p<0.05$) populations, 24 hours post 3μM HYP-PDT. The significant, majority early apoptotic Fb population correlated with the fibroblasts being most susceptible to HYP-PDT and the significant increase in intracellular ROS production. This result correlated with literature stipulating that HYP-PDT causes accumulation of intracellular ROS which can lead to cell death via apoptosis and has been shown in several cancer cells such as cervical cells, glioblastoma cells, melanoma cells and T-lymphocyte leukemic cells (Agostinis et al., 2002; Barathan et al., 2013; Lester M Davids et al., 2008; Huntosova et al., 2012; Kiesslich et al., 2006; Krammer & Verwanger, 2012; Schempp, Simon-haarhaus, Termeer, & Simon, 2001; Theodossiou et al., 2009; A Vantieghem, 1998; Annelies Vantieghem et al., 2007). However, to our knowledge, no studies have shown apoptosis occurring in Fb and Mc post HYP-PDT and since this is ongoing research, further experiments using western blotting techniques will be conducted to confirm apoptosis protein expression.

Interestingly, there was no significant intracellular ROS measured in Mc, but there was evidence of early stage apoptosis 24 hours post 3μM HYP-PDT. This indiscretion may have occurred due to apoptosis analysis being conducted at a much later time point (24 hours) than intracellular ROS which

was measured 30 minutes post HYP-PDT. By this time, the intracellular ROS levels may have overwhelmed the Mc antioxidant system and caused intracellular organelle damage (Engel, Ryan, 2006; Matés, Segura, Alonso, & Márquez, 2008; Schallreuter, 2007). The possible protective effect of melanin HYP-PDT and endogenous antioxidants in pigmented cells are of particular interest to our lab and are currently being investigated.

Surprisingly, treatment with 3μM HYP in the dark resulted in a significant 15% ($p < 0.01$) early apoptotic Kc population, which did not correlate to the cell viability response to HYP treated Kc in the dark. However, HYP in the dark has been shown to have effects on heat shock protein 90 (Hsp 90) ubiquitinylation in a murine mammary adenocarcinoma cell line and a human SCC cell line, which has been suggested to lead to mitotic induced cell death (Blank, Mandel, Keisari, Meruelo, & Lavie, 2004). Hsps are a family of proteins that defend cells from external stress and Hsp 90 is stimulated in stressed Kc (Holland, Roberts, Wood, & Cunliffe, 1993; Jäättelä, 2009; Maytin, 1992). It could be interesting to investigate the effect of HYP-PDT on Hsp 90 in Kc as this will provide further information on how Kc are coping with HYP-PDT treatment.

4.6 Conclusions and Future Directions

The data collected during this project displayed the differential response of primary human skin cells to HYP-PDT (Figure 4.6.1). To date, there have been no studies which have investigated the effects of a HYP-PDT melanomas-killing dose on all 3 primary human skin cell types. We found that 3μM HYP-PDT is cytotoxic to Fb (Figure 4.6.1) and to a lesser extent Mc but the highest HYP-PDT dose we tested, was not cytotoxic to Kc (Figure 4.6.1). This was a favorable finding as Kc are the predominant cell type in the epidermis and are therefore most at risk during PDT of a skin cancer that resides in the epidermis. Future directions include validating HYP-PDT-

induced apoptosis protein pathways induced in normal skin via protein expression of key apoptotic proteins such as Caspases 3; 7 and 8; B-cell lymphoma 2 (Bcl2) and pro-apoptotic protein BAK using western blot analysis (Figure 4.6.1). Furthermore, we intend to investigate the role of melanin and endogenous antioxidants in skin cancer cells with regards protecting the cells from HYP-PDT (Figure 4.6.1)

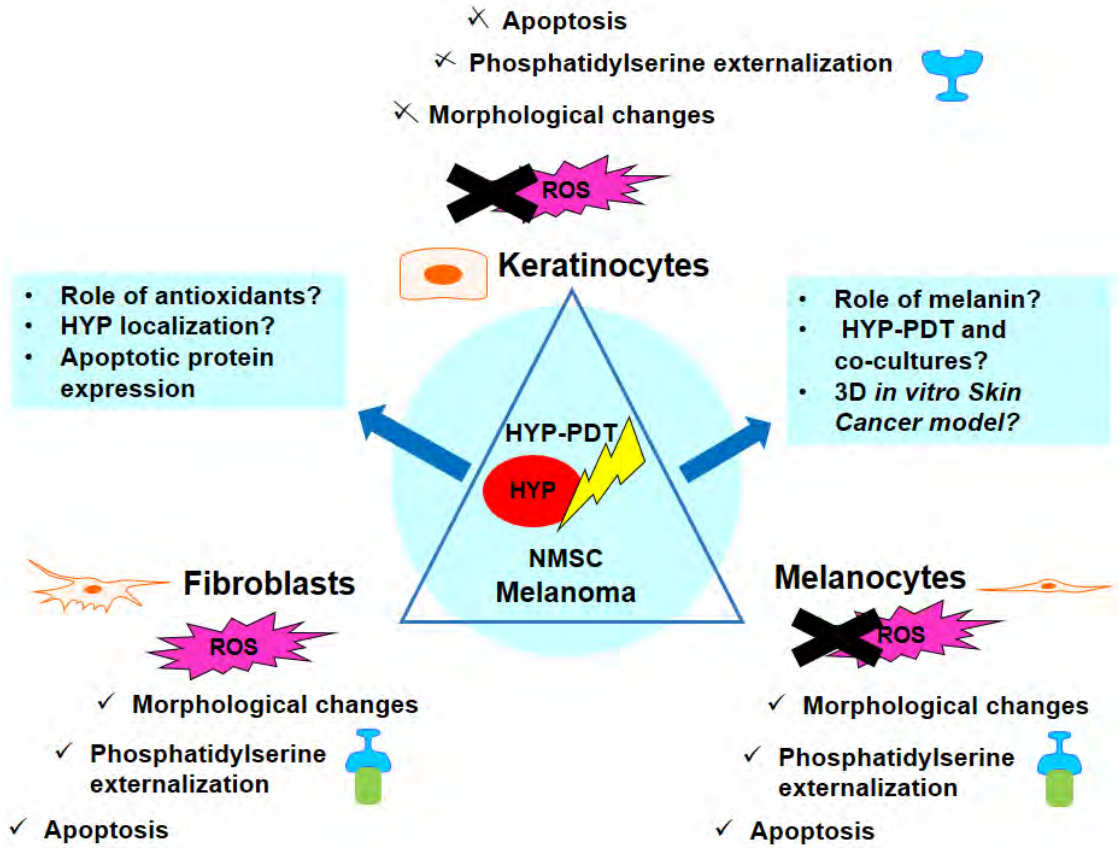

Figure 4.6.1: Summary of results (differential response to HYP-PDT by primary human skin cells and future directions that have stemmed from this project

Additionally, we would like to further asses the effects of HYP-PDT on Mc and Kc co-cultures which are exposed to Fb and skin cancer cell conditioned media; resembling the *in vivo* environmental conditions of skin cells in the

epidermis (Figure 4.6.1). Moreover, we intend to assess the effects of HYP-PDT on a 3D *in vitro* skin equivalent model that includes melanoma cells and recapitulates the microenvironment of a melanoma (Figure 4.6.1); as there is evidence that cancer cells and the tumor microenvironment communicate via paracrine signaling enabling the tumor microenvironment to contribute to tumor progression, proliferation, metastasis and resistance to treatment (Celli, 2013; Junttila & de Sauvage, 2013; Maes, Rubio, Garg, & Agostinis, 2013; Quail & Joyce, 2013). Therefore, it would be worthwhile to investigate the effects of HYP-PDT on a skin cancer microenvironment and to validate the specificity of HYP-PDT for skin cancer cells.

References

Abercrombie, M. (1970). Contact inhibition in tissue culture. *In Vitro*, *6*(2), 128–142. doi:10.1007/BF02616114

Ackroyd, R. (2001). The history of photodetection and photodynamic therapy. *Photochemistry and Photobiology*, *74*(5), 656 – 669.

Agar, N. S., Halliday, G. M., Barnetson, R. S., Ananthaswamy, H. N., Wheeler, M., & Jones, A. M. (2004). The basal layer in human squamous tumors harbors more UVA than UVB fingerprint mutations: a role for UVA in human skin carcinogenesis. *Proceedings of the National Academy of Sciences of the United States of America*, *101*(14), 4954–9. doi:10.1073/pnas.0401141101

Agostinis, P., Berg, K., Cengel, K. A., Foster, T. H., Girotti, A. W., Gollnick, S. O., … Kessel, D. (2011). Photodynamic Therapy of Cancer : An Update. *CA: A Cancer Journal for Clinicians*, *00*(4), 250–281. doi:10.3322/caac.20114.Available

Agostinis, P., Vantieghem, A., Merlevede, W., & de Witte, P. A. M. (2002). Hypericin in cancer treatment: more light on the way. *The International Journal of Biochemistry & Cell Biology*, *34*(3), 221–241. doi:10.1016/S1357-2725(01)00126-1

Ahmed, A. H., Soyer, H. P., Saunders, N., Boukamp, P., & Roberts, M. S. (2008). Non-melanoma skin cancers. *Drug Discovery Today: Disease Mechanisms*, *5*(1), e55–e62. doi:10.1016/j.ddmec.2008.05.007

Alecu, M., Ursaciuc, C., Hãlãlãu, F., Coman, G., Merlevede, W., Waelkens, E., & de Witte, P. (1998). Photodynamic treatment of basal cell carcinoma and squamous cell carcinoma with hypericin. *Anticancer Research*, *18*(6B), 4651–4.

Alexiades-Armenakas, M. (2006). Laser-mediated photodynamic therapy. *Clinics in Dermatology*, *24*(1), 16–25. doi:10.1016/j.clindermatol.2005.10.027

Allison, R. R., Downie, G. H., Cuenca, R., Hu, X.-H., Childs, C. J., & Sibata, C. H. (2004). Photosensitizers in clinical PDT. *Photodiagnosis and Photodynamic Therapy*, *1*(1), 27–42. doi:10.1016/S1572-1000(04)00007-9

Ando, H., Niki, Y., Ito, M., Akiyama, K., Matsui, M. S., Yarosh, D. B., & Ichihashi, M. (2012). Melanosomes are transferred from melanocytes to keratinocytes through the processes of packaging, release, uptake, and dispersion. *The*

Journal of Investigative Dermatology, *132*(4), 1222–9. doi:10.1038/jid.2011.413

Ashkenazi, A., & Dixit, V. M. (1999). Apoptosis control by death and decoy receptors. *Current Opinion in Cell Biology*, *11*(2), 255–260. doi:10.1016/S0955-0674(99)80034-9

Assefa, Z., Vantieghem, A., Declercq, W., Vandenabeele, P., Vandenheede, J. R., Merlevede, W., … Agostinis, P. (1999). The Activation of the c-Jun N-terminal Kinase and p38 Mitogen-activated Protein Kinase Signaling Pathways Protects HeLa Cells from Apoptosis Following Photodynamic Therapy with Hypericin. *Journal of Biological Chemistry*, *274*(13), 8788–8796. doi:10.1074/jbc.274.13.8788

Baldea, I., Filip, A. G., & Napoca, C.-. (2012). Photodynamic Therapy in Melanoma- An Update. *Journal of Physiology and Pharmacology*, *63*(7), 109–118.

Barathan, M., Mariappan, V., Shankar, E. M., Abdullah, B. J. J., Goh, K. L., & Vadivelu, J. (2013). Hypericin-photodynamic therapy leads to interleukin-6 secretion by HepG2 cells and their apoptosis via recruitment of BH3 interacting-domain death agonist and caspases. *Cell DEath and Disease*, *4*(6), e697–10. doi:10.1038/cddis.2013.219

Bernd, A., Simon, S., Bosca, A. R., Kippenberger, S., Alperi, J. D., Miquel, J., … Kaufmann, R. (1999). Phototoxic Effects of Hypericum Extract in Cultures of Human Keratinocytes Compared with Those of Psoralen. *Photochemistry and Photobiology*, *69*(2), 218–221. doi:10.1111/j.1751-1097.1999.tb03276.x

Blank, M., Mandel, M., Keisari, Y., Meruelo, D., & Lavie, G. (2003). Enhanced ubiquitinylation of heat shock protein 90 as a potential mechanism for mitotic cell death in cancer cells induced with hypericin. *Cancer Research*, *63*(23), 8241–7.

Blank, M., Mandel, M., Keisari, Y., Meruelo, D., & Lavie, G. (2004). Enhanced Ubiquitinylation of Heat Shock Protein 90 as a Potential Mechanism for Mitotic Cell Death in Cancer Cells Induced with Hypericin Enhanced Ubiquitinylation of Heat Shock Protein 90 as a Potential Mechanism for Mitotic Cell Death in Cancer Cells In. *Cancer Research*, *63*, 8241–8247.

Boiy, A., Roelandts, R., & de Witte, P. a M. (2011). Photodynamic therapy using topically applied hypericin: comparative effect with methyl-aminolevulinic acid on UV induced skin tumours. *Journal of Photochemistry and Photobiology. B, Biology*, *102*(2), 123–31. doi:10.1016/j.jphotobiol.2010.09.012

Boiy, A., Roelandts, R., & de Witte, P. A. M. (2007). Influence of application and formulation factors on the penetration of hypericin in normal mouse skin and UV induced skin tumors. *Journal of Photochemistry and Photobiology. B, Biology*, *89*(2-3), 156–62. doi:10.1016/j.jphotobiol.2007.10.001

Boiy, A., Roelandts, R., van den Oord, J., & de Witte, P. A. M. (2008). Photosensitizing activity of hypericin and hypericin acetate after topical application on normal mouse skin. *The British Journal of Dermatology*, *158*(2), 360–9. doi:10.1111/j.1365-2133.2007.08329.x

Braathen, L. R., Szeimies, R.-M., Basset-Seguin, N., Bissonnette, R., Foley, P., Pariser, D., … Morton, C. A. (2007). Guidelines on the use of photodynamic therapy for nonmelanoma skin cancer: an international consensus. International Society for Photodynamic Therapy in Dermatology, 2005. *Journal of the American Academy of Dermatology*, *56*(1), 125–43. doi:10.1016/j.jaad.2006.06.006

Bradford, P. T. (2009). Skin cancer in skin of color. *Dermatology Nursing / Dermatology Nurses' Association*, *21*(4), 170–7, 206; quiz 178.

Brown, S. B., Brown, E. A., & Walker, I. (2004). The present and future role of photodynamic therapy in cancer treatment. *The Lancet Oncology*, *5*(8), 497–508. doi:10.1016/S1470-2045(04)01529-3

Bublik, M., Head, C., Benharash, P., Paiva, M., Eshraghi, A., Kim, T., & Saxton, R. (2006). Hypericin and pulsed laser therapy of squamous cell cancer in vitro. *Photomedicine and Laser Surgery*, *24*(3), 341–7. doi:10.1089/pho.2006.24.341

Buytaert, E., Callewaert, G., Hendrickx, N., Scorrano, L., Hartmann, D., Missiaen, L., … Agostinis, P. (2006). Role of endoplasmic reticulum depletion and multidomain proapoptotic BAX and BAK proteins in shaping cell death after hypericin-mediated photodynamic therapy. *FASEB Journal : Official Publication of the Federation of American Societies for Experimental Biology*, *20*(6), 756–8. doi:10.1096/fj.05-4305fje

Cadet, J., Mouret, S., Ravanat, J., & Douki, T. (2012). Photoinduced Damage to Cellular DNA : Direct and Photosensitized. *Photochemistry and Photobiology*, *88*(25), 1048–1065. doi:10.1111/j.1751-1097.2012.01200.x

Calzavara- Pinton, P. G. (2007). Photodynamic therapy: update 2006 Part 1: Photochemistry and photobiology. *Journal of the European Academy of Dermatology and Venereology*, *21*(3).

Calzavara-Pinton, P. G., Venturini, M., & Sala, R. (2007). Photodynamic therapy: update 2006. Part 1: Photochemistry and photobiology. *Journal of*

the European Academy of Dermatology and Venereology : JEADV, *21*(3), 293–302. doi:10.1111/j.1468-3083.2006.01902.x

Castano, A. (2006). Photodynamic therapy and anti-tumour immunity. *Nature Reviews. Cancer*, *6*(7).

Castano, A., Demidova, T., & Hamblin, M. (2004). Mechanisms in photodynamic therapy: part one—photosensitizers, photochemistry and cellular localization. *Photodiagnosis and Photodynamic Therapy*, *1*(4), 279–293. doi:10.1016/S1572-1000(05)00007-4

Celli, J. P. (2013). Stromal interactions as regulators of tumor grpwth and therapeutic response: A potential target for photodynamic therapy? *Israel Journal of Chemistry*, *52*(617), 757–766. doi:10.1002/ijch.201200013.

Chedekel, M. R., & Zeise, L. (1999). Protection of hair and skin from environmental damage with melanin. *SÖFW-Journal*, *125*(2-3), 14–18.

Chen, B., & de Witte, P. A. (2000). Photodynamic therapy efficacy and tissue distribution of hypericin in a mouse P388 lymphoma tumor model. *Cancer Letters*, *150*(1), 111–117. doi:10.1016/S0304-3835(99)00381-X

Dahle, J. (2000). The bystander effect in photodynamic inactivation of cells. *Biochimica et Biophysica Acta (BBA) - General Subjects*, *1475*(3), 273–280. doi:10.1016/S0304-4165(00)00077-5

Dahle, J., Kaalhus, O., Moan, J., & Steen, H. B. (1997). Cooperative effects of photodynamic treatment of cells in microcolonies. *Proceedings of the National Academy of Sciences*, *94*(5), 1773–1778. doi:10.1073/pnas.94.5.1773

Damsky, W. E., Theodosakis, N., & Bosenberg, M. (2014). Melanoma metastasis: new concepts and evolving paradigms. *Oncogene*, *33*(19), 2413–22. doi:10.1038/onc.2013.194

Davids, L. M., & Kleemann, B. (2010). Combating melanoma: The use of photodynamic therapy as a novel, adjuvant therapeutic tool. *Cancer Treatment Reviews*, *37*(6), 465–475. doi:10.1016/j.ctrv.2010.11.007

Davids, L. M., & Kleemann, B. (2013). The Menace of Melanoma : A Photodynamic Approach to Adjunctive Cancer Therapy. In G. Duc & T. Huynh (Eds.), *Melanoma - From Early Detection to Treatment"*.

Davids, L. M., Kleemann, B., Cooper, S., & Kidson, S. H. (2009). Melanomas display increased cytoprotection to hypericin-mediated cytotoxicity through

the induction of autophagy. *Cell Biology International*, *33*(10), 1065–72. doi:10.1016/j.cellbi.2009.06.026

Davids, L. M., Kleemann, B., Kacerovská, D., Pizinger, K., & Kidson, S. H. (2008). Hypericin phototoxicity induces different modes of cell death in melanoma and human skin cells. *Journal of Photochemistry and Photobiology. B, Biology*, *91*(2-3), 67–76. doi:10.1016/j.jphotobiol.2008.01.011

Davies, M. J. (2003). Singlet oxygen-mediated damage to proteins and its consequences. *Biochemical and Biophysical Research Communications*, *305*(3), 761–770. doi:10.1016/S0006-291X(03)00817-9

De Angelis, C. (2008). Side effects related to systemic cancer treatment: are we changing the Promethean experience with molecularly targeted therapies? *Current Oncology (Toronto, Ont.)*, *15*(4), 198–9.

De Gruijl, F. R., van Kranen, H. J., & Mullenders, L. H. . (2001). UV-induced DNA damage, repair, mutations and oncogenic pathways in skin cancer. *Journal of Photochemistry and Photobiology B: Biology*, *63*(1-3), 19–27. doi:10.1016/S1011-1344(01)00199-3

Detty, M. R., Gibson, S. L., & Wagner, S. . (2004). Current clinical and preclinical photosensitizers for use in photodynamic therapy. *Journal of Medicinal Chemistry*, *47*(16).

Dietrich, C., Wallenfang, K., Oesch, F., & Wieser, R. (1997). Differences in the mechanisms of growth control in contact-inhibited and serum-deprived human fibroblasts. *Oncogene*, *15*(22), 2743–7. doi:10.1038/sj.onc.1201439

Dolmans, D. E. J. G. J., Fukumura, D., & Jain, R. K. (2003). Photodynamic therapy for cancer. *Nature Reviews. Cancer*, *3*(5), 380–7. doi:10.1038/nrc1071

Du, H., Li, Y., Olivo, M., Yip, G. W., & Bay, B. (2006). Differential up-regulation of metallothionein isoforms in well-differentiated nasopharyngeal cancer cells in vitro by photoactivated hypericin. *Oncology Reports*, *16*, 1397–1402.

Ehmann, L. M., Heinemann, V., & Wollenberg, A. (2011). [New tyrosine kinase and EGFR inhibitors in cancer therapy. Cardiac and skin toxicity as relevant side effects. Part B: Skin]. *Der Internist*, *52*(11), 1359–64. doi:10.1007/s00108-011-2896-2

Engel, Ryan, H. (2006). Oxidative stress and apoptosis: a new treatment paradigm in cancer. *Frontiers in Bioscience*, *11*(1), 300. doi:10.2741/1798

Fadeel, B., Zhivotosky, B., & Orrenius, S. (1999). All along the watchtower: on the regulation of apoptosis regulators. *FASEB J*, *13*(13), 1647–1657.

Ferenc, P., Solár, P., Kleban, J., Mikes, J., & Fedorocko, P. (2010). Down-regulation of Bcl-2 and Akt induced by combination of photoactivated hypericin and genistein in human breast cancer cells. *Journal of Photochemistry and Photobiology. B, Biology*, *98*(1), 25–34. doi:10.1016/j.jphotobiol.2009.10.004

Fiers, W., Beyaert, R., Declercq, W., & Vandenabeele, P. (1999). More than one way to die: apoptosis, necrosis and reactive oxygen damage. *Oncogene*, *18*(54), 7719–30. doi:10.1038/sj.onc.1203249

Frantz, C., Stewart, K. M., & Weaver, V. M. (2010). The extracellular matrix at a glance. *Journal of Cell Science*, *123*(Pt 24), 4195–200. doi:10.1242/jcs.023820

Freak, J. (2004). Promoting knowledge and awareness of skin cancer. *Nursing Standard*, *18*(35), 45 – 53.

Fukunaga-Kalabis, M., & Herlyn, M. (2012). Beyond ABC: another mechanism of drug resistance in melanoma side population. *The Journal of Investigative Dermatology*, *132*(10), 2317–9. doi:10.1038/jid.2012.220

Garg, A. D., & Agostinis, P. (2014). ER stress, autophagy and immunogenic cell death in photodynamic therapy- induced anti-cancer immune responses. *Photochemical & Photobiological Sciences : Official Journal of the European Photochemistry Association and the European Society for Photobiology*, *13*, 474–487. doi:10.1039/c3pp50333j

Garg, A. D., Dudek, A. M., Ferreira, G. B., Verfaillie, T., Vandenabeele, P., Krysko, D. V, … Agostinis, P. (2013). ROS-induced autophagy in cancer cells assists in evasion from determinants of immunogenic cell death. *Autophagy*, *9*(9).

Gerschenson, L., & Rotello, R. (1992). Apoptosis: a different type of cell death. *FASEB J*, *6*(7), 2450–2455.

Gordon, P. R., Mansur, C. P., & Gilchrest, B. A. (1989). Regulation of Human Melanocyte Growth, Dendricity, and Melanization by Keratinocyte Derived Factors. *Journal of Investigative Dermatology*, *92*(4), 565–572. doi:10.1111/1523-1747.ep12709595

Gray Schopfer, V., Wellbrock, C., & Marais, R. (2007). Melanoma biology and new targeted therapy. *Nature*, *445*(7130), 851 – 857.

Green, D. R., & Walczak, H. (2013). Apoptosis therapy : driving cancers down the road to ruin. *Nature Medicine*, *19*(2), 131–133. doi:10.1038/nm.3076

Gyenge, E. B., Forny, P., Lüscher, D., Laass, A., Walt, H., & Maake, C. (2012). Effects of hypericin and a chlorin based photosensitizer alone or in combination in squamous cell carcinoma cells in the dark. *Photodiagnosis and Photodynamic Therapy*, *9*(4), 321–31. doi:10.1016/j.pdpdt.2012.03.006

Gyenge, Emina, B., Lüscher, D., Forny, P., Antoniol, M., Geisberger, G., Walt, H., … Maake, C. (2013). Photodynamic mechanisms induced by a combination of hypericin and a chlorin based-photosensitizer in head and neck squamous cell carcinoma cells. *Photochemistry and Photobiology*, *89*(1), 150–62. doi:10.1111/j.1751-1097.2012.01217.x

Haass, N. K., & Herlyn, M. (2005). Normal human melanocyte homeostasis as a paradigm for understanding melanoma. *The Journal of Investigative Dermatology. Symposium Proceedings / the Society for Investigative Dermatology, Inc. [and] European Society for Dermatological Research*, *10*(2), 153–63. doi:10.1111/j.1087-0024.2005.200407.x

Hadjur, C., Richard, M. J., Parat, M. O., Favier, A., & Jardon, P. (1995). Photodynamically induced cytotoxicity of hypericin dye on human fibroblast cell line MRC5. *Journal of Photochemistry and Photobiology. B, Biology*, *27*(2), 139–46.

Hadjur, C., Richard, M. J., Parat, M. O., Jardon, P., & Favier, A. (1996). Photodynamic effects of hypericin on lipid peroxidation and antioxidant status in melanoma cells. *Photochemistry and Photobiology*, *64*(2), 375–81.

Halaban, R. (1988). Basic fibroblast growth factor from human keratinocytes is a natural mitogen for melanocytes. *The Journal of Cell Biology*, *107*(4), 1611–1619. doi:10.1083/jcb.107.4.1611

Halaban, R. (2000). The Regulation of Normal Melanocyte Proliferation. *Pigment Cell Research*, *13*(1), 4–14. doi:10.1034/j.1600-0749.2000.130103.x

Hamblin, M., & Huang, Y.-Y. (2013). *Handbook of Photomedicine* (p. 886). CRC Press.

Head, C. S., Luu, Q., Sercarz, J., & Saxton, R. (2006). Photodynamic therapy and tumor imaging of hypericin-treated squamous cell carcinoma. *World Journal of Surgical Oncology*, *4*, 87. doi:10.1186/1477-7819-4-87

Hearing, V. J. (2005). Biogenesis of pigment granules: a sensitive way to regulate melanocyte function. *Journal of Dermatological Science*, *37*(1), 3–14. doi:10.1016/j.jdermsci.2004.08.014

Hengartner, M. O. (2000). The biochemistry of apoptosis. *Nature*, *407*(6805), 770 – 776.

Hirobe, T. (2005). Role of keratinocyte-derived factors involved in regulating the proliferation and differentiation of mammalian epidermal melanocytes. *Pigment Cell Research / Sponsored by the European Society for Pigment Cell Research and the International Pigment Cell Society*, *18*(1), 2–12. doi:10.1111/j.1600-0749.2004.00198.x

Holland, D. B., Roberts, S. G., Wood, E. J., & Cunliffe, W. J. (1993). Cold Shock Induces the Synthesis of Stress Proteins in Human Keratinocytes. *Journal of Investigative Dermatology*, *101*(2), 196–199. doi:10.1111/1523-1747.ep12363791

Hopper, C. (2000). Photodynamic therapy: a clinical reality in the treatment of cancer. *The Lancet Oncology*, *1*(4), 212–219. doi:10.1016/S1470-2045(00)00166-2

Huntosova, V., Nadova, Z., Dzurova, L., Jakusova, V., Sureau, F., & Miskovsky, P. (2012). Cell death response of U87 glioma cells on hypericin photoactivation is mediated by dynamics of hypericin subcellular distribution and its aggregation in cellular organelles. *Photochemical & Photobiological Sciences : Official Journal of the European Photochemistry Association and the European Society for Photobiology*, *11*(9), 1428–36. doi:10.1039/c2pp05409d

Imokawa, G., Yada, Y., & Miyagishi, M. (1992). Endothelins secreted from human keratinocytes are intrinsic mitogens for human melanocytes. *J. Biol. Chem.*, *267*(34), 24675–24680.

Jäättelä, M. (2009). Heat shock proteins as cellular lifeguards. *Annals of Medicine*, *31*(4), 261–271.

Jori, G., & Reddi, E. (1993). The role of lipoproteins in the delivery of tumour-targeting photosensitizers. *International Journal of Biochemistry*, *25*(10), 1369–1375. doi:10.1016/0020-711X(93)90684-7

Joshi, P. G., Nair, N., Begum, G., Joshi, N. B., Sinkar, V. P., & Vora, S. (2007). Melanocyte-keratinocyte interaction induces calcium signalling and melanin transfer to keratinocytes. *Pigment Cell Research / Sponsored by the European Society for Pigment Cell Research and the International Pigment Cell Society*, *20*(5), 380–4. doi:10.1111/j.1600-0749.2007.00397.x

Junttila, M. R., & de Sauvage, F. J. (2013). Influence of tumour micro-environment heterogeneity on therapeutic response. *Nature*, *501*(7467), 346–54. doi:10.1038/nature12626

Kacerovská, D., Pizinger, K., Majer, F., & Smíd, F. (2008). Photodynamic therapy of nonmelanoma skin cancer with topical hypericum perforatum extract--a pilot study. *Photochemistry and Photobiology*, *84*(3), 779–85. doi:10.1111/j.1751-1097.2007.00260.x

Kamuhabwa, A. R., Agostinis, P., D'Hallewin, M. A., Kasran, A., & de Witte, P. A. (2000). Photodynamic activity of hypericin in human urinary bladder carcinoma cells. *Anticancer Research*, *20*(4), 2579–84.

Karioti, A., & Bilia, R. A. (2010). Hypericins as potential leads for new therapeutics. *International Journal of Molecular Sciences*, *11*(2), 562 – 594.

Karrer, S., Szeimies, R.-M., Hohenleutner, U., & Landthaler, M. (2001). Role of Lasers and Photodynamic Therapy in the Treatment of Cutaneous Malignancy. *American Journal of Clinical Dermatology*, *2*(4), 229–237. doi:10.2165/00128071-200102040-00004

Kashef, N., Borghei, Y. S., & Djavid, G. E. (2013). Photodynamic effect of hypericin on the microorganisms and primary human fibroblasts. *Photodiagnosis and Photodynamic Therapy*, *10*(2), 150–5. doi:10.1016/j.pdpdt.2012.11.007

Kerr, J. F., Wyllie, A. H., & Currie, A. R. (1972). Apoptosis: a basic biological phenomenon with wide-ranging implications in tissue kinetics. *British Journal of Cancer*, *26*(4), 239–57.

Kiesslich, T., Krammer, B., & Plaetzer, K. (2006). Cellular mechanisms and prospective applications of hypericin in photodynamic therapy. *Current Medicinal Chemistry*, *13*(18), 2189–204.

Kleban, J., Szilárdiová, B., Mikes, J., Horváth, V., Sacková, V., Brezáni, P., … Fedorocko, P. (2006). Pre-treatment of HT-29 cells with 5-LOX inhibitor (MK-886) induces changes in cell cycle and increases apoptosis after photodynamic therapy with hypericin. *Journal of Photochemistry and Photobiology. B, Biology*, *84*(2), 79–88. doi:10.1016/j.jphotobiol.2006.02.003

Kleemann, B., Loos, B., Lang, D., Scriba, T., & Davids, L. (2014). St John's Wort (Hypericum perforatum L.) Photomedicine: Hypericin-Photodynamic Therapy induces Metastatic Melanoma Cell Death. *PloS One*, *Accepted*.

Kohen, R. (1999). Skin antioxidants: their role in aging and in oxidative stress--new approaches for their evaluation. *Biomedicine & Pharmacotherapy = Biomédecine & Pharmacothérapie*, *53*(4), 181–92. doi:10.1016/S0753-3322(99)80087-0

Konan, Y. N., Gurny, R., & Allémann, E. (2002). State of the art in the delivery of photosensitizers for photodynamic therapy. *Journal of Photochemistry and Photobiology B: Biology*, *66*(2), 89–106. doi:10.1016/S1011-1344(01)00267-6

Krammer, B., & Verwanger, T. (2012). Molecular Response to Hypericin-Induced Photodamage. *Current Medical Chemistry*, *19*(6), 793–798.

Kubin, A., Loew, H. G., Burner, U., Jessner, G., Kolbabek, H., & Wierrani, F. (2008). How to make hypericin water-soluble. *Die Pharmazie*, *63*(4), 263–9.

Kubin, A., Wierrani, F., Burner, U., Ualth, G., & Grünberger, W. (2005). Hypericin--the facts about a controversial agent. *Current Pharmaceutical Design*, *11*(2), 233–53.

Langer, M., Flores-Genger, H., Sevelda, P., Fiegl, J., Ringler, M., & Kubista, E. (1989). [Side effects of adjuvant therapies of breast cancer: their significance for the patient]. *Wiener Klinische Wochenschrift*, *101*(4), 134–8.

Lauth, M., Unden, A. B., & Toftgård, R. (2004). Non-melanoma skin cancer: pathogenesis and mechanisms. *Drug Discovery Today: Disease Mechanisms*, *1*(2), 267–272. doi:10.1016/j.ddmec.2004.09.005

Lavie, G., Mazur, Y., Lavie, D., & Meruelo, D. (1995). The chemical and biological properties of hypericin—a compound with a broad spectrum of biological activities. *Medicinal Research Reviews*, *15*(2), 111–119. doi:10.1002/med.2610150203

Lens, M. B., & Dawes, M. (2004). Global perspectives of contemporary epidemiological trends of cutaneous malignant melanoma. *British Journal of Dermatology*, *150*(2), 179 – 185.

Levine, B., & Klionsky, D. J. (2004). Development by Self-DigestionMolecular Mechanisms and Biological Functions of Autophagy. *Developmental Cell*, *6*(4), 463–477. doi:10.1016/S1534-5807(04)00099-1

Maes, H., Rubio, N., Garg, A. D., & Agostinis, P. (2013). Autophagy: shaping the tumor microenvironment and therapeutic response. *Trends in Molecular Medicine*, *19*(7), 428–46. doi:10.1016/j.molmed.2013.04.005

Mang, T. S. (2004). Lasers and light sources for PDT: past, present and future. *Photodiagnosis and Photodynamic Therapy*, *1*(1), 43–48. doi:10.1016/S1572-1000(04)00012-2

Marino, G., Niiso-Santo, M., Baechrecke, E. . H., & Guido, K. (2014). Self-consumption: the interplay of autophagy and apoptosis. *Nature Reviews.*

Molecular Cell Biology, *15*(2), 81–94. doi:10.1038/nrm3735.Self-consumption

Martin, K., & Barrett, J. (2002). Reactive oxygen species as double-edged swords in cellular processes: low-dose cell signaling versus high-dose toxicity. *Human & Experimental Toxicology*, *21*(2), 71–75. doi:10.1191/0960327102ht213oa

Matés, J. M., Segura, J. A., Alonso, F. J., & Márquez, J. (2008). Intracellular redox status and oxidative stress: implications for cell proliferation, apoptosis, and carcinogenesis. *Archives of Toxicology*, *82*(5), 273–99. doi:10.1007/s00204-008-0304-z

Maytin, E. V. (1992). Differential effects of heat shock and UVB light upon stress protein expression in epidermal keratinocytes. *J. Biol. Chem.*, *267*(32), 23189–23196.

Melnikova, V. O., & Ananthaswamy, H. N. (2005). Cellular and molecular events leading to the development of skin cancer. *Mutation Research*, *571*(1-2), 91–106. doi:10.1016/j.mrfmmm.2004.11.015

Meyskens Jr., F. L., Farmer, P., & Fruehauf, J. P. (2001). Redox Regulation in Human Melanocytes and Melanoma. *Pigment Cell Research*, *14*(3), 148–154. doi:10.1034/j.1600-0749.2001.140303.x

Mikeš, J., Jendželovský, R., & Fedoročko, P. (2013). *Cellular Aspects of Photodynamic Therapy with Hypericin*.

Miller, A. J., & Mihm, M. C. (2006). Mechanisms of Disease Melanoma. *The New England Journal of Medicine*, *355*(1), 51–65.

Miller, A. L. (1998). St. John's Wort (Hypericum perforatum): clinical effects on depression and other conditions. *Alternative Medicine Review : A Journal of Clinical Therapeutic*, *3*(1), 18–26.

Moan, J., & Berg, K. (1991). The photodegrdation of Porphyrins in cells can be used to estimate the lifetime of singlet oxygen. *Photochemistry and Photobiology*, *53*(4), 549–553. doi:10.1111/j.1751-1097.1991.tb03669.x

Mojzisova, H., Bonneau, S., & Brault, D. (2007). Structural and physico-chemical determinants of the interactions of macrocyclic photosensitizers with cells. *European Biophysics Journal : EBJ*, *36*(8), 943–53. doi:10.1007/s00249-007-0204-9

Morton, C. A., McKenna, K. E., & Rhodes, L. E. (2008). Guidelines for topical photodynamic therapy: update. *The British Journal of Dermatology*, *159*(6), 1245–66. doi:10.1111/j.1365-2133.2008.08882.x

Mottaz, J. H., & Zelickson, A. S. (1967). Melanin Transfer: A Possible Phagocytic Process1. *The Journal of Investigative Dermatology*, *49*(6), 605–610. doi:10.1038/jid.1967.187

Nahrstedt, A., & Butterweck, V. (2010). Lessons learned from herbal medicinal products: the example of St. John's Wort (perpendicular). *Journal of Natural Products*, *73*(5), 1015–21. doi:10.1021/np1000329

Nakazawa, K., Nakazawa, H., Collombel, C., & Damour, O. (1995). Keratinocyte Extracellular Matrix-Mediated Regulation of Normal Human Melanocyte Functions. *Pigment Cell Research*, *8*(1), 10–18. doi:10.1111/j.1600-0749.1995.tb00769.x

Narayanan, D. L., Saladi, R. N., & Fox, J. L. (2010). Ultraviolet radiation and skin cancer. *International Journal of Dermatology*, *49*(9), 978–86. doi:10.1111/j.1365-4632.2010.04474.x

Oleinick, N. L., & Evans, H. H. (2010). The Photobiology of Photodynamic Therapy: Cellular Targets and Mechanisms.

Ortonne, J.-P. (2002). Photoprotective properties of skin melanin. *British Journal of Dermatology*, *146*(s61), 7–10. doi:10.1046/j.1365-2133.146.s61.3.x

Otten, J., Johnson, G. S., & Pastan, I. (1971). Cyclic AMP levels in fibroblasts: Relationship to growth rate and contact inhibition of growth. *Biochemical and Biophysical Research Communications*, *44*(5), 1192–1198. doi:10.1016/S0006-291X(71)80212-7

Ouyang, L., Shi, Z., Zhao, S., Wang, F.-T., Zhou, T.-T., Liu, B., & Bao, J.-K. (2012). Programmed cell death pathways in cancer: a review of apoptosis, autophagy and programmed necrosis. *Cell Proliferation*, *45*(6), 487–98. doi:10.1111/j.1365-2184.2012.00845.x

Pfeifer, G. P., & Besaratinia, A. (2012). UV wavelength-dependent DNA damage and human non-melanoma and melanoma skin cancer. *Photochemical & Photobiological Sciences : Official Journal of the European Photochemistry Association and the European Society for Photobiology*, *11*(1), 90–7. doi:10.1039/c1pp05144j

Picardo, M., Grammatico, P., Roccella, F., Roccella, M., Grandinetti, M., del Porto, G., & Passi, S. (1996). Imbalance in the Antioxidant Pool in Melanoma Cells and Normal Melanocytes from Patients with Melanoma.

Journal of Investigative Dermatology, *107*(3), 322–326. doi:10.1111/1523-1747.ep12363163

Plaetzer, K., Krammer, B., Berlanda, J., Berr, F., & Kiesslich, T. (2009). Photophysics and photochemistry of photodynamic therapy: fundamental aspects. *Lasers in Medical Science*, *24*(2), 259–68. doi:10.1007/s10103-008-0539-1

Powell, J., & Soon, C. (2002). Physiology of the Skin. *Surgery (Oxford)*, *20*(6), ii–vi. doi:10.1383/surg.20.6.0.14639

Quail, D. F., & Joyce, J. A. (2013). Microenvironmental regulation of tumor progression and metastasis. *Nature Medicine*, *19*(11), 1423–37. doi:10.1038/nm.3394

Rezusta, A., López-Chicón, P., Paz-Cristobal, M. P., Alemany-Ribes, M., Royo-Díez, D., Agut, M., … Gilaberte, Y. (2012). In vitro fungicidal photodynamic effect of hypericin on Candida species. *Photochemistry and Photobiology*, *88*(3), 613–9. doi:10.1111/j.1751-1097.2011.01053.x

Robertson, C. A., Evans, D. H., & Abrahamse, H. (2009). Photodynamic therapy (PDT): a short review on cellular mechanisms and cancer research applications for PDT. *Journal of Photochemistry and Photobiology. B, Biology*, *96*(1), 1–8. doi:10.1016/j.jphotobiol.2009.04.001

Ross, K., Cherpelis, B., Lien, M., & Fenske, N. (2013). Spotlighting the role of photodynamic therapy in cutaneous malignancy: an update and expansion. *Dermatologic Surgery : Official Publication for American Society for Dermatologic Surgery [et Al.]*, *39*(12), 1733–44. doi:10.1111/dsu.12319

Rubio, N. N., Coupienne, I., Di Valentin, E., Heirman, I., Grooten, J., Piette, J., … Valentin, E. Di. (2012). Spatiotemporal autophagic degradation of oxidatively damaged organelles after photodynamic stress is amplified by mitochondrial reactive oxygen species. *Autophagy*, *8*(9), 1312–24. doi:10.4161/auto.20763

Sacková, V., Fedorocko, P., Szilárdiová, B., Mikes, J., & Kleban, J. (2006). Hypericin-induced photocytotoxicity is connected with G2/M arrest in HT-29 and S-phase arrest in U937 cells. *Photochemistry and Photobiology*, *82*(5), 1285–91. doi:10.1562/2006-02-22-RA-806

Sander, C. S., Chang, H., Hamm, F., Elsner, P., & Thiele, J. J. (2004). Role of oxidative stress and the antioxidant network in cutaneous carcinogenesis. *International Journal of Dermatology*, *43*(5), 326–35. doi:10.1111/j.1365-4632.2004.02222.x

Sanovic, R., Krammer, B., Grumboeck, S., & Verwanger, T. (2009). Time-resolved gene expression profiling of human squamous cell carcinoma cells during the apoptosis process induced by photodynamic treatment with hypericin. *International Journal of Oncology*, *35*(4), 921–39.

Saraste, A. (2000). Morphologic and biochemical hallmarks of apoptosis. *Cardiovascular Research*, *45*(3), 528–537. doi:10.1016/S0008-6363(99)00384-3

Schallreuter, K. U. (2007). Advances in melanocyte basic science research. *Dermatologic Clinics*, *25*(3), 283–91, vii. doi:10.1016/j.det.2007.04.010

Schempp, C. M., Simon-haarhaus, B., Termeer, C. C., & Simon, J. C. (2001). Hypericin photo-induced apoptosis involves the tumor necrosis factor-related apoptosis-inducing ligand (TRAIL) and activation of. *Cell Proliferation*, *493*, 26–30.

Scott, G., Leopardi, S., Printup, S., & Madden, B. C. (2002). Filopodia are conduits for melanosome transfer to keratinocytes. *J. Cell Sci.*, *115*(7), 1441–1451.

Seiberg, M. (2001). Keratinocyte-Melanocyte Interactions During Melanosome Transfer. *Pigment Cell Research*, *14*(4), 236–242. doi:10.1034/j.1600-0749.2001.140402.x

Seitz, G., Krause, R., Fuchs, J., Heitmann, H., Armeanu, S., Ruck, P., & Warmann, S. W. (2008). In vitro photodynamic therapy in pediatric epithelial liver tumors promoted by hypericin, 1277–1282. doi:10.3892/or

Sharma, K. V, Bowers, N., & Davids, L. M. (2011). Photodynamic therapy-induced killing is enhanced in depigmented metastatic melanoma cells. *Cell Biology International*, *35*(9), 939–44. doi:10.1042/CBI20110103

Sharma, K. V, & Davids, L. M. (2012). Hypericin-PDT-induced rapid necrotic death in human squamous cell carcinoma cultures after multiple treatment. *Cell Biology International*, *36*(12), 1261–6. doi:10.1042/CBI20120108

Sharma, K. V, Davids, L. M., & Krishna V. Sharma and Lester M.Davids. (2012). Depigmentation in melanomas increases the efficacy of hypericin-mediated photodynamic-induced cell death. *Photodiagnosis and Photodynamic Therapy*, *9*(2), 156–63. doi:10.1016/j.pdpdt.2011.09.003

Shen, S., Kepp, O., & Kroemer, G. (2012). The end of autophagic cell death? *Autophagy*, *8*(January), 1–3.

Shindo, Y., Witt, E., Han, D., Epstein, W., & Packer, L. (1994). Enzymic and Non-Enzymic Antioxidants in Epidermis and Dermis of Human Skin. *Journal of Investigative Dermatology*, *102*(1), 122–124. doi:10.1111/1523-1747.ep12371744

Siboni, G., Weitman, H., Freeman, D., Mazur, Y., Malik, Z., & Ehrenberg, B. (2002). The correlation between hydrophilicity of hypericins and helianthrone: internalization mechanisms, subcellular distribution and photodynamic action in colon carcinoma cells. *Photochemical & Photobiological Sciences*, *1*(7), 483–491. doi:10.1039/b202884k

Silverberg, M. J., Leyden, W., Warton, E. M., Quesenberry, C. P., Engels, E. A., & Asgari, M. M. (2013). HIV infection status, immunodeficiency, and the incidence of non-melanoma skin cancer. *Journal of the National Cancer Institute*, *105*(5), 350–60. doi:10.1093/jnci/djs529

Simon, H.-U., Haj-Yehia, A., & Levi-Schaffer, F. (2000). Role of reactive oxygen species (ROS) in apoptosis induction. *Apoptosis*, *5*(5), 415–418. doi:10.1023/A:1009616228304

Skalkos, D., Gioti, E., Stalikas, C. D., Meyer, H., Papazoglou, T. G., & Filippidis, G. (2006). Photophysical properties of Hypericum perforatum L. extracts--novel photosensitizers for PDT. *Journal of Photochemistry and Photobiology. B, Biology*, *82*(2), 146–51. doi:10.1016/j.jphotobiol.2005.11.001

Splinter, R., & Hooper, B. A. (2007). *An introduction to biomedical optics. Ty*. Taylor&Francis.

Stapleton, M., & Rhodes, L. (2003). Photosensitizers for photodynamic therapy of cutaneous disease. *Journal of Dermatological Treatment*, *14*(2), 107–112. doi:10.1080/09546630310012127

Svanberg, K., Andersson, T., Killander, D., Wang, I., Stenram, U., Andersson-Engels, S., … Svanberg, S. (1994). Photodynamic therapy of non-melanoma malignant tumours of the skin using topical δ-amino levulinic acid sensitization and laser irradiation. *British Journal of Dermatology*, *130*(6), 743–751. doi:10.1111/j.1365-2133.1994.tb03412.x

Swalwell, H., Latimer, J., Haywood, R. M., & Birch-Machin, M. A. (2012). Investigating the role of melanin in UVA/UVB- and hydrogen peroxide-induced cellular and mitochondrial ROS production and mitochondrial DNA damage in human melanoma cells. *Free Radical Biology & Medicine*, *52*(3), 626–34. doi:10.1016/j.freeradbiomed.2011.11.019

Tan, S., Wood, M., & Maher, P. (2002). Oxidative Stress Induces a Form of Programmed Cell Death with Characteristics of Both Apoptosis and Necrosis in Neuronal Cells. *Journal of Neurochemistry*, *71*(1), 95–105. doi:10.1046/j.1471-4159.1998.71010095.x

Theodossiou, T. A., Hothersall, J. S., Witte, P. A. De, Pantos, A., & Agostinis, P. (2009). The Multifaceted Photocytotoxic Profile of Hypericin. *Molecular Pharmaceutics*, *6*(6), 1775–1789. doi:10.1021/mp900166q

Thompson, J. F., Scolyer, R. A., & Kefford, R. F. (2005). Cutaneous melanoma. *Lancet*, *365*(9460), 687–701. doi:10.1016/S0140-6736(05)17951-3

Tobin, D. J. (2006). Biochemistry of human skin--our brain on the outside. *Chemical Society Reviews*, *35*(1), 52–67. doi:10.1039/b505793k

Traynor, N. J., Beattie, P. E., Ibbotson, S. H., Moseley, H., Ferguson, J., & Woods, J. A. (2005). Photogenotoxicity of hypericin in HaCaT keratinocytes: implications for St. John's Wort supplements and high dose UVA-1 therapy. *Toxicology Letters*, *158*(3), 220–4. doi:10.1016/j.toxlet.2005.03.012

Valyi-Nagy, I. T., Murphy, G. F., Mancianti, M. L., Whitaker, D., & Herlyn, M. (1990). Phenotypes and interactions of human melanocytes and keratinocytes in an epidermal reconstruction model. *Laboratory Investigation; a Journal of Technical Methods and Pathology*, *62*(3), 314–24.

Van de Putte, M., Roskams, T., Vandenheede, J. R., Agostinis, P., & de Witte, P. A. M. (2005). Elucidation of the tumoritropic principle of hypericin. *British Journal of Cancer*, *92*(8), 1406–13. doi:10.1038/sj.bjc.6602512

Van Den Bossche, K., Naeyaert, J.-M., & Lambert, J. (2006). The quest for the mechanism of melanin transfer. *Traffic (Copenhagen, Denmark)*, *7*(7), 769–78. doi:10.1111/j.1600-0854.2006.00425.x

Vandenabeele, P., Galluzzi, L., Vanden Berghe, T., & Kroemer, G. (2010). Molecular mechanisms of necroptosis: an ordered cellular explosion. *Nature Reviews. Molecular Cell Biology*, *11*(10), 700–14. doi:10.1038/nrm2970

Vandongen, G., Visser, G., & Vrouenraets, M. (2004). Photosensitizer-antibody conjugates for detection and therapy of cancer. *Advanced Drug Delivery Reviews*, *56*(1), 31–52. doi:10.1016/j.addr.2003.09.003

Vantieghem, A. (1998). Hypericin-induced photosensitization of HeLa cells leads to apoptosis or necrosis Involvement of cytochrome c and procaspase-3 activation in the mechanism of apoptosis. *FEBS Letters*, *440*(1-2), 19–24. doi:10.1016/S0014-5793(98)01416-1

Vantieghem, A., Xu, Y., Declercq, W., Vandenabeele, P., Denecker, G., Vandenheede, J. R., … Witte, P. A. De. (2007). Different Pathways Mediate Cytochrome c Release After Photodynamic Therapy with Hypericin. *Photochemistry and Photobiology*, *74*(2), 133–142. doi:10.1562/0031-8655(2001)0740133DPMCCR2.0.CO2

Vittar, N. B. R., Lamberti, M., Pansa, M. F., Vera, R. E., Rodriguez, M. E., Cogno, I. S., … Rivarola, V. A. (2013). Ecological photodynamic therapy : New trend to disrupt the intricate networks within tumor ecosystem. *BBA - Reviews on Cancer*, *1835*(1), 86–99. doi:10.1016/j.bbcan.2012.10.004

Vittar, N. R., Lamberti, M. J., Pansa, M. F., Vera, R. E., Rodriguez, M. E., Cogno, I. S., … Vittar, R. (2013). Direct and indirect photodynamic therapy effects on the cellular and molecular components of the tumor microenvironment. *BBA - Reviews on Cancer*, *1835*(1), 86–99. doi:10.1016/j.bbcan.2012.10.004

Vo-Dinh, T. (2003). *Biomedical Photonics Handbook* (p. 1872). CRC Press.

Wan, M. T., & Lin, J. Y. (2014). Current evidence and applications of photodynamic therapy in dermatology. *Clinical, Cosmetic and Investigational Dermatology*, *7*, 145–63. doi:10.2147/CCID.S35334

Wang, X.-L., Wang, H.-W., Guo, M.-X., & Xu, S.-Z. (2008). Treatment of skin cancer and pre-cancer using topical ALA-PDT--a single hospital experience. *Photodiagnosis and Photodynamic Therapy*, *5*(2), 127–33. doi:10.1016/j.pdpdt.2008.05.003

Wood, J. M., Jimbow, K., Boissy, R. E., Slominski, A., Plonka, P. M., Slawinski, J., … Tosk, J. (1999). What's the use of generating melanin? *Experimental Dermatology*, *8*(2), 153–164. doi:10.1111/j.1600-0625.1999.tb00365.x

Zeitouni, N., Oseroff, A., & Shieh, S. (2003). Photodynamic therapy for nonmelanoma skin cancers Current review and update. *Molecular Immunology*, *39*(17-18), 1133–1136. doi:10.1016/S0161-5890(03)00083-X

Zhao, B., & He, Y.-Y. (2010). Recent advances in the prevention and treatment of skin cancer using photodynamic therapy. *Expert Review of Anticancer Therapy*, *10*(11), 1797–809. doi:10.1586/era.10.154

Zobayed, S. M. A., Afreen, F., Goto, E., & Kozai, T. (2006). Plant-environment interactions: Accumulation of hypericin in dark glands of Hypericum perforatum. *Annals of Botany*, *98*(4), 793–804. doi:10.1093/aob/mcl169

Websites:

http://kids.britannica.com/elementary/art-89672/Human-skin-has-three-layers-the-epidermis-the-dermis-and

http://droualb.faculty.mjc.edu/Lecture%20Notes/Unit%201/Integumentary%20with%20figures.html

Appendix A: Solutions

1.12.1. Separating Epidermis and Dermis from Skin Tissue

Work in a petri-dish in a drop of 1xPBS and antibiotics

Gently grasp epidermis layer with forceps tip

Hold Dermis in place with tweezers

Gently pull the epidermis away from the dermis in one movement

1.13.

1.13.1. Dulbecco's Modified Eagle's Medium (DMEM) (pH 7.4, 1L)

DMEM powder	27.06g

$NaHCO_3$	7.4g
Autoclaved ddH_20	qs

Sterilize through a 0.2µm filter and store in aliquots at 4°C

1.13.2. Fetal Calf Serum (FCS) (500ml)

FCS	500ml

Heat inactivate at 56°C (water bath) for 20 minutes

Allow to cool and store in aliquots at -20°C

1.13.3. Penicillin (100U/ml)/Streptomycin (100µg/ml)

Penicillin (1662U/mg)	3g
Streptomycin (750U/mg)	5g
ddH_20	100ml

Sterilize through a 0.2µm filter and store aliquots at -20°C

1.13.4. Trypsin (0.05%) Supplemented with 0.1% Glucose (100ml) (pH 7.3)

Trypsin (BD Biosciences, USA)	0.05g
Glucose	0.1g
ddH_2O	100ml

sterilize through a 0.2µm filter and store at -20°C

1.13.5. Complete Fibroblast Medium (400ml) (pH 7.4)

FCS (100%)	40ml
Penicillin/streptomycin (100x)	4ml
DMEM	qs

sterilize through a 0.2µm filter and store at 4°C

1.13.6. Ham's F10 (500ml)

Hams F10 powder	4.93g
$NaHCO_3$	0.2g

sterilize through a 0.2µm filter and store at 4°C

1.13.7. Complete Melanocyte Specific Medium (FETI) (500ml) (p.H 7.4)

FCS (Lonza)	10ml
Ultroser G	5ml
bFGF (10µg/ml)	100µl
Endothelin (10µg/ml)	100µl
TPA (40µM)	200µl
IBMX (5mM)	5ml
Penicillin/Streptomycin	5ml
Ham's F10	ds

sterilize through a 0.2µm filter and store at -20°C

1.13.8. Complete Keratinocyte Specific Medium (KSFM) Gibco® (500ml)

KSFM (synthetically defined keratinocyte medium)	500ml
Bovine pituitary extract (BPE) Gibco®	25mg
Epidermal growth factor (EGF) Gibco ®	2.5µg/ml
Penicillin/streptomycin (100X)	5ml

sterilize through a 0.2µm filter and store at -20°C

1.13.9. Ham's F12 (700ml)

Ham's F12 Gibco®	1.86g
ddH_2O	sq

sterilize through a 0.2µm filter and store at 4°C

1.13.10. GREEN'S Medium for Keratinocytes (400ml) (pH 7.3)

Ham's F12	100ml
Insulin (3.85mg/ml)	500µl
Hydrocortisone (0.2mg/ml)	800µl
Cholera Toxin ($1x10^{-7}$M)	400µl
T/T3 (5mg/ml)	400µl
EFG (10µg/ml)	400µl
Penicillin/ Streptomycin (100X)	4ml
Gentamycin (10mg/ml, 1%)	8ml
Sodium Bicarbonate (7.5% a.q.)	4ml
Hepes Buffer (1M) (pH 7.3)	8ml
FCS (Lonza) (IH)	40ml
Ham's F12	sq

sterilize through a 0.2µm filter and store at -20°C

1.13.11. Trypsin/ EDTA (100ml)

Trypsin (0.05%) (BD, Biosciences, USA)	0.05g
EDTA anhydrous (0.02%) (Sigma-Aldrich, USA)	0.02g
ddH_2O	100ml

sterilize through a 0.2µm filter and store at -20°C

1.13.12. Phosphate Buffered Saline (1xPBS) (pH 7.4) (1L)

NaCl (0.14M)	8g
Na_2HPO_4 (8.8M)	1.26g
KCl (2.7M)	0.2g

KH_2PO_4 (1.47M)	0.2g
ddH_2O	qs

Autoclave and store at 4°C

1.13.13. Mycoplasma Test (Hoechst Dye)

Grow cells on coverslips for a period of 7 days without antibiotics

Remove culture medium

Wash with 1xPBS

Fix cells with 1ml glacial acetic acid : methanol (1:3) for 6 mins

Discard Hoechst and wash cells 3X with 1xPBS

Mount coverslips onto glass slides in Mowiol

View slides using fluorescent microscopy

1.14. Hypericin-Induced Photodynamic Therapy (HYP-PDT)

1.15.

1.15.1. Hypericin (HYP) Stock Solution (2mM)

Hypericin powder	1mg
Dimethyl sulfoxide (100%)	1ml

1.16. Fluorescence Based ROS Assay

1.17.

1.17.1. DCF-DA Working Stock Solution Preparation (1mM)

DCF-DA (100mM)	10µl
1xPBS	990µl

1.18. Microscopy Slide Preparation

1.19.

1.19.1. 4% Paraformaldehyde (PFA) (100ml)

PFA (Merck, Germany)	4g
1xPBS	qs

Heat at 50°C to dissolve and store in aliquots at -20°C

1.19.2. Mowiol

Mowiol (Sigma-Aldrich, USA)	2.4g
Glycerol (Merck, South Africa)	6g
Tris buffer (0.2M) (pH 8.5)	12ml
ddH2O	6ml

Stir for a few hours at 50°C

Centrifuge at 12000 rpm for 20 mins

Store supernatant in 1ml aliquots at -20

1.20. Fluorescent Activated Cell Sorting (FACS)

1.20.1. Hepes Buffer (12mM) (15ml) (pH 7.4)

Hepes	0.04289g
ddHO	sq

Make up fresh on the day of FACS experiment

1.20.2. Annexin V-FITC Binding Buffer (13ml)

Hepes buffer (12mM)	10.833ml
NaCl (1M)	1.82ml
$CaCl_2$ (100mM)	325µl
ddH_2O	22µl

1.20.3. Propidium Iodide (PI) (50µg/ml)

Propidium iodide stock (1mg/ml)	50µl
ddH_2O	950µl